Covariant LQG in numerics: real, complex critical points, and ongoing developments

Dongxue Qu

Perimeter Institute

M. Han, H. Liu, DQ, 2404.10563 (2024),
M. Han, DQ, C. Zhang, 2404.02796 (2024),
M. Han, H. Liu, DQ, F. Vidotto, C. Zhang, 2402.07984 (2024),
M. Han, H. Liu, DQ, 2301.02930 (2023)

Loops'24@Florida

Outline

- Motivation
- Spinfoam overviews
- Real and complex critical point
    - ☆ Numerical algorithm of constructing boundary data and real critical point
    - ☆ Computing complex critical points
- Cosmological dynamics from spinfoam with scalar matter

Outline

- Motivation
- Spinfoam overviews
- Real and complex critical point
  - Numerical algorithm of constructing boundary data and real critical point
  - Computing complex critical points
- Cosmological dynamics from spinfoam with scalar matter

Motivation

Motivation

- Spinfoam theory is a covariant approach of LQG
- Spinfoam amplitude defines transition amplitude of LQG states.

Motivation

- Spinfoam theory is a covariant approach of LQG
- Spinfoam amplitude defines transition amplitude of LQG states.
- Main challenge: the difficulty of computing spinfoam amplitude $\Longrightarrow$ Recent progress in numerics on spinfoam models
  - sl2cfoam based on $15j$ + boosters [Dona, Fanizza, Sarno, Speziale, Gozzini 2018-2023]
  - Spinfoam renormalization [Bahr, Dittrich, Steinhaus, 2016-2023]
  - Effective spinfoam model [Asante, Dittrich, Haggard, 2020-2023]
  - Lefschetz thimble, Monte-Carlo [Steinhaus 2024, Donà, Frisoni and Vidotto, 2023, Han, Huang, Liu and DQ, 2020-2021]
  - Complex critical point and asymptotic expansion [Han, Huang, Liu, DQ, 2020-2024]

Motivation

- Spinfoam theory is a covariant approach of LQG
- Spinfoam amplitude defines transition amplitude of LQG states.
- Main challenge: the difficulty of computing spinfoam amplitude $\Longrightarrow$ Recent progress in numerics on spinfoam models
  - sl2cfoam based on $15j$ + boosters [Dona, Fanizza, Sarno, Speziale, Gozzini 2018-2023]
  - Spinfoam renormalization [Bahr, Dittrich, Steinhaus, 2016-2023]
  - Effective spinfoam model [Asante, Dittrich, Haggard, 2020-2023]
  - Lefschetz thimble, Monte-Carlo [Steinhaus 2024, Donà, Frisoni and Vidotto, 2023, Han, Huang, Liu and DQ, 2020-2021]
  - Complex critical point and asymptotic expansion [Han, Huang, Liu, DQ, 2020-2024]
- The method of complex critical points: A generalized stationary phase approximation of spinfoam amplitude

Motivation

- Spinfoam theory is a covariant approach of LQG
- Spinfoam amplitude defines transition amplitude of LQG states.
- Main challenge: the difficulty of computing spinfoam amplitude $\Longrightarrow$ Recent progress in numerics on spinfoam models
  - sl2cfoam based on $15j$ + boosters [Dona, Fanizza, Sarno, Speziale, Gozzini 2018-2023]
  - Spinfoam renormalization [Bahr, Dittrich, Steinhaus, 2016-2023]
  - Effective spinfoam model [Asante, Dittrich, Haggard, 2020-2023]
  - Lefschetz thimble, Monte-Carlo [Steinhaus 2024, Donà, Frisoni and Vidotto, 2023, Han, Huang, Liu and DQ, 2020-2021]
  - Complex critical point and asymptotic expansion [Han, Huang, Liu, DQ, 2020-2024]
- The method of complex critical points: A generalized stationary phase approximation of spinfoam amplitude
  - Numerical algorithm of constructing boundary data and real critical point

Motivation

- Spinfoam theory is a covariant approach of LQG
- Spinfoam amplitude defines transition amplitude of LQG states.
- Main challenge: the difficulty of computing spinfoam amplitude $\Longrightarrow$ Recent progress in numerics on spinfoam models
  - sl2cfoam based on $15j$ + boosters [Dona, Fanizza, Sarno, Speziale, Gozzini 2018-2023]
  - Spinfoam renormalization [Bahr, Dittrich, Steinhaus, 2016-2023]
  - Effective spinfoam model [Asante, Dittrich, Haggard, 2020-2023]
  - Lefschetz thimble, Monte-Carlo [Steinhaus 2024, Donà, Frisoni and Vidotto, 2023, Han, Huang, Liu and DQ, 2020-2021]
  - Complex critical point and asymptotic expansion [Han, Huang, Liu, DQ, 2020-2024]
- The method of complex critical points: A generalized stationary phase approximation of spinfoam amplitude
  - Numerical algorithm of constructing boundary data and real critical point
  - Deformation of boundary data and computing complex critical points

Motivation

Application of complex critical point method

Motivation

Application of complex critical point method

- The semiclassical analysis of spinfoam quantum gravity: Look at the large-j behavior:

$$\frac{\text{area}}{\ell_p^2} \sim \gamma\sqrt{j(j+1)}, \quad \text{area} \gg \ell_p^2$$

[Asante, Bahr, Barrett, Bianchi, Bonzom, Conrady, Ding, Dittrich, Dona, Engle, Freidel, Gozzini, Haggard, Han, Hellmann, Huang, Kaminski, Kisielowski, Liu, Livine, Magliaro, Perini, Pereira, Riello, Rovelli, Sahlmann, Sarno, Speziale, Zhang, etc.]

Barbero-Immirzi parameter

Motivation

Application of complex critical point method

- The semiclassical analysis of spinfoam quantum gravity: Look at the large-j behavior:

$$\frac{\text{area}}{\ell_p^2} \sim \gamma\sqrt{j(j+1)}, \quad \text{area} \gg \ell_p^2$$

[Asante, Bahr, Barrett, Bianchi, Bonzom, Conrady, Ding, Dittrich, Dona, Engle, Freidel, Gozzini, Haggard, Han, Hellmann, Huang, Kaminski, Kisielowski, Liu, Livine, Magliaro, Perini, Pereira, Riello, Rovelli, Sahlmann, Sarno, Speziale, Zhang, etc.]

Barbero-Immirzi parameter

- Extract properties of effective theory from the spinfoam amplitude in the large-j regime.

Motivation

Application of complex critical point method

- The semiclassical analysis of spinfoam quantum gravity: Look at the large-j behavior:

$$\frac{\text{area}}{\ell_p^2} \sim \gamma\sqrt{j(j+1)}, \quad \text{area} \gg \ell_p^2$$

[Asante, Bahr, Barrett, Bianchi, Bonzom, Conrady, Ding, Dittrich, Dona, Engle, Freidel, Gozzini, Haggard, Han, Hellmann, Huang, Kaminski, Kisielowski, Liu, Livine, Magliaro, Perini, Pereira, Riello, Rovelli, Sahlmann, Sarno, Speziale, Zhang, etc.]

Barbero-Immirzi parameter

- Extract properties of effective theory from the spinfoam amplitude in the large-j regime.

- New development: understanding of quantum cosmology from spinfoam theory, investigate the effective dynamics of cosmology from the large-j spinfoam amplitude.

Outline

- Motivation
- Spinfoam overviews
- Real and complex critical point
    - Numerical algorithm of constructing boundary data and real critical point
    - Computing complex critical points
- Cosmological dynamics from spinfoam with scalar matter

Spinfoam overview

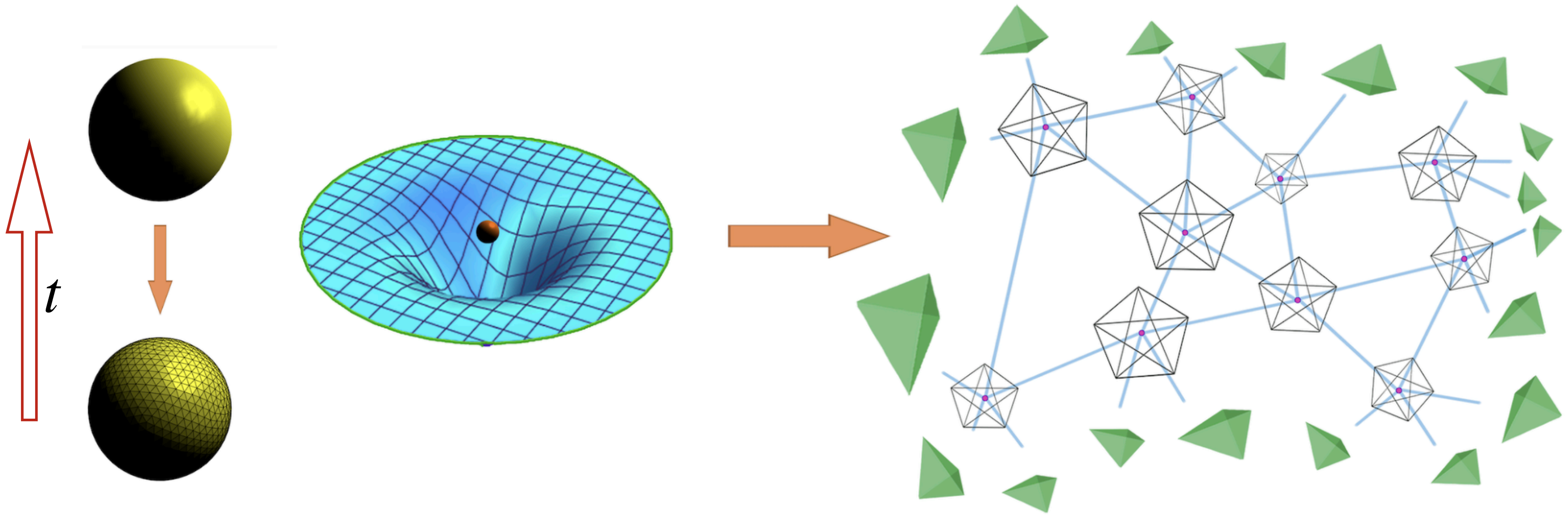

Covariant path integral formulation of Quantum Gravity (QG):

$$Z(h_f, h_i) = \int_{h_i}^{h_f} \mathscr{D}[g] e^{\frac{i}{\ell_P^2} \int_{\mathscr{M}} \mathrm{d}^4 x \sqrt{-g} R},$$

Summing over histories of 3-geometries:

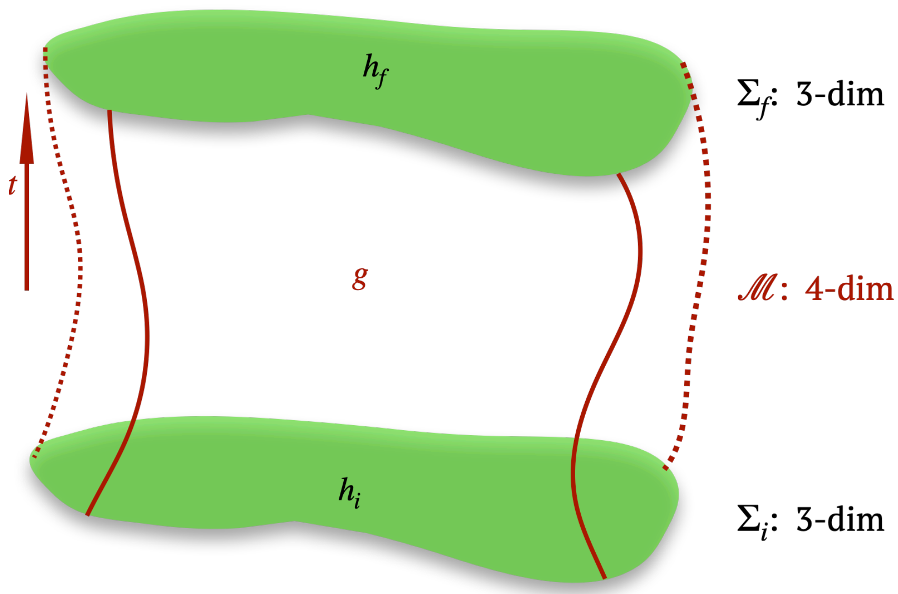

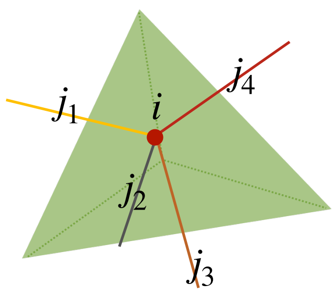

Inspired by [F. Vidotto, Loops'24 Summer School], [E. Livine, 2024], [C, Rovelli, F. Vidotto, 2014]

Spinfoam

Covariant path integral formulation of Quantum Gravity (QG):

$$Z(h_f, h_i) = \int_{h_i}^{h_f} \mathscr{D}[g] e^{\frac{i}{\ell_P^2}\int_{\mathscr{M}} d^4x\sqrt{-g}R},$$

Summing over histories of 3-geometries:

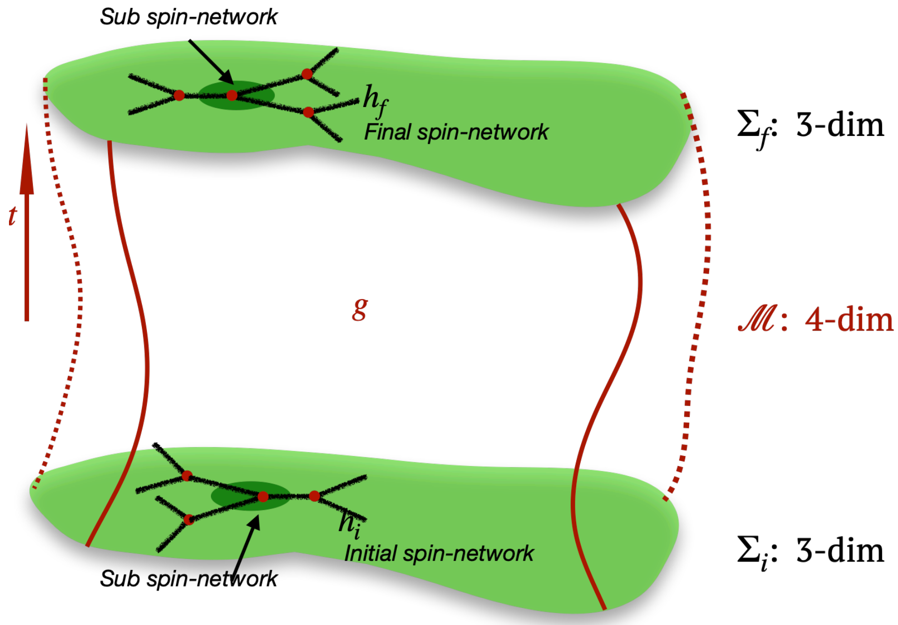

Adapt into LQG framework:

Quantum 3-geometry = Spin-network state (Γ, j_l, i_n)

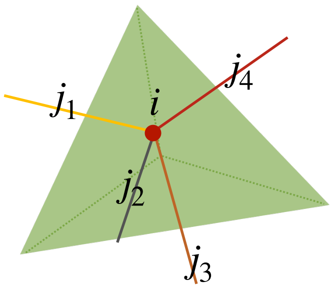

Inspired by [F. Vidotto, Loops'24 Summer School], [E. Livine, 2024], [C, Rovelli, F. Vidotto, 2014]

Spinfoam

Covariant path integral formulation of Quantum Gravity (QG):

$$Z(h_f, h_i) = \int_{h_i}^{h_f} \mathscr{D}[g] e^{\frac{i}{\ell_p^2}\int_{\mathscr{M}} \mathrm{d}^4 x \sqrt{-g}R},$$

Summing over histories of 3-geometries:

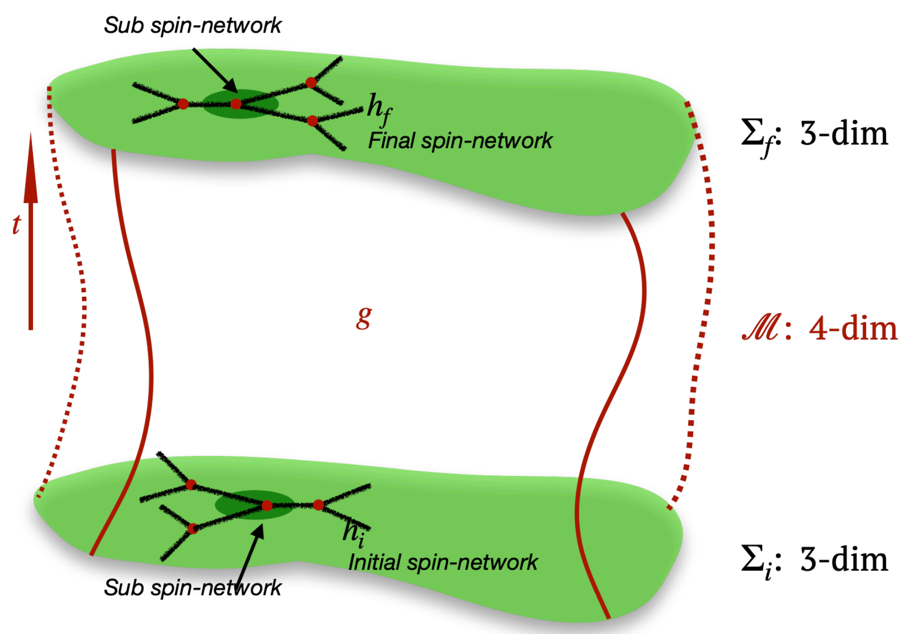

Adapt into LQG framework:

Quantum 3-geometry = Spin-network state (Γ, j_l, i_n)

- Spins $j_l \in \mathrm{irrep}[SU(2)]$
- Intertwiners $i_n \in \mathrm{Inv}[V_{j_1} \otimes \cdots \otimes V^*_{j_n}]$

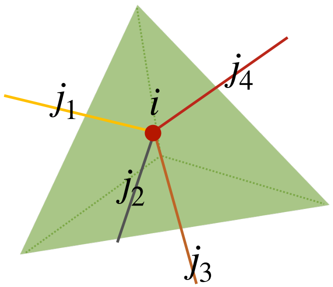

Inspired by [F. Vidotto, Loops’24 Summer School], [E. Livine, 2024], [C, Rovelli, F. Vidotto, 2014]

Spinfoam

Covariant path integral formulation of Quantum Gravity (QG):

$$Z(h_f, h_i) = \int_{h_i}^{h_f} \mathscr{D}[g] e^{\frac{i}{\ell_p^2}\int_{\mathscr{M}} \mathrm{d}^4x\sqrt{-g}R},$$

Summing over histories of 3-geometries:

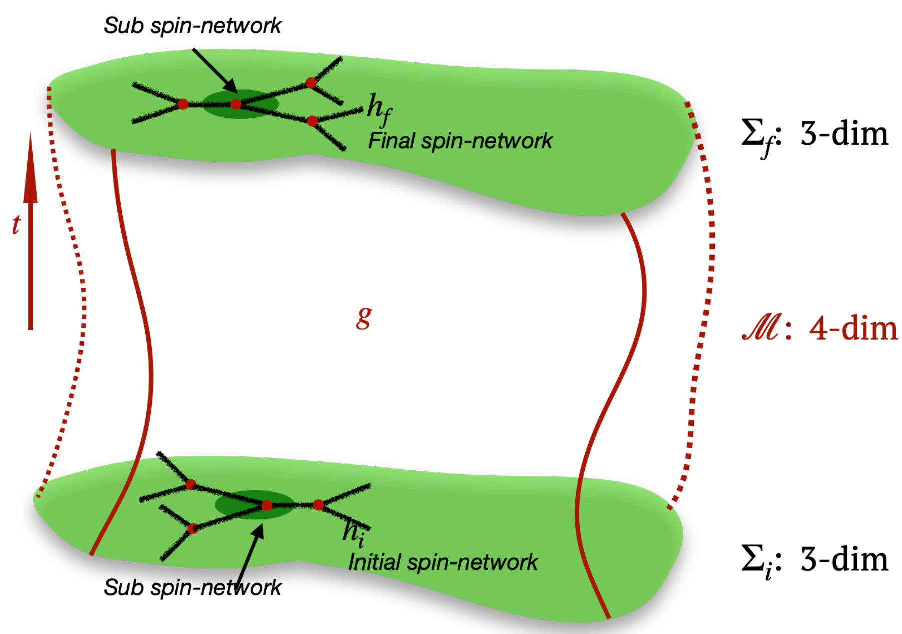

Adapt into LQG framework:

Quantum 3-geometry = Spin-network state (Γ, j_l, i_n)

- Spins $j_l \in$ irrep[SU(2)]
- Intertwiners $i_n \in \mathrm{Inv}[V_{j_1} \otimes \cdots \otimes V^*_{j_n}]$

LQG Hilbert space on graph Γ:

$\mathscr{H}_\Gamma = L^2\left(\mathrm{SU}(2)^{\#\text{ of links}}/\mathrm{SU}(2)^{\#\text{ of nodes}}\right)$

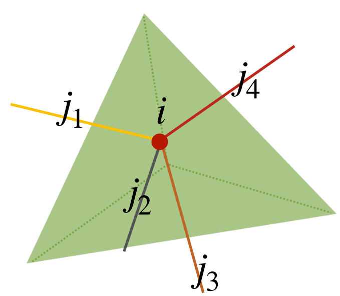

Inspired by [F. Vidotto, Loops'24 Summer School], [E. Livine, 2024], [C, Rovelli, F. Vidotto, 2014]

Spinfoam

Covariant path integral formulation of Quantum Gravity (QG):

$$Z(h_f, h_i) = \int_{h_i}^{h_f} \mathscr{D}[g] e^{\frac{i}{\ell_P^2}\int_{\mathscr{M}} \mathrm{d}^4x\sqrt{-g}R},$$

Summing over histories of 3-geometries:

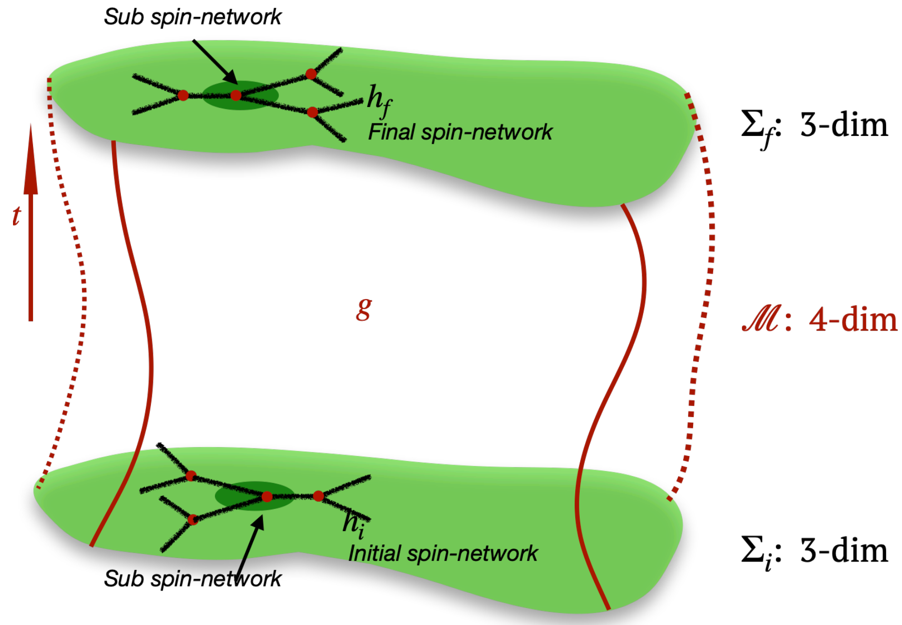

Adapt into LQG framework:

Quantum 3-geometry = Spin-network state (Γ, j_l, i_n)

- Spins $j_l \in \mathrm{irrep}[\mathrm{SU}(2)]$
- Intertwiners $i_n \in \mathrm{Inv}[V_{j_1} \otimes \cdots \otimes V^*_{j_n}]$

LQG Hilbert space on graph Γ:
$\mathscr{H}_\Gamma = L^2\left(\mathrm{SU}(2)^{\#\text{ of links}}/\mathrm{SU}(2)^{\#\text{ of nodes}}\right)$

Nodes: quantum polyhedron (quantum number i_n)

Links: quanta of area (quantum number j_l)

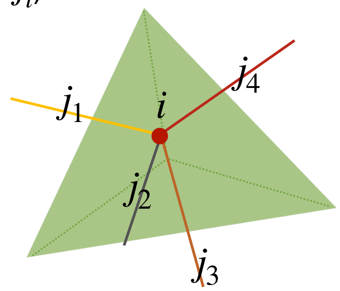

Inspired by [F. Vidotto, Loops'24 Summer School], [E. Livine, 2024], [C, Rovelli, F. Vidotto, 2014]

Spinfoam

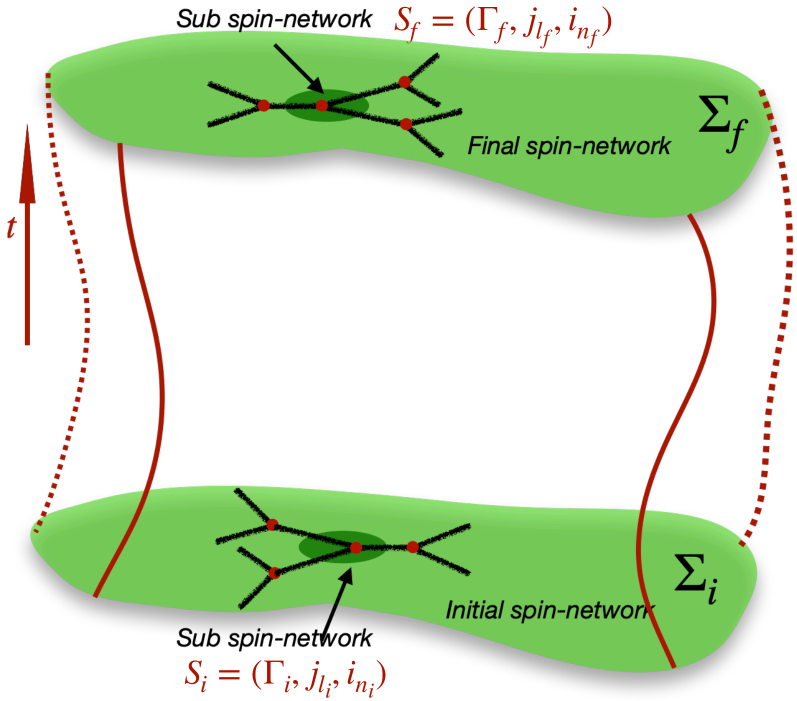

Inspired by [F. Vidotto, Loops'24 Summer School], [E. Livine, 2024], [C, Rovelli, F. Vidotto, 2014]

Spinfoam

Histories of spin-networks = Spinfoam

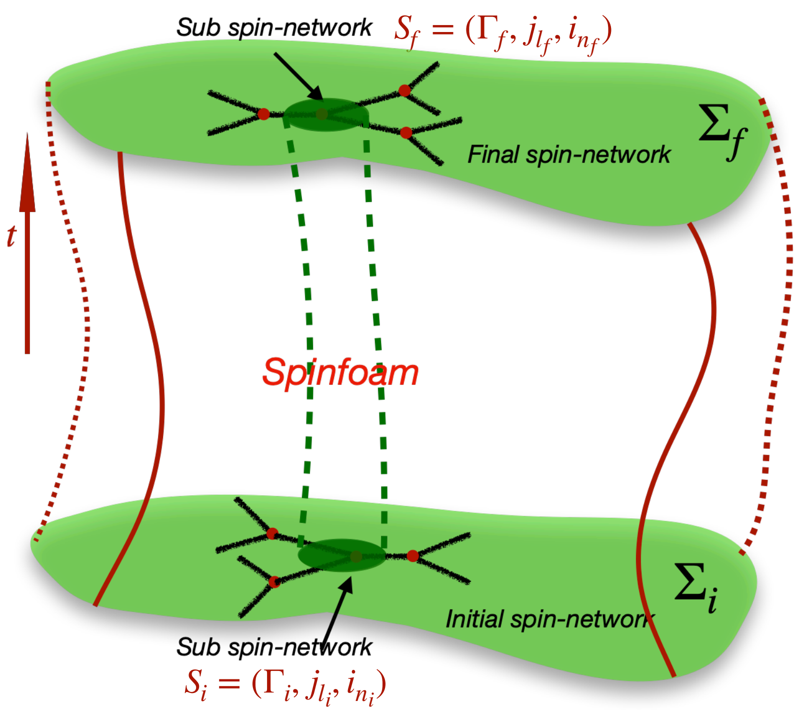

Inspired by [F. Vidotto, Loops'24 Summer School], [E. Livine, 2024], [C, Rovelli, F. Vidotto, 2014]

Spinfoam

[E. Livine, 2024]

Histories of spin-networks = Spinfoam

Spatial imprint	Spinfoam cell	Algebra	Geometry
Link l	Face f	Spin j_l	Area
Node n	Edge e	Intertwiner i_n	Volume
Transition	Vertex v	Amplitude A	4d event

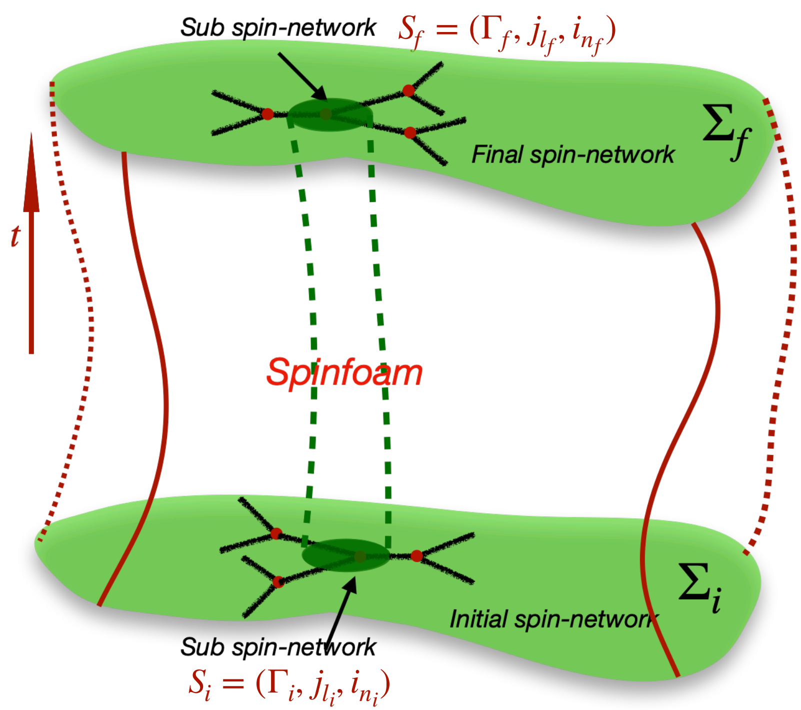

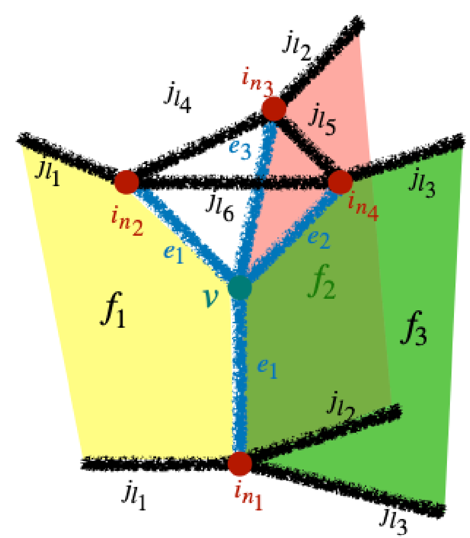

Inspired by [F. Vidotto, Loops'24 Summer School], [E. Livine, 2024], [C, Rovelli, F. Vidotto, 2014]

Spinfoam

[E. Livine, 2024]

Histories of spin-networks = Spinfoam

Spatial imprint	Spinfoam cell	Algebra	Geometry
Link l	Face f	Spin j_l	Area
Node n	Edge e	Intertwiner i_n	Volume
Transition	Vertex v	Amplitude A	4d event

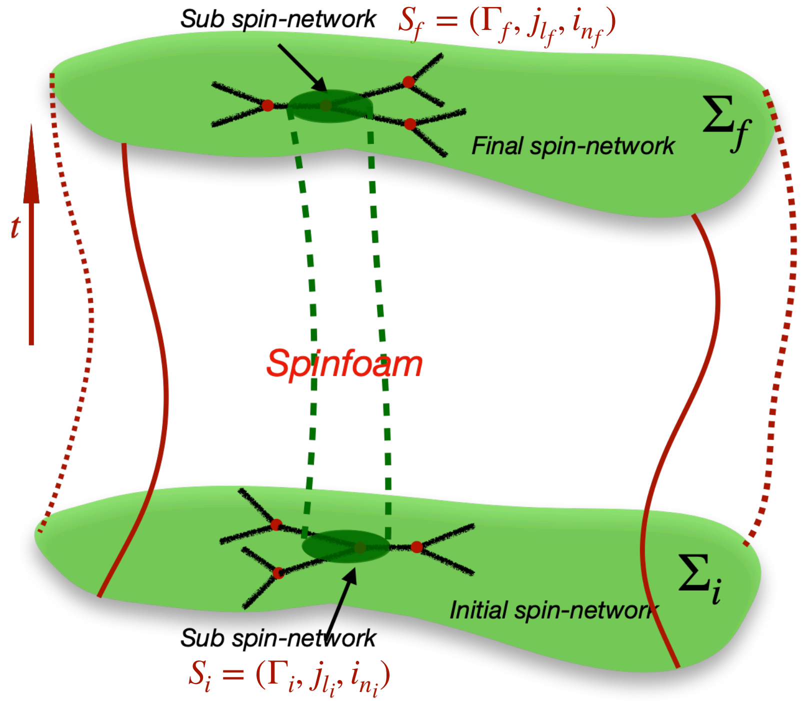

Spinfoam amplitude: $A(\mathscr{K}^*, S_i, S_f)$

2-complex   Boundary 3-geometries

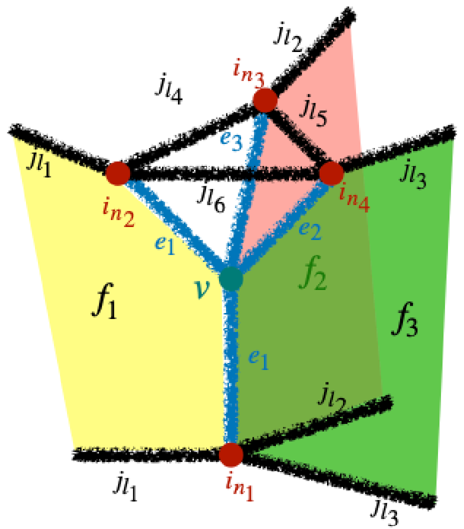

Inspired by [F. Vidotto, Loops'24 Summer School], [E. Livine, 2024], [C, Rovelli, F. Vidotto, 2014]

Spinfoam

To study the quantum dynamics in LQG: spinfoam amplitude.

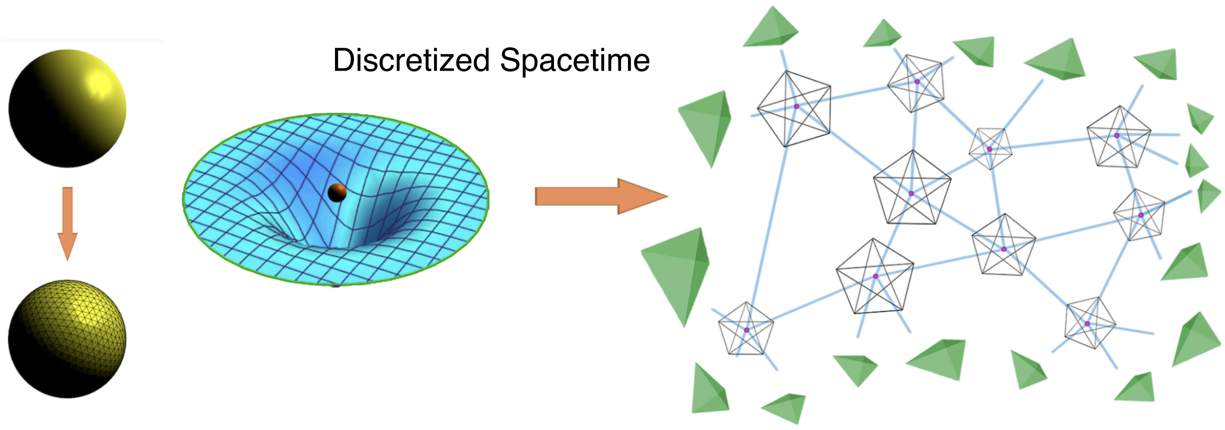

[M. Han, DQ, et al 2023]

Spinfoam

To study the quantum dynamics in LQG: spinfoam amplitude.

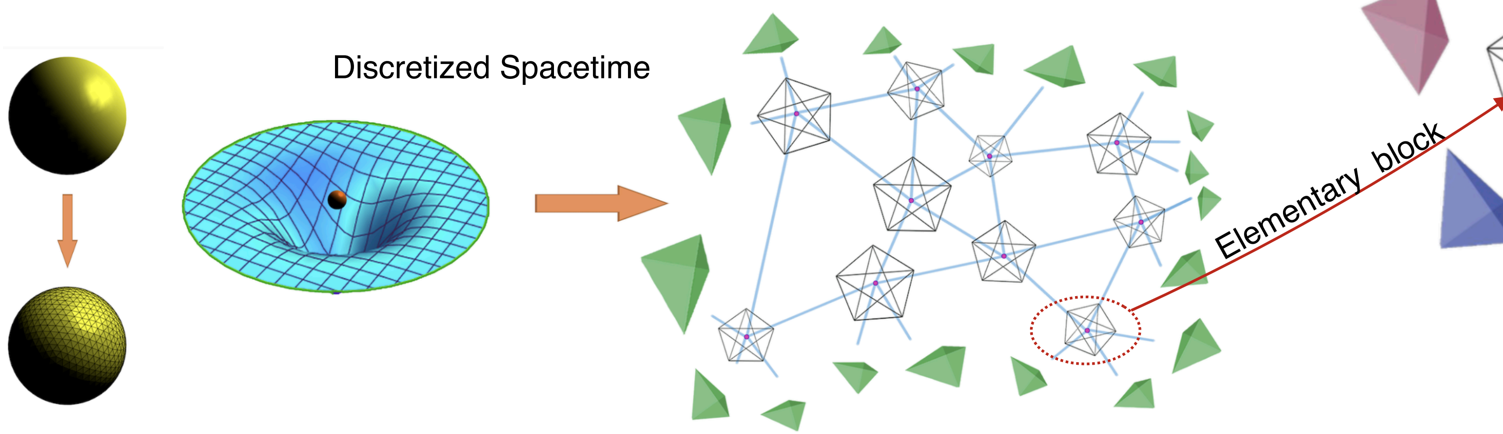

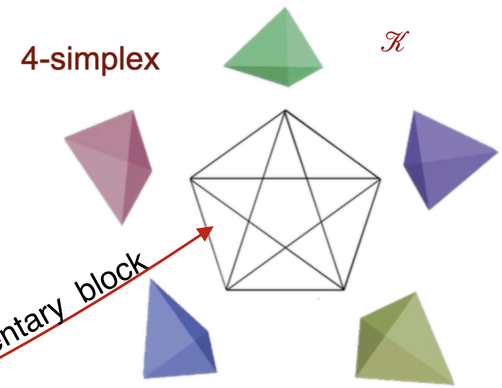

[M. Han, DQ, et al 2023]

Spinfoam

To study the quantum dynamics in LQG: spinfoam amplitude.

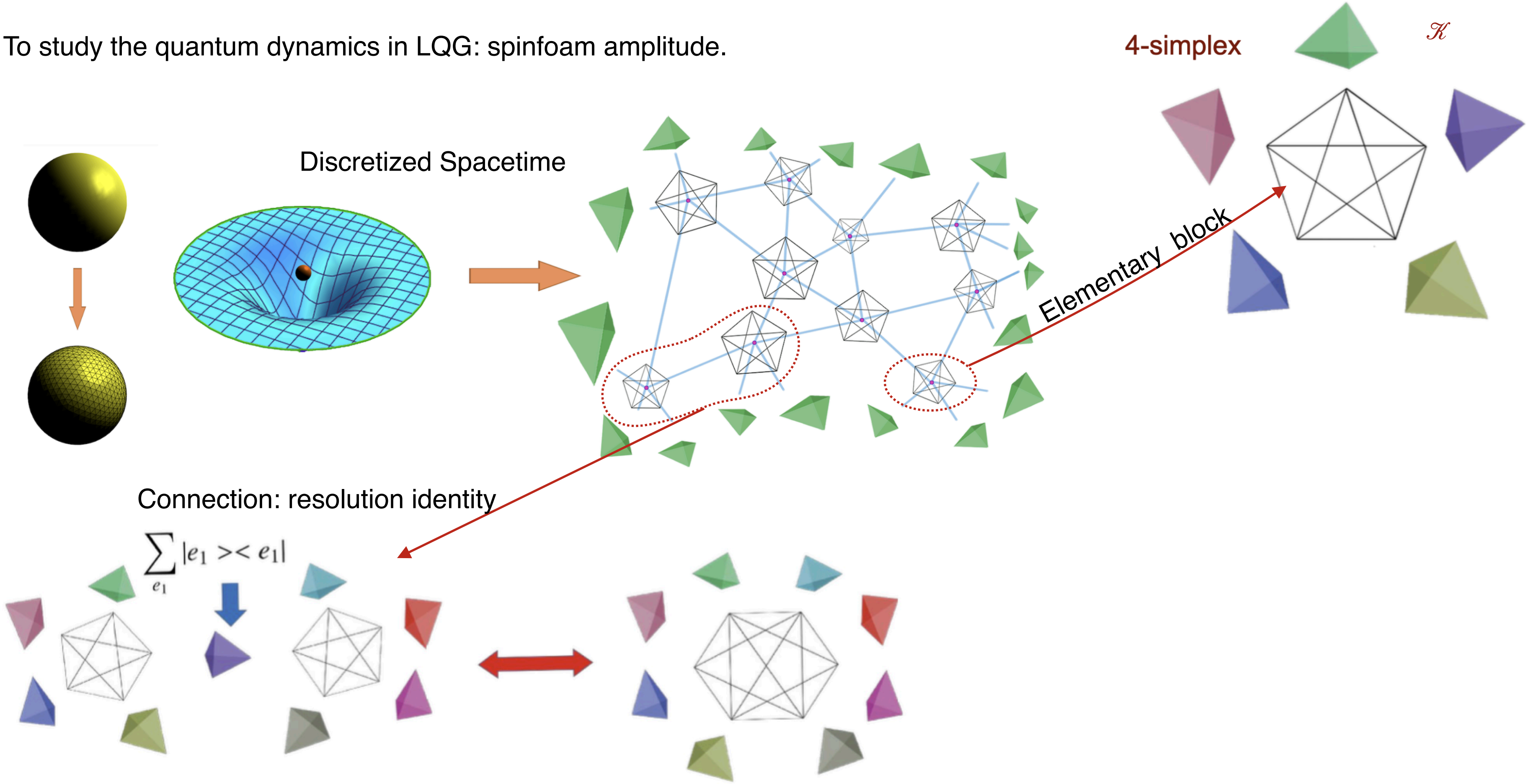

$$\langle x_f, t_f | x_i, t_i \rangle = \int dx_{N-1}\, dx_{N-2} \ldots dx_1 \,\langle x_f, t_f | x_{N-1}, t_{N-1} \rangle \langle x_{N-1}, t_{N-1} | x_{N-2}, t_{N-2} \rangle \ldots \langle x_2, t_2 | x_1, t_1 \rangle$$

[M. Han, DQ, et al 2023]

Spinfoam amplitude

A spinfoam $= (\mathscr{K}^*, j_f, i_e)$

4-d triangulation	$\mathscr{K}$	2 - complex	$\mathscr{K}^*$
4-simplex	σ	Vertex	v
Tetrahedron	τ	Oriented edge	e
Triangle	t	Oriented Face	f

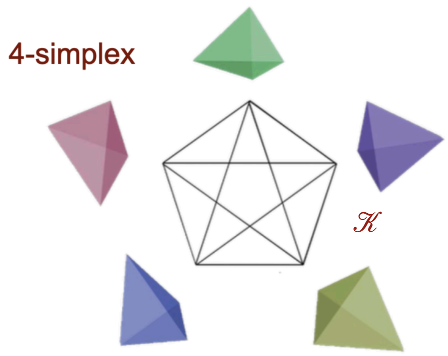

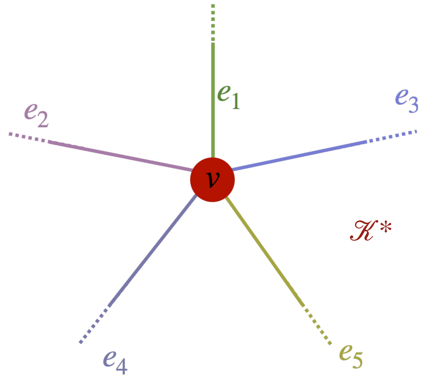

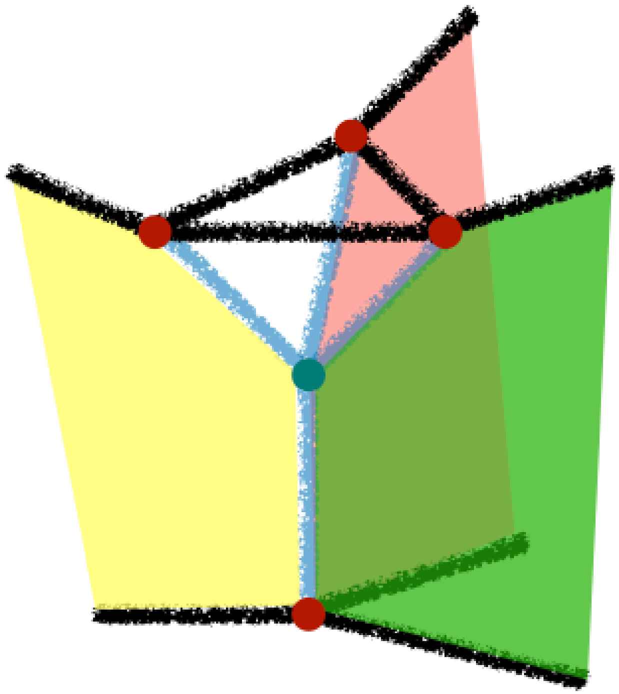

Spinfoam amplitude

$$\text{A spinfoam} = (\mathscr{K}^*, j_f, i_e)$$

4-d triangulation	$\mathscr{K}$	2 - complex	$\mathscr{K}^*$
4-simplex	σ	Vertex	v
Tetrahedron	τ	Oriented edge	e
Triangle	t	Oriented Face	f

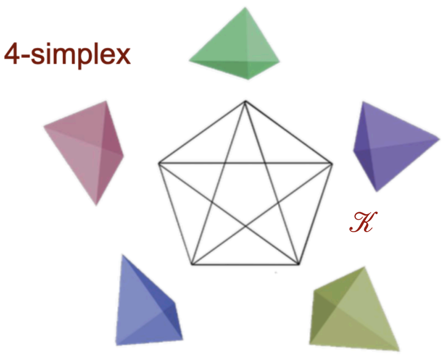

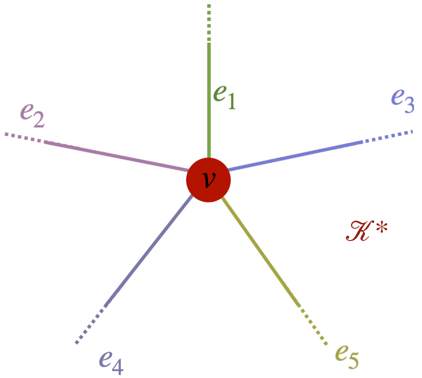

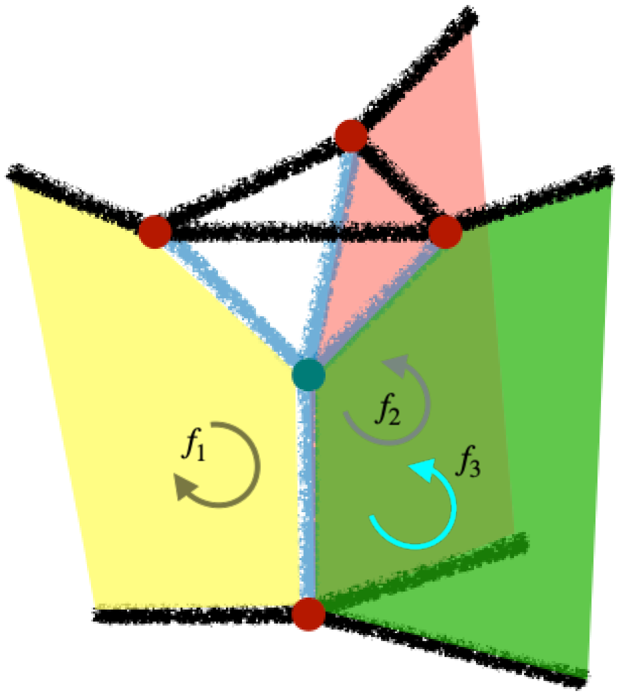

Spinfoam amplitude

A spinfoam $= (\mathscr{K}^*, j_f, i_e)$

4-d triangulation $\mathscr{K}$	2 - complex $\mathscr{K}^*$
4-simplex σ	Vertex v
Tetrahedron τ	Oriented edge e
Triangle t	Oriented Face f

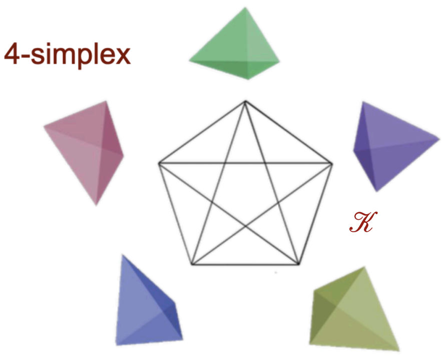

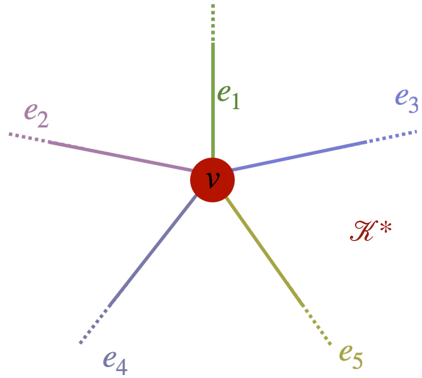

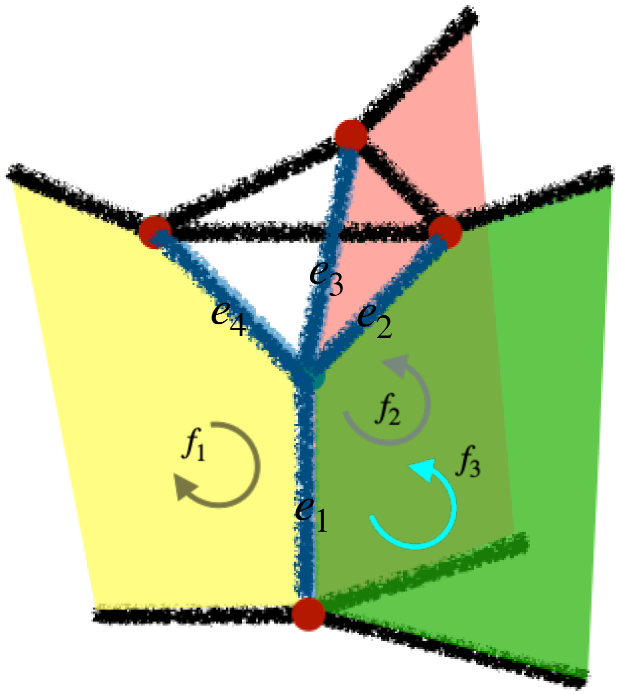

Spinfoam amplitude

A spinfoam $= (\mathscr{K}^*, j_f, i_e)$

4-d triangulation	$\mathscr{K}$	2 - complex	$\mathscr{K}^*$
4-simplex	σ	Vertex	v
Tetrahedron	τ	Oriented edge	e
Triangle	t	Oriented Face	f

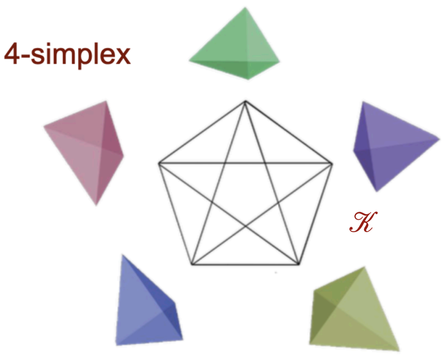

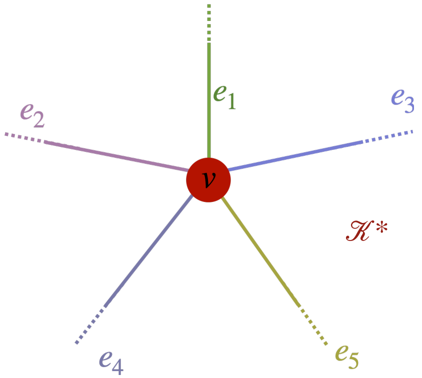

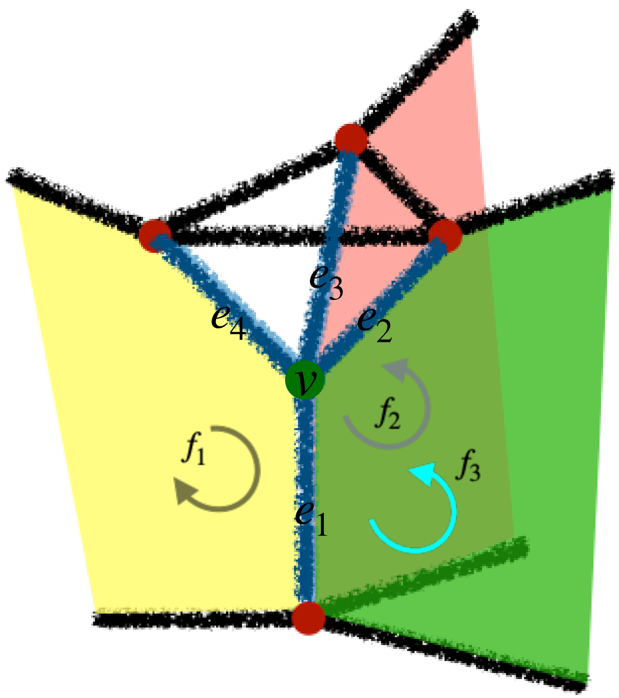

Spinfoam amplitude

A spinfoam $= (\mathscr{K}^*, j_f, i_e)$

4-d triangulation $\mathscr{K}$	2 - complex $\mathscr{K}^*$
4-simplex σ	Vertex v
Tetrahedron τ	Oriented edge e
Triangle t	Oriented Face f

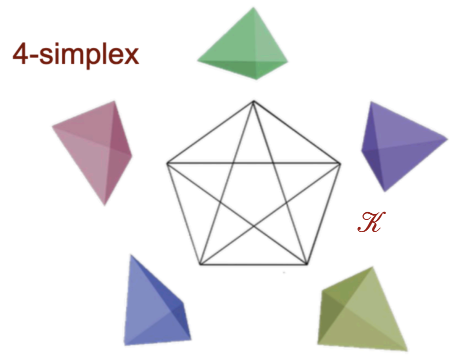

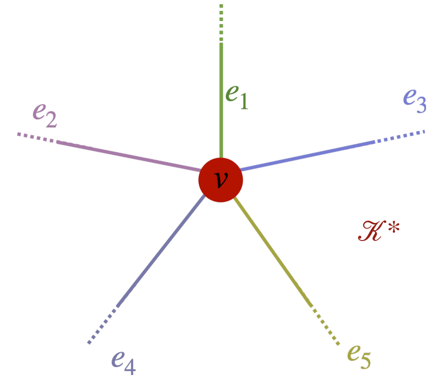

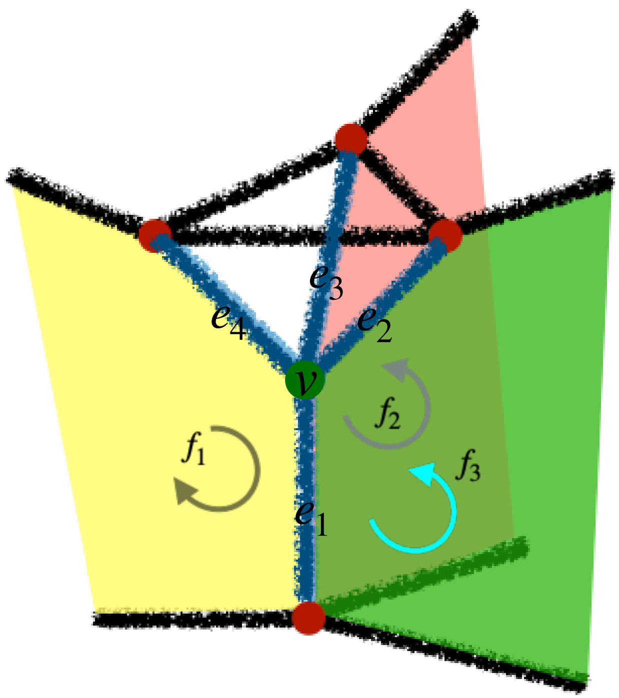

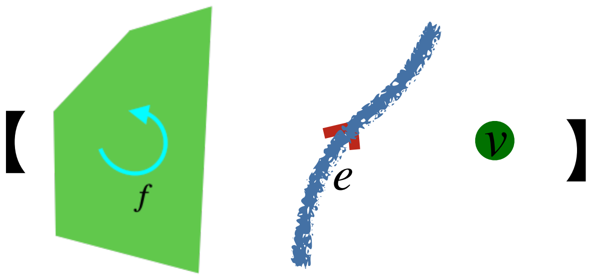

Spinfoam amplitude

A spinfoam $= (\mathscr{K}^*, j_f, i_e)$

4-d triangulation $\mathscr{K}$	2 - complex $\mathscr{K}^*$
4-simplex σ	Vertex v
Tetrahedron τ	Oriented edge e
Triangle t	Oriented Face f

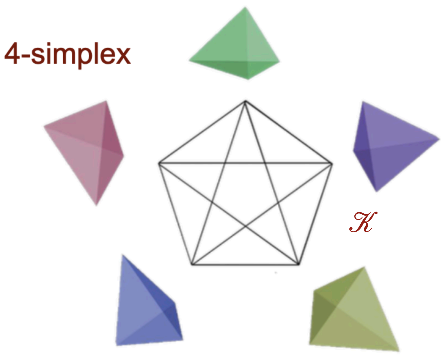

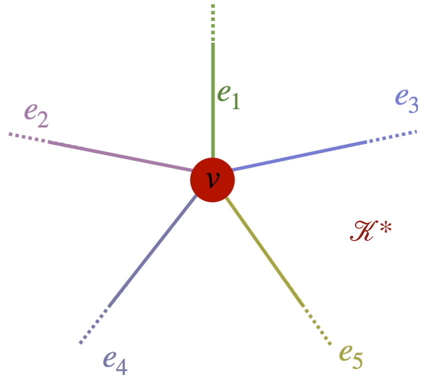

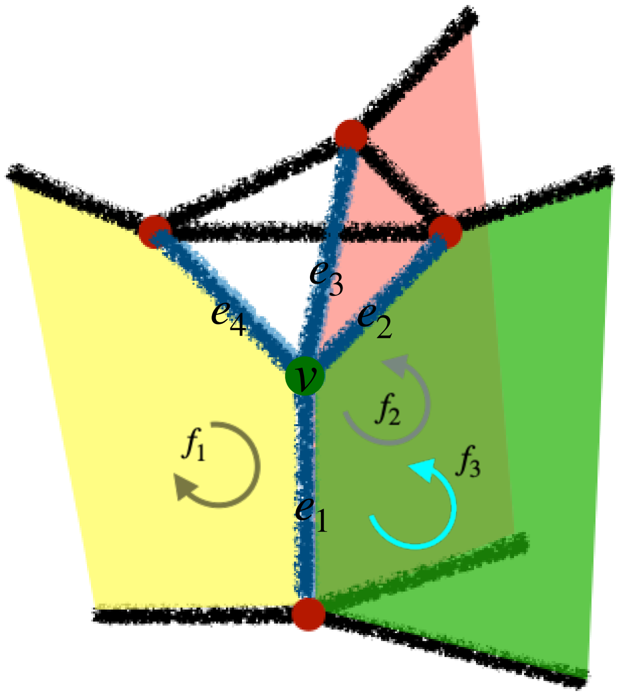

Spinfoam amplitude

A spinfoam $= (\mathcal{K}^*, j_f, i_e)$

4-d triangulation $\mathcal{K}$	2 - complex $\mathcal{K}^*$
4-simplex σ	Vertex v
Tetrahedron τ	Oriented edge e
Triangle t	Oriented Face f

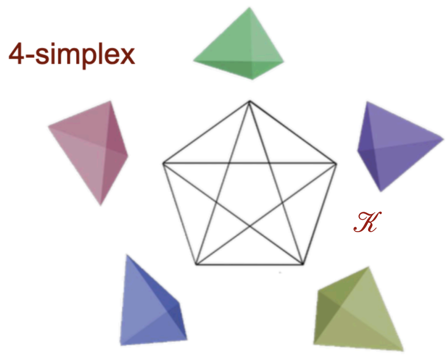

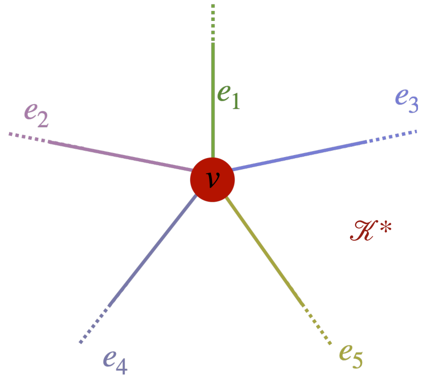

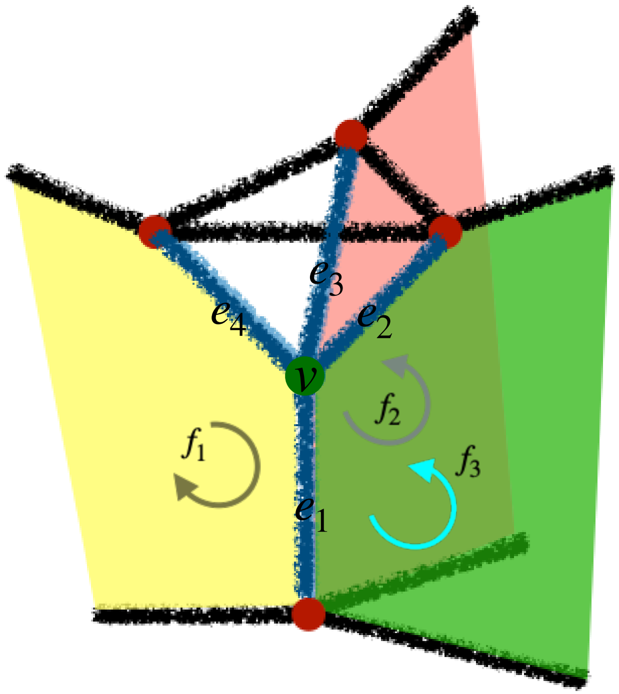

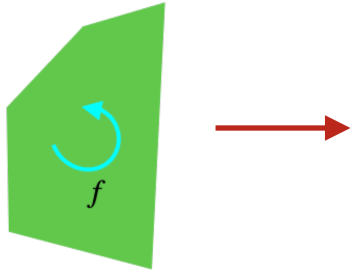

SU(2) spins j_f

Spinfoam amplitude

A spinfoam $= (\mathscr{K}^*, j_f, i_e)$

4-d triangulation $\mathscr{K}$	2 - complex $\mathscr{K}^*$
4-simplex σ	Vertex v
Tetrahedron τ	Oriented edge e
Triangle t	Oriented Face f

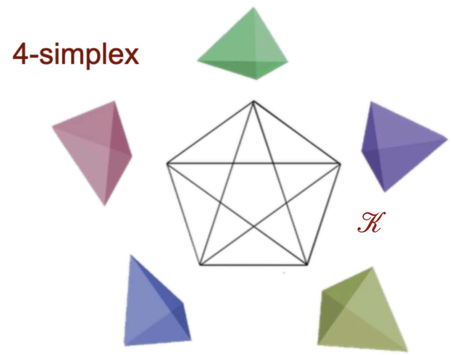

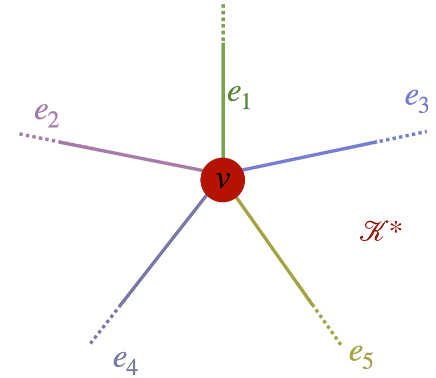

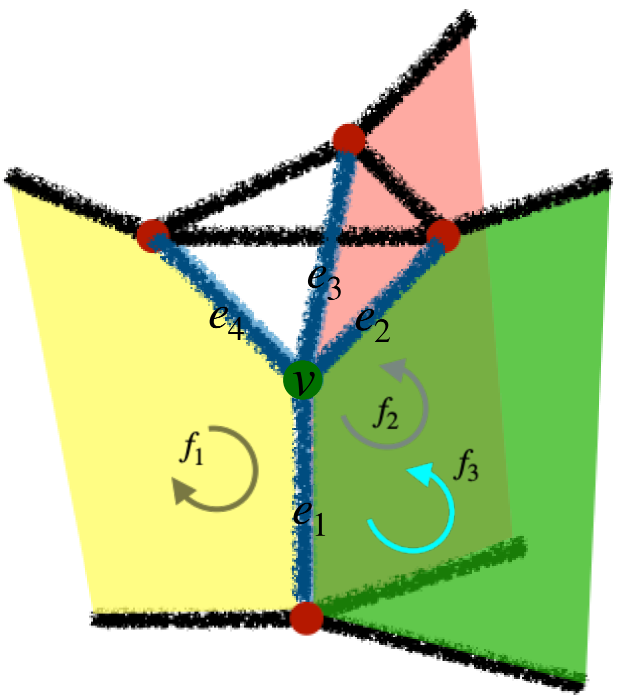

Spinfoam amplitude

A spinfoam $= (\mathscr{K}^*, j_f, i_e)$

4-d triangulation $\mathscr{K}$	2 - complex $\mathscr{K}^*$
4-simplex σ	Vertex v
Tetrahedron τ	Oriented edge e
Triangle t	Oriented Face f

4-simplex

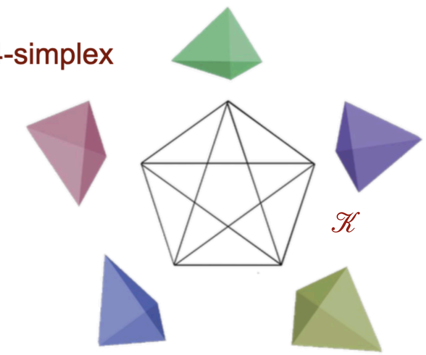

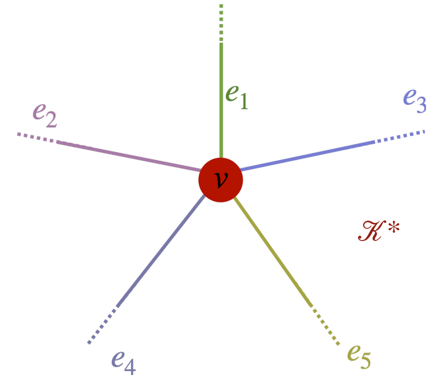

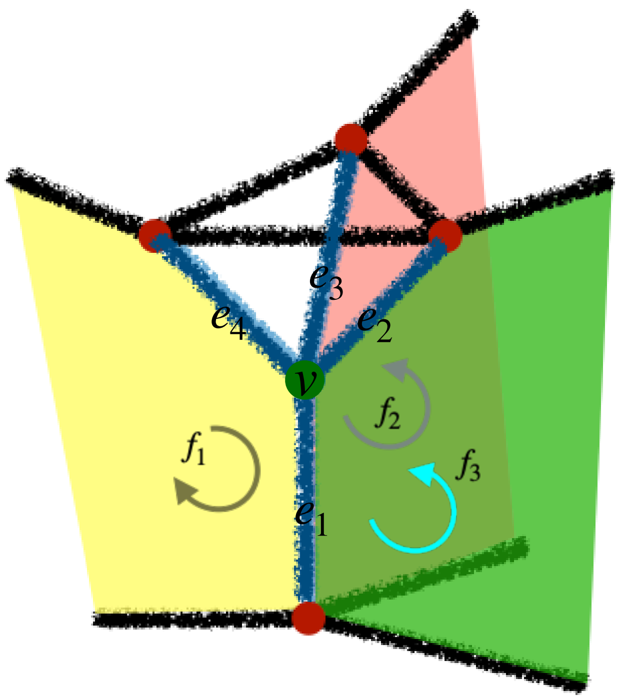

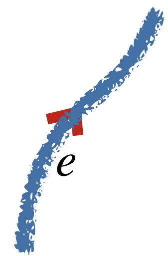

SU(2) intertwiner i_e

$$i_e \in \mathrm{Inv}[V_{j_{f_1}} \otimes \cdots \otimes V^*_{j_{f_n}}]$$

Spinfoam amplitude

A spinfoam $= (\mathscr{K}^*, j_f, i_e)$

4-d triangulation $\mathscr{K}$	2 - complex $\mathscr{K}^*$
4-simplex σ	Vertex v
Tetrahedron τ	Oriented edge e
Triangle t	Oriented Face f

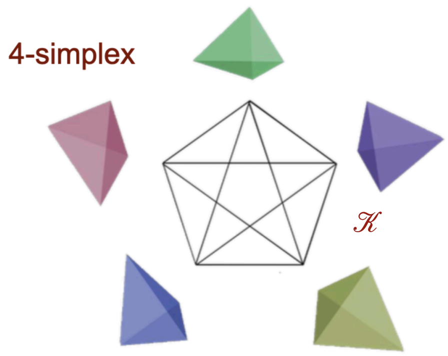

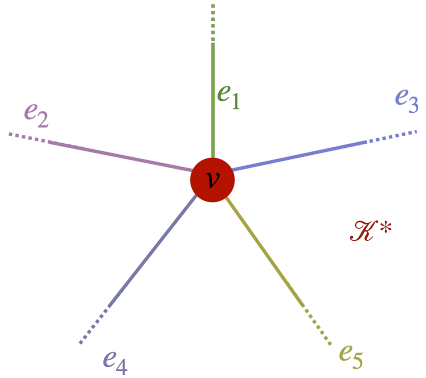

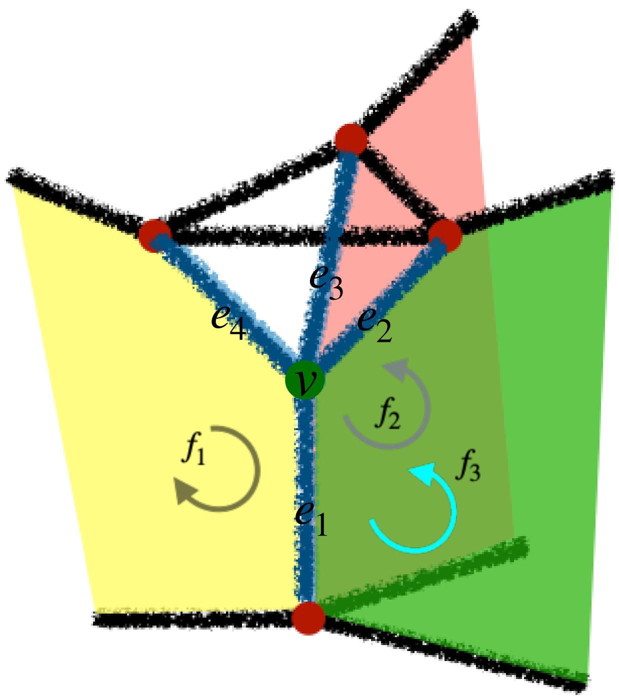

Spinfoam amplitude

A spinfoam $= (\mathscr{K}^*, j_f, i_e)$

4-d triangulation $\mathscr{K}$	2 - complex $\mathscr{K}^*$
4-simplex σ	Vertex v
Tetrahedron τ	Oriented edge e
Triangle t	Oriented Face f

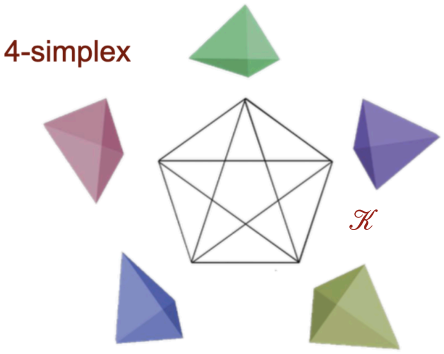

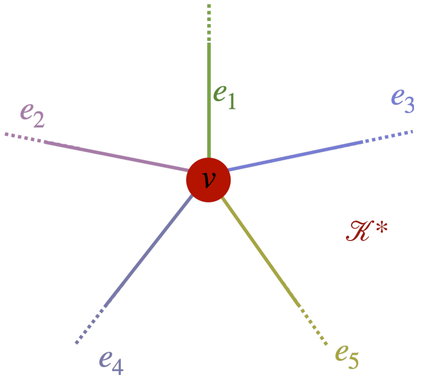

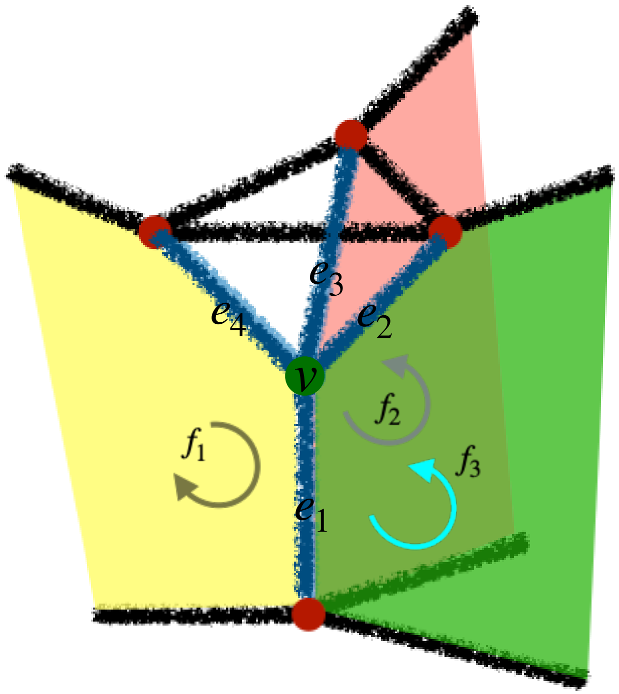

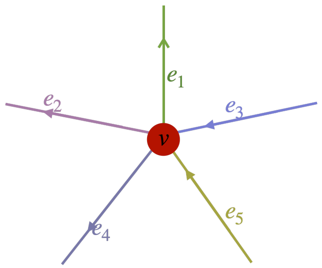

$= A_v(j_f, i_e)$

Spinfoam amplitude

A spinfoam $= (\mathscr{K}^*, j_f, i_e)$

4-d triangulation	$\mathscr{K}$	2 - complex	$\mathscr{K}^*$
4-simplex	σ	Vertex	v
Tetrahedron	τ	Oriented edge	e
Triangle	t	Oriented Face	f

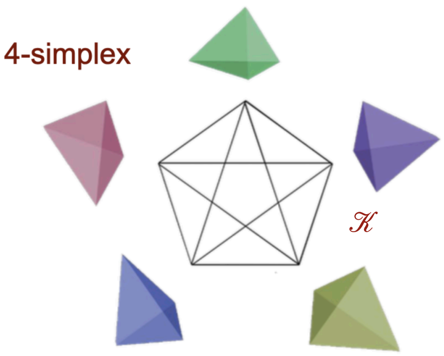

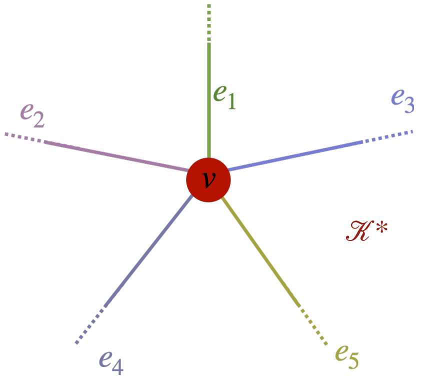

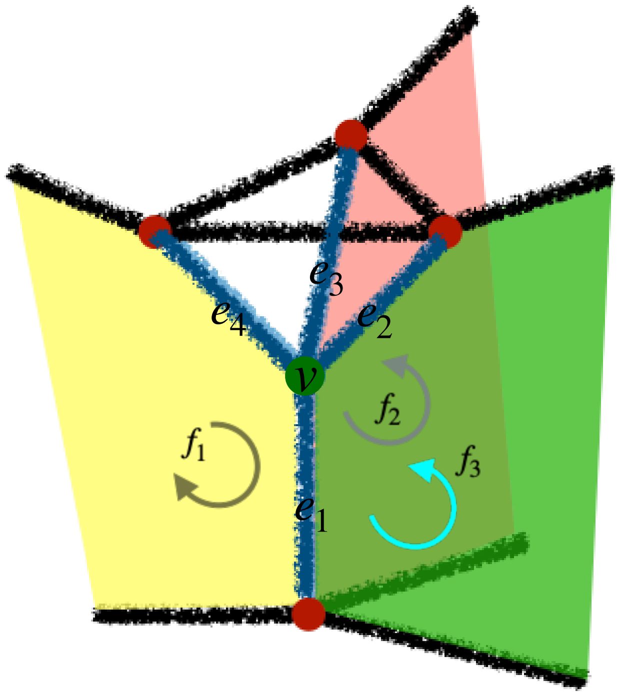

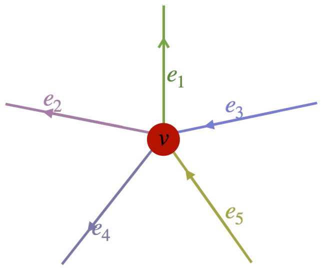

$= A_v(j_f, i_e)$

Spinfoam amplitude: $A = \sum_{j_f, i_e} \prod_f W(j_f) \prod_v A_v(j_f, i_e)$

Spinfoam amplitude

A spinfoam $= (\mathcal{K}^*, j_f, i_e)$

4-d triangulation $\mathcal{K}$	2 - complex $\mathcal{K}^*$
4-simplex σ	Vertex v
Tetrahedron τ	Oriented edge e
Triangle t	Oriented Face f

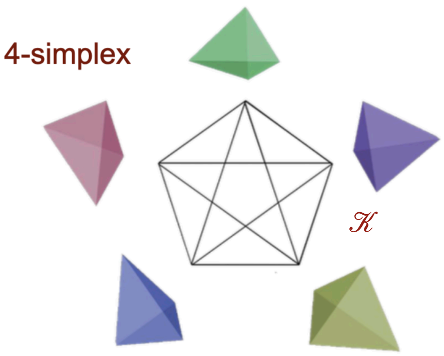

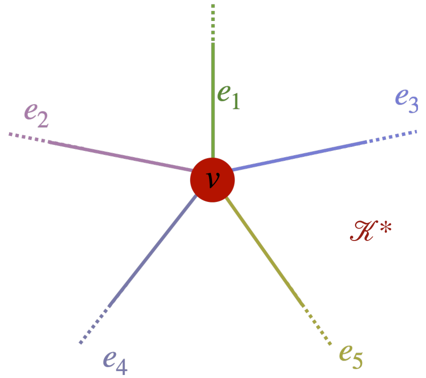

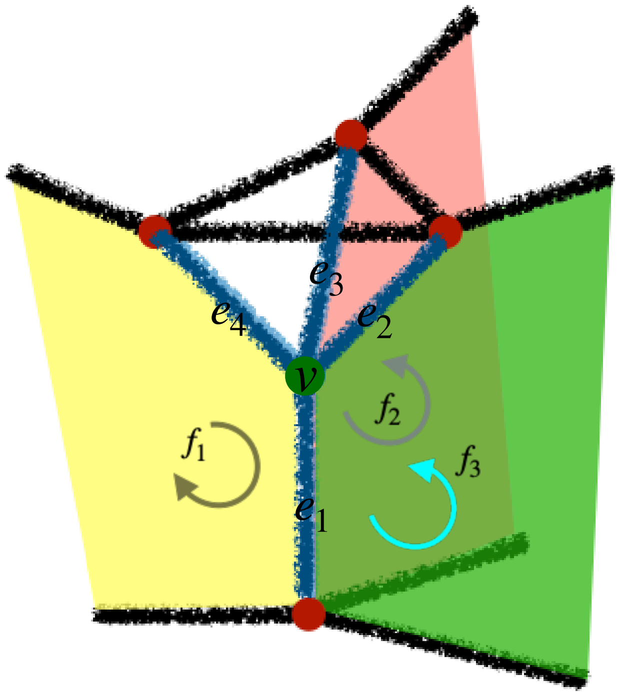

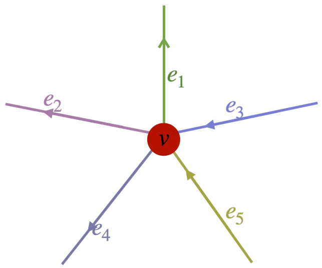

$= A_v(j_f, i_e)$

Spinfoam amplitude: $A = \sum_{j_f, i_e} \prod_f W(j_f) \prod_v A_v(j_f, i_e)$

$$A_v(j_f, i_e) := \mathrm{Tr}\left(\otimes_e I_e \otimes_{e'} I^*_{e'} \right)$$

outgoing e incoming e'

EPRL spinfoam model

EPRL spinfoam model

Spinfoam amplitude: $A = \sum_{j_f, i_e} \prod_f W(j_f) \prod_v A_v(j_f, i_e)$

$$A_v(j_f, i_e) := \mathrm{Tr}\left(\otimes_e I_e \otimes_{e'} I^*_{e'} \right)$$

I_e is SL(2,ℂ) intertwiner determined by SU(2) intertwiner i_e

EPRL spinfoam model

Spinfoam amplitude: $A = \sum_{j_f, i_e} \prod_f W(j_f) \prod_v A_v(j_f, i_e)$

$$A_v(j_f, i_e) := \mathrm{Tr}\left(\otimes_e I_e \otimes_{e'} I^*_{e'} \right)$$

I_e is SL(2,ℂ) intertwiner determined by SU(2) intertwiner i_e

$$Y : \begin{bmatrix} \text{SU(2) unitary irrep.} \\ j_f \end{bmatrix} \to \begin{bmatrix} \text{SL(2,}\mathbb{C}\text{) unitary irrep.} \\ (\rho, k) = (\gamma j_f, j_f) \end{bmatrix}$$

$$Y : |j, m\rangle \to |\gamma j, j; j, m\rangle$$

EPRL spinfoam model

Spinfoam amplitude: $A = \sum_{j_f, i_e} \prod_f W(j_f) \prod_v A_v(j_f, i_e)$

$$A_v(j_f, i_e) := \mathrm{Tr}\left(\otimes_e I_e \otimes_{e'} I^*_{e'} \right)$$

I_e is SL(2,ℂ) intertwiner determined by SU(2) intertwiner i_e

$$Y : \begin{bmatrix} \text{SU(2) unitary irrep.} \\ j_f \end{bmatrix} \to \begin{bmatrix} \text{SL(2,}\mathbb{C}\text{) unitary irrep.} \\ (\rho, k) = (\gamma j_f, j_f) \end{bmatrix}$$

$$Y : |j, m\rangle \to |\gamma j, j; j, m\rangle$$

$$I_e = P^{\mathrm{Inv}}_{\mathrm{SL}(2,\mathbb{C})} \circ Y(i_e)$$

EPRL spinfoam model

Spinfoam amplitude: $A = \sum_{j_f, i_e} \prod_f W(j_f) \prod_v A_v(j_f, i_e)$

$$A_v(j_f, i_e) := \mathrm{Tr}\left(\otimes_e I_e \otimes_{e'} I^*_{e'} \right)$$

I_e is SL(2,ℂ) intertwiner determined by SU(2) intertwiner i_e

$$Y : \begin{bmatrix} \text{SU(2) unitary irrep.} \\ j_f \end{bmatrix} \to \begin{bmatrix} \text{SL(2,}\mathbb{C}\text{) unitary irrep.} \\ (\rho, k) = (\gamma j_f, j_f) \end{bmatrix}$$

$$Y : |j, m\rangle \to |\gamma j, j; j, m\rangle$$

$$I_e = P^{\mathrm{Inv}}_{\mathrm{SL}(2,\mathbb{C})} \circ Y(i_e)$$

EPRL spinfoam model

Spinfoam amplitude: $A = \sum_{j_f, i_e} \prod_f W(j_f) \prod_v A_v(j_f, i_e)$

$$A_v(j_f, i_e) := \mathrm{Tr}\left(\otimes_e I_e \otimes_{e'} I^*_{e'} \right)$$

I_e is SL(2,ℂ) intertwiner determined by SU(2) intertwiner i_e

$$Y: \begin{bmatrix} \text{SU(2) unitary irrep.} \\ j_f \end{bmatrix} \to \begin{bmatrix} \text{SL(2,}\mathbb{C}\text{) unitary irrep.} \\ (\rho, k) = (\gamma j_f, j_f) \end{bmatrix}$$

$$Y: |j, m\rangle \to |\gamma j, j; j, m\rangle$$

$$I_e = P^{\mathrm{Inv}}_{\mathrm{SL}(2,\mathbb{C})} \circ Y(i_e)$$

$A_v(j_f, i_e)$: **EPRL vertex amplitude**

EPRL spinfoam model

Spinfoam amplitude: $A = \sum_{j_f, i_e} \prod_f W(j_f) \prod_v A_v(j_f, i_e)$

$$A_v(j_f, i_e) := \mathrm{Tr}\left(\otimes_e I_e \otimes_{e'} I^*_{e'} \right)$$

I_e is SL(2,ℂ) intertwiner determined by SU(2) intertwiner i_e

$$Y : \begin{bmatrix} \text{SU(2) unitary irrep.} \\ j_f \end{bmatrix} \to \begin{bmatrix} \text{SL(2,ℂ) unitary irrep.} \\ (\rho, k) = (\gamma j_f, j_f) \end{bmatrix}$$

$$Y : |j, m\rangle \to |\gamma j, j; j, m\rangle$$

$$I_e = P^{\mathrm{Inv}}_{\mathrm{SL}(2,\mathbb{C})} \circ Y(i_e)$$

$A_v(j_f, i_e)$: **EPRL vertex amplitude**

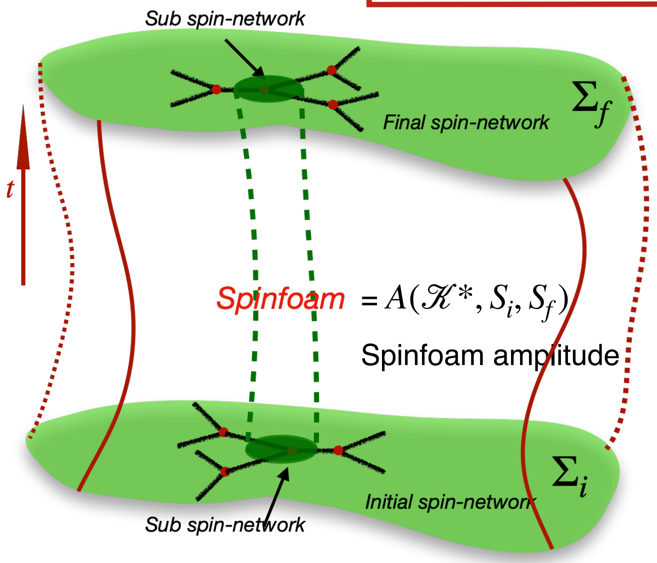

EPRL Spinfoam amplitude:

$$A = \sum_{j_f, i_e} \prod_f \dim(j_f) \prod_v A_v(j_f, i_e)$$

Finite by removing SL(2,ℂ) gauge freedom

EPRL model and Hnybida-Conrady extension model

Path integral formulation of spinfoam amplitude:

$$A(\mathscr{K}) = \sum_{\{j_h\}} \prod_h \dim(j_h) \int [\mathrm{d}X] e^{S[j_h, X]} .$$

$$S = \sum_v S_v, \qquad S_v = \sum_{(e,e')} \left(S_{vef} + S_{ve'f} \right) .$$

[J. Simao and S. Steinhaus, 2021], [H. Liu and M. Han, 2019], [W. Kaminski, M. Kisielowski, H. Sahlmann, 2018], [M. Han, 2013], [Barrett et al, 2010]

EPRL model and Hnybida-Conrady extension model

Path integral formulation of spinfoam amplitude:

$$A(\mathscr{K}) = \sum_{\{j_h\}} \prod_h \dim(j_h) \int [\mathrm{d}X] e^{S[j_h, X]}.$$

$$S = \sum_v S_v, \qquad S_v = \sum_{(e,e')} \left(S_{vef} + S_{ve'f}\right).$$

$$\tilde{\xi}_{ef} = \begin{cases} \xi_{ef} & \text{SU(2) spinor} \\ \xi^{\pm}_{ef} & \text{SU(1,1) spinor} \end{cases}$$

- Half-edge action S_{vef} for spacelike face (EPRL model + Hnybida-Conrady extension model):

$$S_{vef} = j_f \left\{ 2\ln\left[\left(m_{ef}\langle\tilde{\xi}_{ef}, Z_{vef}\rangle\right)^{\frac{\kappa_{vef}+\epsilon_e}{2}} \left(m_{ef}\langle Z_{vef}, \tilde{\xi}_{ef}\rangle\right)^{\frac{-\kappa_{vef}+\epsilon_e}{2}}\right] + \left(\iota\gamma\kappa_{vef} - \epsilon_e\right)\ln\left[m_{ef}\langle Z_{vef}, Z_{vef}\rangle\right]\right\}, \qquad Z_{vef} = g^{\mathrm{T}}_{ve} z_{vf} \tag{1}$$

- Half-edge action S_{vef} for timelike face (Hnybida-Conrady extension model):

$$S_{vef} = j_f \left[2\ln\left(\sqrt{\frac{\langle l^+_{ef}, Z_{vef}\rangle}{\langle Z_{vef}, l^+_{ef}\rangle}}\right)^{\kappa_{vef}} - \frac{\iota}{\gamma}\kappa_{vef}\ln\left(\langle l^+_{ef}, Z_{vef}\rangle\langle Z_{vef}, l^+_{ef}\rangle\right)\right]. \tag{2}$$

[J. Simao and S. Steinhaus, 2021], [H. Liu and M. Han, 2019], [W. Kaminski, M. Kisielowski, H. Sahlmann, 2018], [M. Han, 2013], [Barrett et al, 2010]

EPRL model and Hnybida-Conrady extension model

Path integral formulation of spinfoam amplitude:

$$A(\mathcal{K}) = \sum_{\{j_h\}} \prod_h \dim(j_h) \int [\mathrm{d}X] e^{S[j_h, X]}.$$

$$S = \sum_v S_v, \qquad S_v = \sum_{(e,e')} \left(S_{vef} + S_{ve'f} \right).$$

$\tilde{\xi}_{ef} = \begin{cases} \xi_{ef} & \text{SU(2) spinor} \\ \xi^{\pm}_{ef} & \text{SU(1,1) spinor} \end{cases}$

- Half-edge action S_{vef} for spacelike face (EPRL model + Hnybida-Conrady extension model):

$$S_{vef} = j_f \left\{ 2 \ln \left[\left(m_{ef} \langle \tilde{\xi}_{ef}, Z_{vef} \rangle \right)^{\frac{\kappa_{vef} + \epsilon_e}{2}} \left(m_{ef} \langle Z_{vef}, \tilde{\xi}_{ef} \rangle \right)^{\frac{-\kappa_{vef} + \epsilon_e}{2}} \right] + \left(\iota \gamma \kappa_{vef} - \epsilon_e \right) \ln \left[m_{ef} \langle Z_{vef}, Z_{vef} \rangle \right] \right\}, \qquad Z_{vef} = g^{\mathrm{T}}_{ve} z_{vf} \tag{1}$$

- Half-edge action S_{vef} for timelike face (Hnybida-Conrady extension model):

$$S_{vef} = j_f \left[2 \ln \left(\sqrt{\frac{\langle l^{+}_{ef}, Z_{vef} \rangle}{\langle Z_{vef}, l^{+}_{ef} \rangle}} \right)^{\kappa_{vef}} - \frac{\iota}{\gamma} \kappa_{vef} \ln \left(\langle l^{+}_{ef}, Z_{vef} \rangle \langle Z_{vef}, l^{+}_{ef} \rangle \right) \right]. \tag{2}$$

Boundary data: spins j_b (face areas), and SU(2) spinors ξ_{ef}, or SU(1,1) spinors $\xi^{\pm}_{ef}$, l^{+}_{ef} (tetrahedron face normals).

Integration variables X: $g_{ve} \in \mathrm{SL}(2,\mathbb{C})$, $z_{vf} \in \mathbb{CP}^1$ and (may include) SU(1,1) spinors $\xi^{\pm}_{ef}$, l^{+}_{ef}.

[J. Simao and S. Steinhaus, 2021], [H. Liu and M. Han, 2019], [W. Kaminski, M. Kisielowski, H. Sahlmann, 2018], [M. Han, 2013], [Barrett et al, 2010]

EPRL model and Hnybida-Conrady extension model

Path integral formulation of spinfoam amplitude:

$$A(\mathscr{K}) = \sum_{\{j_h\}} \prod_h \dim(j_h) \int [\mathrm{d}X] e^{S[j_h, X]} .$$

$$S = \sum_v S_v, \qquad S_v = \sum_{(e,e')} \left(S_{vef} + S_{ve'f}\right) .$$

$$\tilde{\xi}_{ef} = \begin{cases} \xi_{ef} & \text{SU(2) spinor} \\ \xi_{ef}^{\pm} & \text{SU(1,1) spinor} \end{cases}$$

- Half-edge action S_{vef} for spacelike face (EPRL model + Hnybida-Conrady extension model):

$$S_{vef} = j_f \left\{ 2 \ln \left[\left(m_{ef} \langle \tilde{\xi}_{ef}, Z_{vef} \rangle \right)^{\frac{\kappa_{vef} + \epsilon_e}{2}} \left(m_{ef} \langle Z_{vef}, \tilde{\xi}_{ef} \rangle \right)^{\frac{-\kappa_{vef} + \epsilon_e}{2}} \right] + \left(\imath \gamma \kappa_{vef} - \epsilon_e \right) \ln \left[m_{ef} \langle Z_{vef}, Z_{vef} \rangle \right] \right\}, \qquad Z_{vef} = g_{ve}^{\mathrm{T}} z_{vf} \tag{1}$$

- Half-edge action S_{vef} for timelike face (Hnybida-Conrady extension model):

$$S_{vef} = j_f \left[2 \ln \left(\sqrt{\frac{\langle l_{ef}^{+}, Z_{vef} \rangle}{\langle Z_{vef}, l_{ef}^{+} \rangle}} \right)^{\kappa_{vef}} - \frac{\imath}{\gamma} \kappa_{vef} \ln \left(\langle l_{ef}^{+}, Z_{vef} \rangle \langle Z_{vef}, l_{ef}^{+} \rangle \right) \right] . \tag{2}$$

Boundary data: spins j_b (face areas), and SU(2) spinors ξ_{ef}, or SU(1,1) spinors $\xi_{ef}^{\pm}$, l_{ef}^{+} (tetrahedron face normals).

Integration variables X: $g_{ve} \in \mathrm{SL}(2,\mathbb{C})$, $z_{vf} \in \mathbb{CP}^1$ and (may include) SU(1,1) spinors $\xi_{ef}^{\pm}$, l_{ef}^{+}.

Path integral formulation of spinfoam amplitude is important to semi-classical analysis.

[J. Simao and S. Steinhaus, 2021], [H. Liu and M. Han, 2019], [W. Kaminski, M. Kisielowski, H. Sahlmann, 2018], [M. Han, 2013], [Barrett et al, 2010]

Outline

- Motivation
- Spinfoam overviews
- Real and complex critical point
  - Numerical algorithm of constructing boundary data and real critical point
  - Computing complex critical points
- Cosmological dynamics from spinfoam with scalar matter

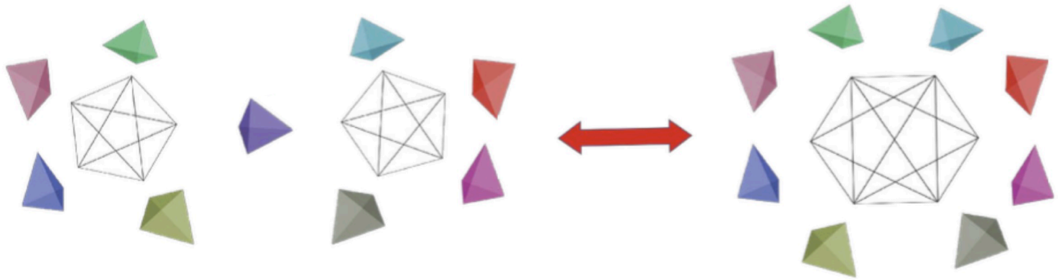

Numerical algorithm of constructing boundary data and critical point

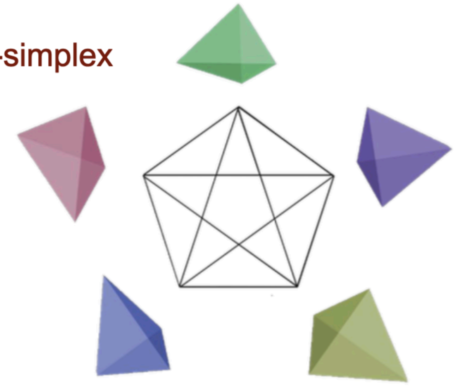

arXiv: 2404.10563

M. Han, H. Liu, DQ (2024.04)

https://github.com/dqu2017/Real-and-Complex-Critical-Points

Real critical point of vertex amplitude

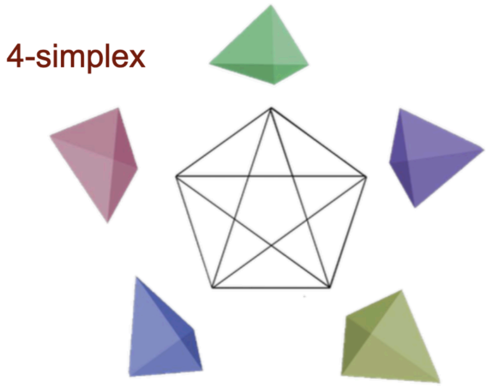

Real critical point of vertex amplitude

- To probe the large-j regime, we scale spins $j_f \to \lambda j_f$ with $\lambda \gg 1$,

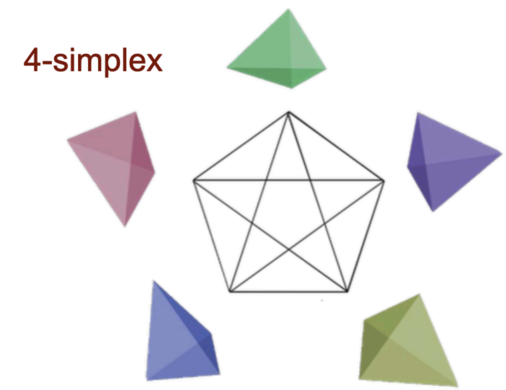

Real critical point of vertex amplitude

- To probe the large-j regime, we scale spins $j_f \to \lambda j_f$ with $\lambda \gg 1$,

$$A_v(\lambda j_f, \tilde{\xi}_{ef}, l_{ef}^{\pm}) = \int [\mathrm{d}g_{ve}\mathrm{d}z_{vf}]\, e^{\lambda S_v}\,.$$

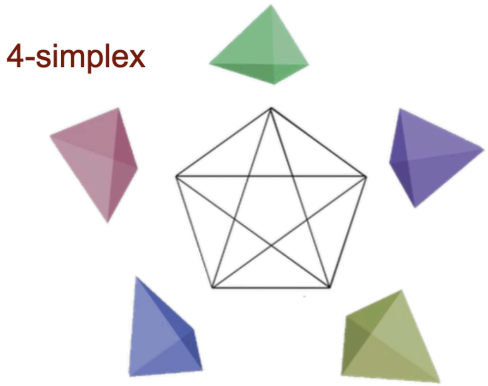

Real critical point of vertex amplitude

- To probe the large-j regime, we scale spins $j_f \to \lambda j_f$ with $\lambda \gg 1$,

$$A_v(\lambda j_f, \tilde{\xi}_{ef}, l_{ef}^{\pm}) = \int [\mathrm{d}g_{ve}\mathrm{d}z_{vf}]\, e^{\lambda S_v}\,.$$

- Applying the stationary phase approximation:

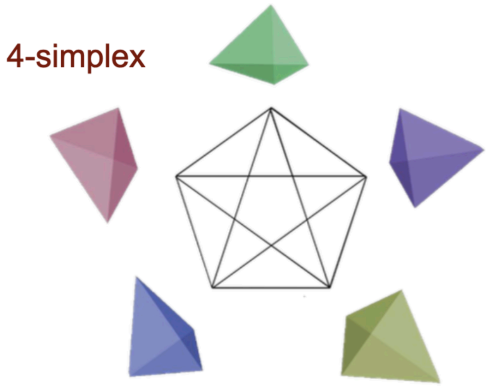

Real critical point of vertex amplitude

- To probe the large-j regime, we scale spins $j_f \to \lambda j_f$ with $\lambda \gg 1$,

$$A_v(\lambda j_f, \tilde{\xi}_{ef}, l_{ef}^{\pm}) = \int [\mathrm{d}g_{ve}\mathrm{d}z_{vf}]\, e^{\lambda S_v}\,.$$

- Applying the stationary phase approximation:

$$\delta_g S_v = \delta_z S_v = 0, \quad \mathrm{Re}(S_v) = 0.$$ The solution is called *(real) critical point.*

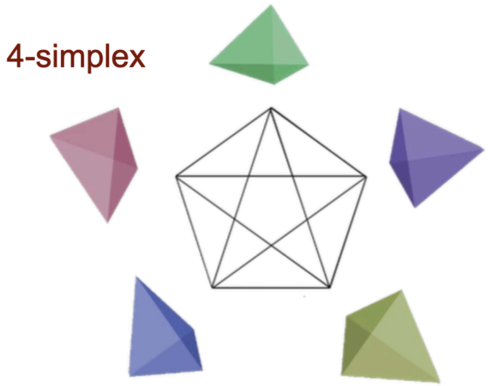

Real critical point of vertex amplitude

- To probe the large-j regime, we scale spins $j_f \to \lambda j_f$ with $\lambda \gg 1$,

$$A_v(\lambda j_f, \tilde{\xi}_{ef}, l^{\pm}_{ef}) = \int [\mathrm{d}g_{ve}\mathrm{d}z_{vf}]\, e^{\lambda S_v}.$$

- Applying the stationary phase approximation:

$$\delta_g S_v = \delta_z S_v = 0, \quad \mathrm{Re}(S_v) = 0.$$ The solution is called *(real) critical point.*

Stationary phase analysis of spinfoam: critical points $\Longrightarrow$ Discrete geometries [Barrett et al, 2010]

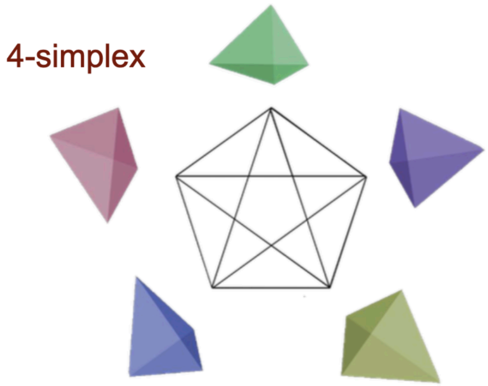

Real critical point of vertex amplitude

- To probe the large-j regime, we scale spins $j_f \to \lambda j_f$ with $\lambda \gg 1$,

$$A_v(\lambda j_f, \tilde{\xi}_{ef}, l^{\pm}_{ef}) = \int [\mathrm{d}g_{ve} \mathrm{d}z_{vf}]\, e^{\lambda S_v}.$$

- Applying the stationary phase approximation:

$$\delta_g S_v = \delta_z S_v = 0, \quad \mathrm{Re}(S_v) = 0.$$ The solution is called *(real) critical point.*

Stationary phase analysis of spinfoam: critical points $\Longrightarrow$ Discrete geometries [Barrett et al, 2010]

Practical viewpoint for physical scenario

Discrete geometries $\Longrightarrow$ boundary data and critical points

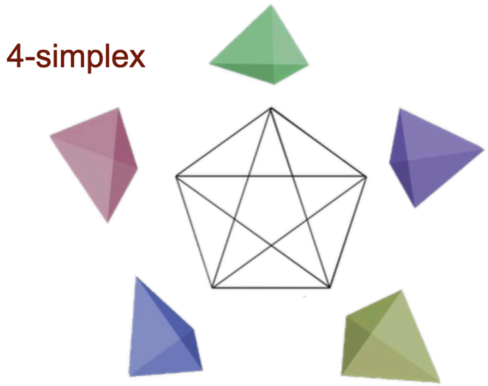

Boundary data and critical point

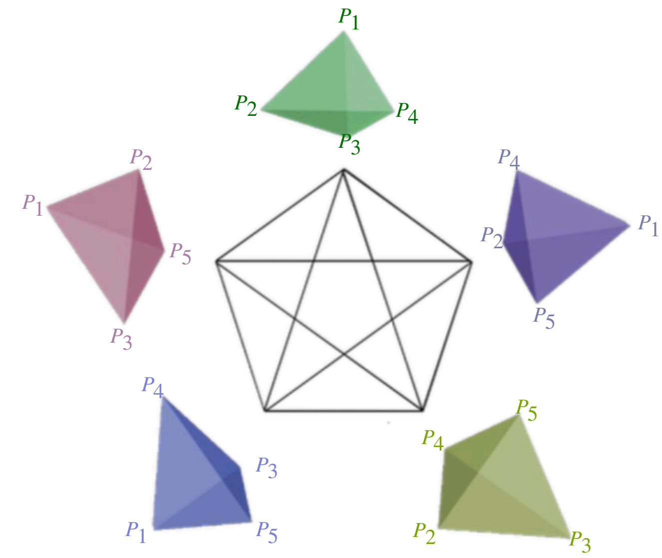

[J. Simao and S. Steinhaus, 2021] [P. Dona, M. Fanizza, G. Sarno, S. Speziale 2019], [W. Kaminski, M. Kisielowski, H. Sahlmann, 2018], [Barrett et al, 2010]

Boundary data and critical point

Start with a flat 4-simplex with 4D coordinates

Squared edge lengths: $s_{ij}^2 < 0 \rightarrow$ timelike edges;

$s_{ij}^2 > 0 \rightarrow$ spacelike edges.

$$P_1 = (0,0,0,0), \quad P_2 = (0,0,0,1), \quad P_3 = (0,0,1,1),$$
$$P_4 = (0,1,1,1), \quad P_5 = (\tfrac{1}{2},1,1,1)\,.$$
$$s_{ij}^2 = \left(1,2,3,\frac{11}{4},1,2,\frac{7}{4},1,\frac{3}{4},-\frac{1}{4}\right)$$

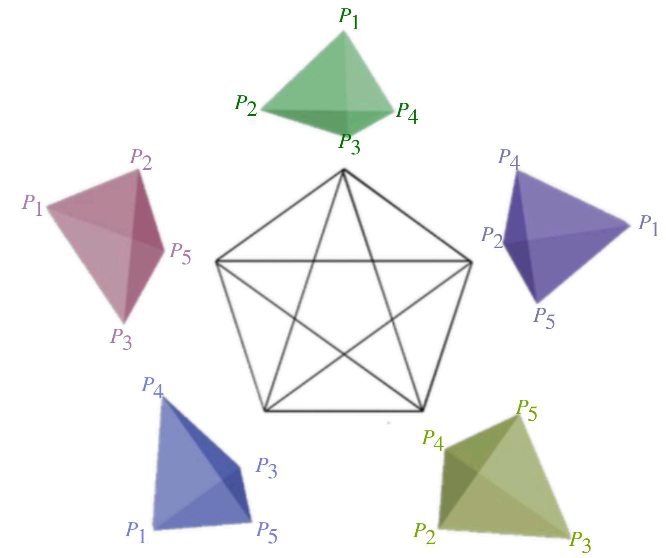

[J. Simao and S. Steinhaus, 2021] [P. Dona, M. Fanizza, G. Sarno, S. Speziale 2019], [W. Kaminski, M. Kisielowski, H. Sahlmann, 2018], [Barrett et al, 2010]

Boundary data and critical point

Start with a flat 4-simplex with 4D coordinates

Squared edge lengths: $s_{ij}^2 < 0 \rightarrow$ timelike edges;

$s_{ij}^2 > 0 \rightarrow$ spacelike edges.

4-d normal outgoing normalized vector N_{ve}

$\mathrm{sign}(e_i) < 0 \rightarrow$ spacelike tetrahedron;

$\mathrm{sign}(e_i) > 0 \rightarrow$ timelike tetrahedron.

$P_1 = (0,0,0,0), \quad P_2 = (0,0,0,1), \quad P_3 = (0,0,1,1),$

$P_4 = (0,1,1,1), \quad P_5 = (\frac{1}{2},1,1,1)\,.$

$$s_{ij}^2 = \left(1,2,3,\frac{11}{4},1,2,\frac{7}{4},1,\frac{3}{4},-\frac{1}{4}\right)$$

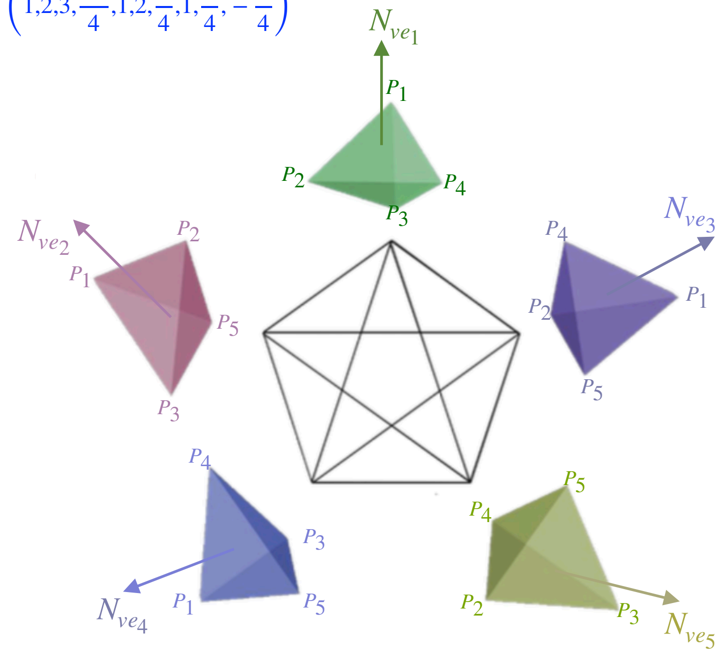

$\mathrm{sign}(e_i) = (+1, +1, -1, -1, -1)$

[J. Simao and S. Steinhaus, 2021] [P. Dona, M. Fanizza, G. Sarno, S. Speziale 2019], [W. Kaminski, M. Kisielowski, H. Sahlmann, 2018], [Barrett et al, 2010]

Boundary data and critical point

Start with a flat 4-simplex with 4D coordinates

↓ Squared edge lengths: $s_{ij}^2 < 0 \rightarrow$ timelike edges;

$s_{ij}^2 > 0 \rightarrow$ spacelike edges.

4-d normal outgoing normalized vector N_{ve}

↓ $\mathrm{sign}(e_i) < 0 \rightarrow$ spacelike tetrahedron;

$\mathrm{sign}(e_i) > 0 \rightarrow$ timelike tetrahedron.

Dihedral angles $\theta_{e,e'}$ of N_{ve} and $N_{ve'}$

↓

$P_1 = (0,0,0,0), \quad P_2 = (0,0,0,1), \quad P_3 = (0,0,1,1),$

$P_4 = (0,1,1,1), \quad P_5 = (\frac{1}{2},1,1,1).$

$s_{ij}^2 = \left(1,2,3,\frac{11}{4},1,2,\frac{7}{4},1,\frac{3}{4},-\frac{1}{4}\right)$

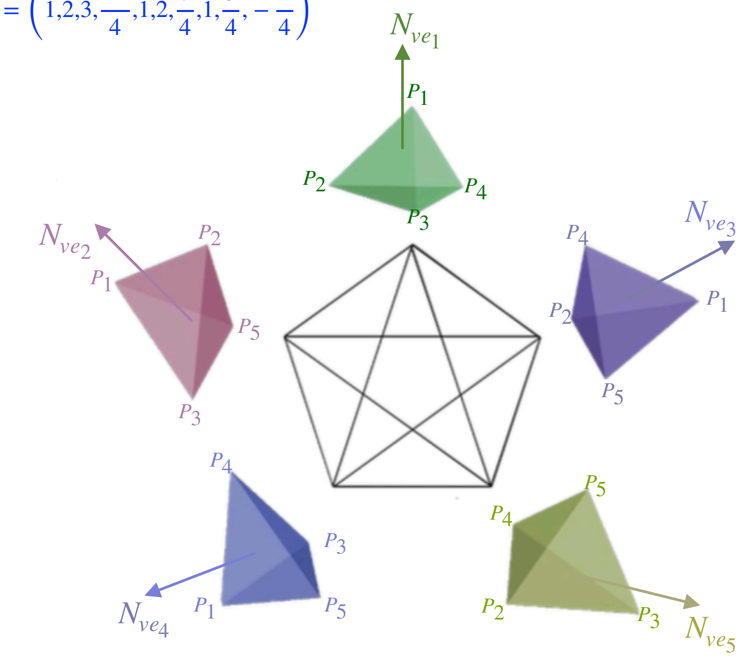

$\mathrm{sign}(e_i) = (+1, +1, -1, -1, -1)$

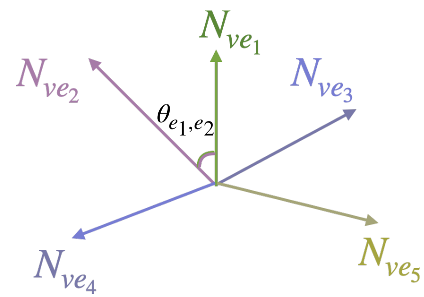

[J. Simao and S. Steinhaus, 2021] [P. Dona, M. Fanizza, G. Sarno, S. Speziale 2019], [W. Kaminski, M. Kisielowski, H. Sahlmann, 2018], [Barrett et al, 2010]

Boundary data and critical point

Start with a flat 4-simplex with 4D coordinates

↓ Squared edge lengths: $s_{ij}^2 < 0 \rightarrow$ timelike edges;
$s_{ij}^2 > 0 \rightarrow$ spacelike edges.

4-d normal outgoing normalized vector N_{ve}

↓ $\text{sign}(e_i) < 0 \rightarrow$ spacelike tetrahedron;
$\text{sign}(e_i) > 0 \rightarrow$ timelike tetrahedron.

Dihedral angles $\theta_{e,e'}$ of N_{ve} and $N_{ve'}$

↓

SO(1,3) group elements Λ_{ve} and SL(2,ℂ) solution g_{ve}

$P_1 = (0,0,0,0), \quad P_2 = (0,0,0,1), \quad P_3 = (0,0,1,1),$

$P_4 = (0,1,1,1), \quad P_5 = (\frac{1}{2},1,1,1).$

$s_{ij}^2 = \left(1,2,3,\frac{11}{4},1,2,\frac{7}{4},1,\frac{3}{4},-\frac{1}{4}\right)$

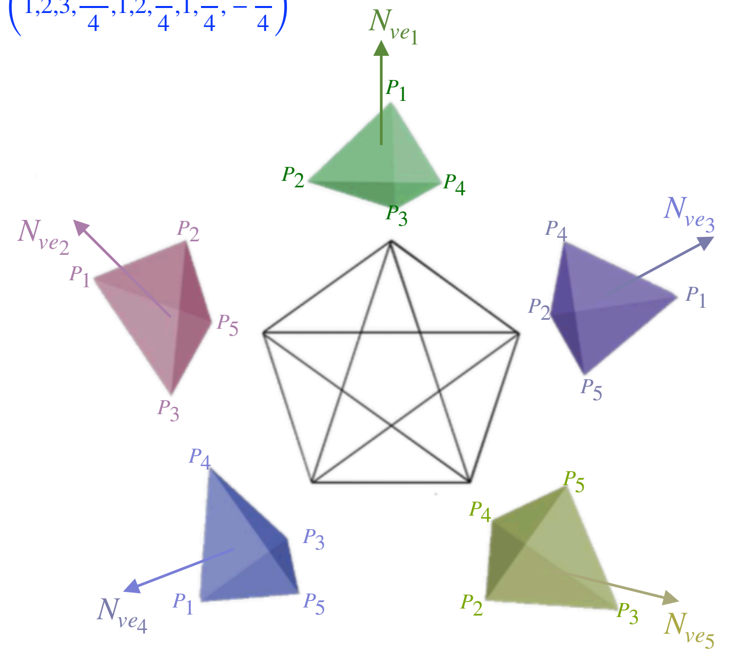

$\text{sign}(e_i) = (+1, +1, -1, -1, -1)$

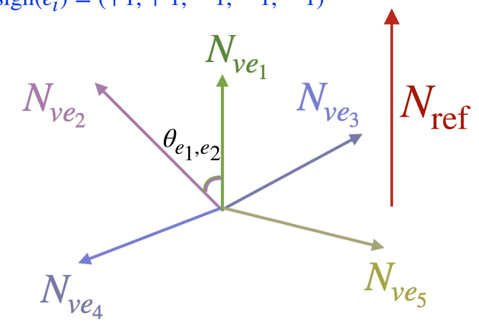

[J. Simao and S. Steinhaus, 2021] [P. Dona, M. Fanizza, G. Sarno, S. Speziale 2019], [W. Kaminski, M. Kisielowski, H. Sahlmann, 2018], [Barrett et al, 2010]

Boundary data and critical point

Start with a flat 4-simplex with 4D coordinates

↓ Squared edge lengths: $s_{ij}^2 < 0 \rightarrow$ timelike edges;

$s_{ij}^2 > 0 \rightarrow$ spacelike edges.

4-d normal outgoing normalized vector N_{ve}

↓ $\mathrm{sign}(e_i) < 0 \rightarrow$ spacelike tetrahedron;

$\mathrm{sign}(e_i) > 0 \rightarrow$ timelike tetrahedron.

Dihedral angles $\theta_{e,e'}$ of N_{ve} and $N_{ve'}$

↓

SO(1,3) group elements Λ_{ve} and SL(2,ℂ) solution g_{ve}

↓ $A_f = \begin{cases} \gamma j_f, & \text{spacelike triangle} \\ j_f, & \text{timelike triangle} \end{cases}, \quad j_f \in \mathbb{N}_0/2$ ↓

Triangle areas A_f

SU(2) or SU(1,1) spinors ξ_{ef} and $l_{ef}^{\pm}$ to each face

$P_1 = (0,0,0,0), \quad P_2 = (0,0,0,1), \quad P_3 = (0,0,1,1),$

$P_4 = (0,1,1,1), \quad P_5 = (\frac{1}{2},1,1,1).$

$s_{ij}^2 = \left(1,2,3,\frac{11}{4},1,2,\frac{7}{4},1,\frac{3}{4},-\frac{1}{4}\right)$

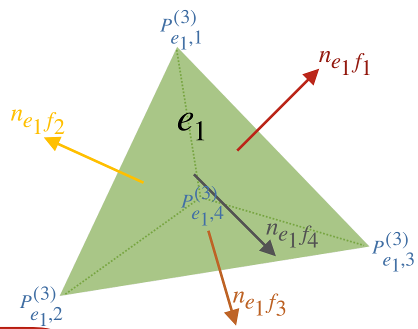

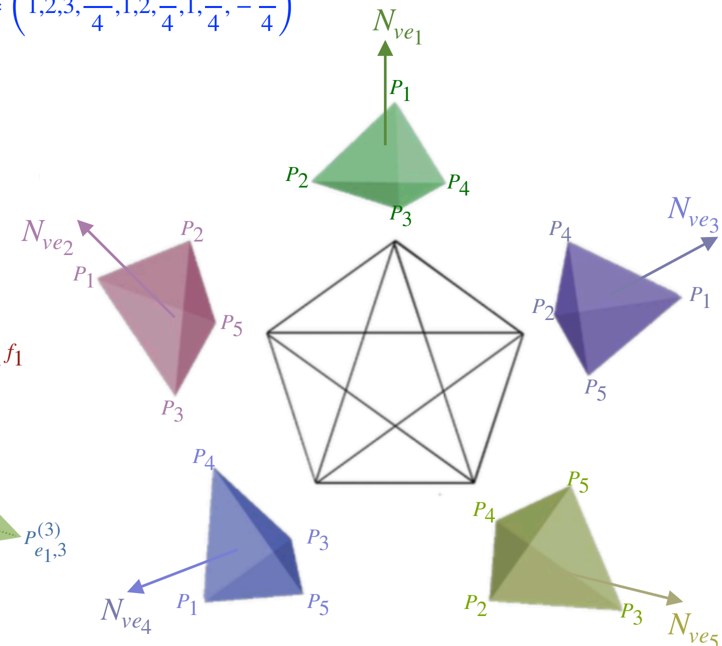

$\mathrm{sign}(e_i) = (+1,+1,-1,-1,-1)$

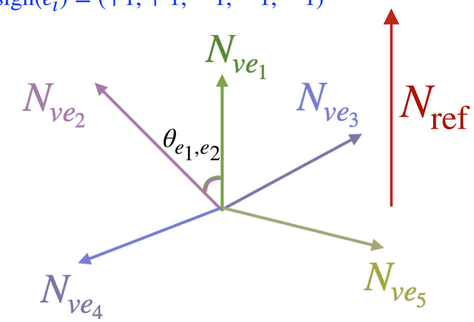

[J. Simao and S. Steinhaus, 2021] [P. Dona, M. Fanizza, G. Sarno, S. Speziale 2019], [W. Kaminski, M. Kisielowski, H. Sahlmann, 2018], [Barrett et al, 2010]

Boundary data and critical point

Start with a flat 4-simplex with 4D coordinates

↓ Squared edge lengths: $s_{ij}^2 < 0 \rightarrow$ timelike edges; $s_{ij}^2 > 0 \rightarrow$ spacelike edges.

4-d normal outgoing normalized vector N_{ve}

↓ $\mathrm{sign}(e_i) < 0 \rightarrow$ spacelike tetrahedron; $\mathrm{sign}(e_i) > 0 \rightarrow$ timelike tetrahedron.

Dihedral angles $\theta_{e,e'}$ of N_{ve} and $N_{ve'}$

↓

SO(1,3) group elements Λ_{ve} and SL(2,ℂ) solution g_{ve}

↓ $A_f = \begin{cases} \gamma j_f, & \text{spacelike triangle} \\ j_f, & \text{timelike triangle} \end{cases}, \quad j_f \in \mathbb{N}_0/2$

Triangle areas A_f

SU(2) or SU(1,1) spinors ξ_{ef} and $l_{ef}^{\pm}$ to each face

↓

Decide triangle orientations $\kappa_{ef} = \pm 1$

$P_1 = (0,0,0,0), \quad P_2 = (0,0,0,1), \quad P_3 = (0,0,1,1),$

$P_4 = (0,1,1,1), \quad P_5 = (\frac{1}{2},1,1,1).$

$s_{ij}^2 = \left(1,2,3,\frac{11}{4},1,2,\frac{7}{4},1,\frac{3}{4},-\frac{1}{4}\right)$

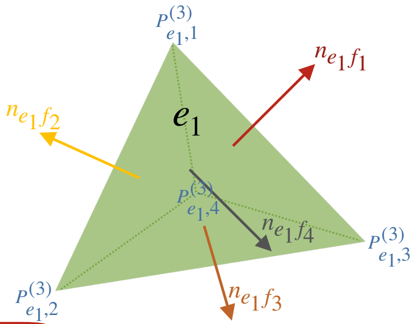

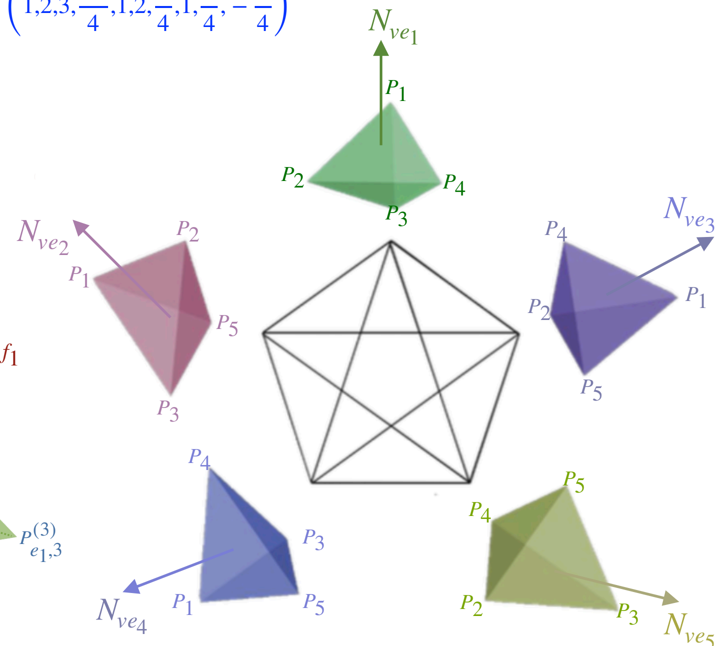

$\mathrm{sign}(e_i) = (+1,+1,-1,-1,-1)$

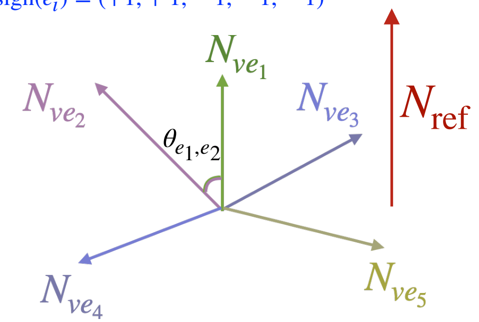

[J. Simao and S. Steinhaus, 2021] [P. Dona, M. Fanizza, G. Sarno, S. Speziale 2019], [W. Kaminski, M. Kisielowski, H. Sahlmann, 2018], [Barrett et al, 2010]

Boundary data and critical point

Start with a flat 4-simplex with 4D coordinates

↓ Squared edge lengths: $s_{ij}^2 < 0 \rightarrow$ timelike edges;

$s_{ij}^2 > 0 \rightarrow$ spacelike edges.

4-d normal outgoing normalized vector N_{ve}

↓ $\mathrm{sign}(e_i) < 0 \rightarrow$ spacelike tetrahedron;

$\mathrm{sign}(e_i) > 0 \rightarrow$ timelike tetrahedron.

Dihedral angles $\theta_{e,e'}$ of N_{ve} and $N_{ve'}$

↓

SO(1,3) group elements Λ_{ve} and SL(2,ℂ) solution g_{ve}

$A_f = \begin{cases} \gamma j_f, & \text{spacelike triangle} \\ j_f, & \text{timelike triangle} \end{cases}, \quad j_f \in \mathbb{N}_0/2$

Triangle areas A_f

SU(2) or SU(1,1) spinors ξ_{ef} and $l_{ef}^{\pm}$ to each face

↓

Decide triangle orientations $\kappa_{ef} = \pm 1$

↓

$z_{vf} \in \mathbb{CP}^1$ up to a complex scaling

$z_{vf} \propto_{\mathbb{C}} \begin{cases} (g_{ve}^{\mathrm{T}})^{-1}\xi_{ef}, & \text{spacelike face in spacelike tetrahedron} \\ (g_{ve}^{\mathrm{T}})^{-1}\xi_{ef}^{\pm}, & \text{spacelike face in timelike tetrahedron} \\ (g_{ve}^{\mathrm{T}})^{-1}l_{ef}^{-}, & \text{timelike face in timelike tetrahedron} \end{cases}$

$P_1 = (0,0,0,0), \quad P_2 = (0,0,0,1), \quad P_3 = (0,0,1,1),$

$P_4 = (0,1,1,1), \quad P_5 = (\frac{1}{2},1,1,1).$

$s_{ij}^2 = \left(1,2,3,\frac{11}{4},1,2,\frac{7}{4},1,\frac{3}{4},-\frac{1}{4}\right)$

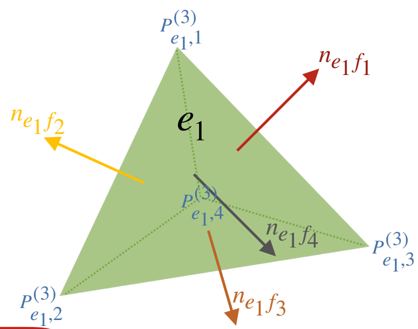

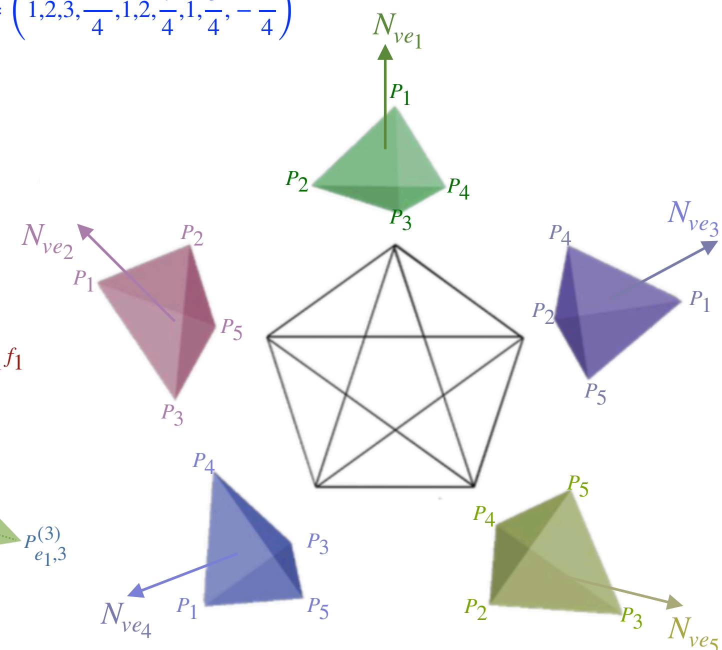

$\mathrm{sign}(e_i) = (+1,+1,-1,-1,-1)$

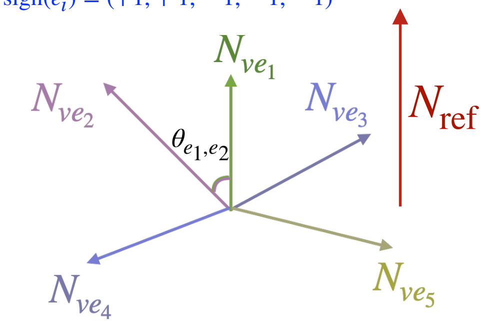

[J. Simao and S. Steinhaus, 2021] [P. Dona, M. Fanizza, G. Sarno, S. Speziale 2019], [W. Kaminski, M. Kisielowski, H. Sahlmann, 2018], [Barrett et al, 2010]

4-simplex action

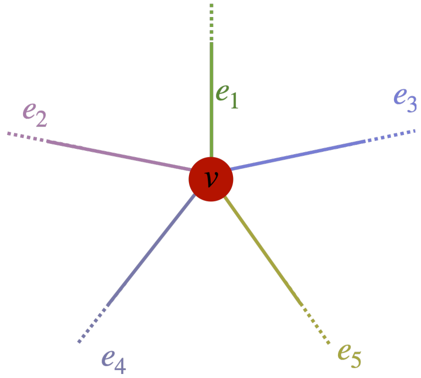

[J. Simao and S. Steinhaus, 2021], [H. Liu and M. Han, 2019], [W. Kaminski, M. Kisielowski, H. Sahlmann, 2018]

4-simplex action

From the 4-simplex geometry $\Longrightarrow$ Boundary data $(j_f, \tilde{\xi}_{ef}, l^{\pm}_{ef})$ and critical point (g^0_{ve}, z^0_{vf})

$$P_1 = (0,0,0,0), \quad P_2 = (0,0,0,1), \quad P_3 = (0,0,1,1), \quad P_4 = (0,1,1,1), \quad P_5 = (\tfrac{1}{2},1,1,1)\,.$$

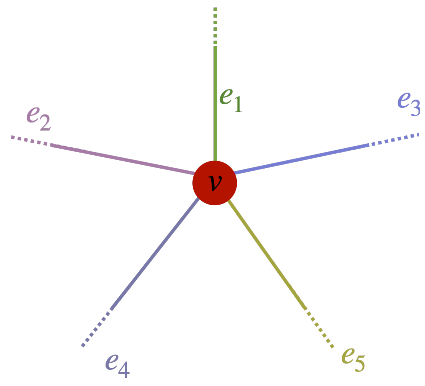

[J. Simao and S. Steinhaus, 2021], [H. Liu and M. Han, 2019], [W. Kaminski, M. Kisielowski, H. Sahlmann, 2018]

4-simplex action

From the 4-simplex geometry $\Longrightarrow$ Boundary data $(j_f, \tilde{\xi}_{ef}, l^{\pm}_{ef})$ and critical point (g^0_{ve}, z^0_{vf})

$\Downarrow$

Continuous gauge freedom in S_v and gauge fixing

$$P_1 = (0,0,0,0), \quad P_2 = (0,0,0,1), \quad P_3 = (0,0,1,1), \quad P_4 = (0,1,1,1), \quad P_5 = (\tfrac{1}{2},1,1,1)\,.$$

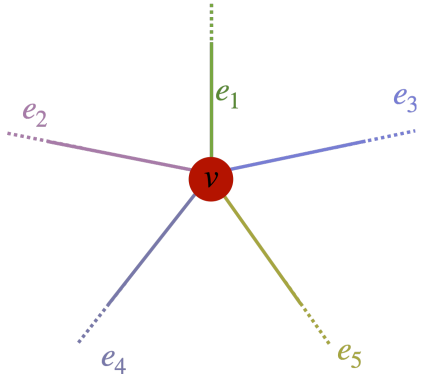

[J. Simao and S. Steinhaus, 2021], [H. Liu and M. Han, 2019], [W. Kaminski, M. Kisielowski, H. Sahlmann, 2018]

4-simplex action

From the 4-simplex geometry $\Longrightarrow$ Boundary data $(j_f, \tilde{\xi}_{ef}, l^{\pm}_{ef})$ and critical point (g^0_{ve}, z^0_{vf})

⇓

Continuous gauge freedom in S_v and gauge fixing

⇓

$$P_1 = (0,0,0,0), \quad P_2 = (0,0,0,1), \quad P_3 = (0,0,1,1),$$
$$P_4 = (0,1,1,1), \quad P_5 = (\tfrac{1}{2},1,1,1)\,.$$

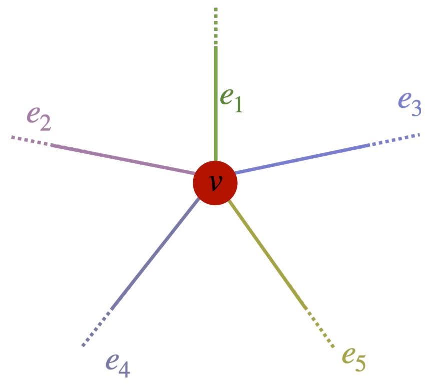

[J. Simao and S. Steinhaus, 2021], [H. Liu and M. Han, 2019], [W. Kaminski, M. Kisielowski, H. Sahlmann, 2018]

4-simplex action

From the 4-simplex geometry $\Longrightarrow$ Boundary data $(j_f, \tilde{\xi}_{ef}, l^{\pm}_{ef})$ and critical point (g^0_{ve}, z^0_{vf})

$$P_1 = (0,0,0,0), \quad P_2 = (0,0,0,1), \quad P_3 = (0,0,1,1),$$
$$P_4 = (0,1,1,1), \quad P_5 = (\tfrac{1}{2},1,1,1)\,.$$

$\Downarrow$

Continuous gauge freedom in S_v and gauge fixing

$\Downarrow$

Real parametrization of integrated variables g_{ve}, z_{vf}

$$g_{ve} = \begin{pmatrix} 1 + \frac{x^1_{ve} + i y^1_{ve}}{\sqrt{2}} & \frac{x^2_{ve} + i y^2_{ve}}{\sqrt{2}} \\ \frac{x^3_{ve} + i y^3_{ve}}{\sqrt{2}} & \mu_{ve} \end{pmatrix} \in \mathrm{SL}(2,\mathbb{C}), \qquad z_{vf} = (1, x_{vf} + i\, y_{vf}) \in \mathbb{CP}^1,$$

$\Downarrow$ $x^{(i)}_{ve}, y^{(i)}_{ve}, x_{vf}, y_{vf}$ are real numbers.

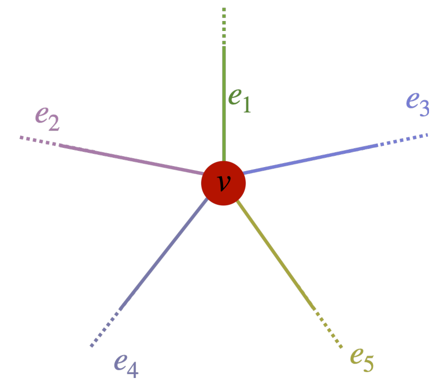

[J. Simao and S. Steinhaus, 2021], [H. Liu and M. Han, 2019], [W. Kaminski, M. Kisielowski, H. Sahlmann, 2018]

4-simplex action

From the 4-simplex geometry $\Longrightarrow$ Boundary data $(j_f, \tilde{\xi}_{ef}, l^{\pm}_{ef})$ and critical point (g^0_{ve}, z^0_{vf})

$P_1 = (0,0,0,0), \quad P_2 = (0,0,0,1), \quad P_3 = (0,0,1,1),$
$P_4 = (0,1,1,1), \quad P_5 = (\frac{1}{2},1,1,1)\,.$

$\Downarrow$

Continuous gauge freedom in S_v and gauge fixing

$\Downarrow$

Real parametrization of integrated variables g_{ve}, z_{vf}

$$g_{ve} = \begin{pmatrix} 1 + \frac{x^1_{ve} + iy^1_{ve}}{\sqrt{2}} & \frac{x^2_{ve} + iy^2_{ve}}{\sqrt{2}} \\ \frac{x^3_{ve} + iy^3_{ve}}{\sqrt{2}} & \mu_{ve} \end{pmatrix} \in \mathrm{SL}(2,\mathbb{C}), \qquad z_{vf} = (1, x_{vf} + i\, y_{vf}) \in \mathbb{CP}^1,$$

$\Downarrow$ $x^{(i)}_{ve}, y^{(i)}_{ve}, x_{vf}, y_{vf}$ are real numbers.

4-simplex action $S_v[g_{ve}, z_{vf}; j_f, \tilde{\xi}_{ef}, l^{\pm}_{ef}] = S_v(x_{ve}, y_{ve}, x_{vf}, y_{vf}),$

$S_v(x_{ve}, y_{ve}, x_{vf}, y_{vf})$ is a function of 44 real variables

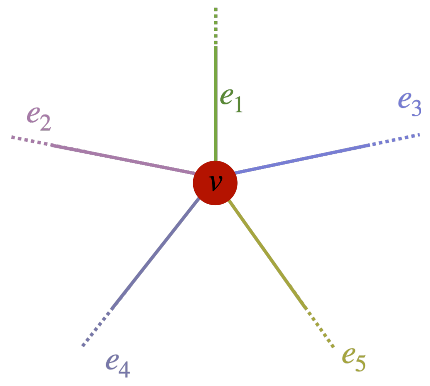

[J. Simao and S. Steinhaus, 2021], [H. Liu and M. Han, 2019], [W. Kaminski, M. Kisielowski, H. Sahlmann, 2018]

4-simplex action

From the 4-simplex geometry $\Longrightarrow$ Boundary data $(j_f, \tilde{\xi}_{ef}, l^{\pm}_{ef})$ and critical point (g^0_{ve}, z^0_{vf})

$P_1 = (0,0,0,0), \quad P_2 = (0,0,0,1), \quad P_3 = (0,0,1,1),$
$P_4 = (0,1,1,1), \quad P_5 = (\frac{1}{2},1,1,1)\,.$

$\Downarrow$

Continuous gauge freedom in S_v and gauge fixing

$\Downarrow$

Real parametrization of integrated variables g_{ve}, z_{vf}

$$g_{ve} = \begin{pmatrix} 1 + \frac{x^1_{ve} + iy^1_{ve}}{\sqrt{2}} & \frac{x^2_{ve} + iy^2_{ve}}{\sqrt{2}} \\ \frac{x^3_{ve} + iy^3_{ve}}{\sqrt{2}} & \mu_{ve} \end{pmatrix} \in \mathrm{SL}(2,\mathbb{C}), \qquad z_{vf} = (1, x_{vf} + i\, y_{vf}) \in \mathbb{CP}^1,$$

$\Downarrow$ $x^{(i)}_{ve}, y^{(i)}_{ve}, x_{vf}, y_{vf}$ are real numbers.

4-simplex action $S_v[g_{ve}, z_{vf}; j_f, \tilde{\xi}_{ef}, l^{\pm}_{ef}] = S_v(x_{ve}, y_{ve}, x_{vf}, y_{vf}),$

$S_v(x_{ve}, y_{ve}, x_{vf}, y_{vf})$ is a function of 44 real variables

https://github.com/dqu2017/Real-and-Complex-Critical-Points

```
actv = vertexaction[area, bdyxi, zvariablesall, gvariablesall, kappa, sgndet, tetn0sign, tetareasign];
actv /. crit // N // ExpandAll // Chop
```

$(0. - 0.958305\, i) - \frac{0. + 0.620279\, i}{\gamma}$

```
daction = D[actv, {variablesAll}];
(daction /. crit) // N // Expand // Chop
```

```
{0, 0, 0, 0, 0, 0, 0, 0, 0, 0, 0, 0, 0, 0, 0, 0, 0, 0, 0,
 0, 0, 0, 0, 0, 0, 0, 0, 0, 0, 0, 0, 0, 0, 0, 0, 0, 0, 0, 0, 0, 0, 0, 0, 0}
```

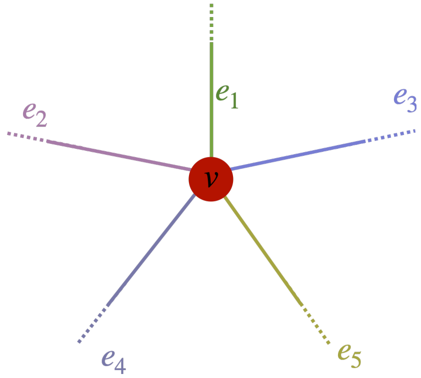

[J. Simao and S. Steinhaus, 2021], [H. Liu and M. Han, 2019], [W. Kaminski, M. Kisielowski, H. Sahlmann, 2018]

Spinfoam on a simplicial complex

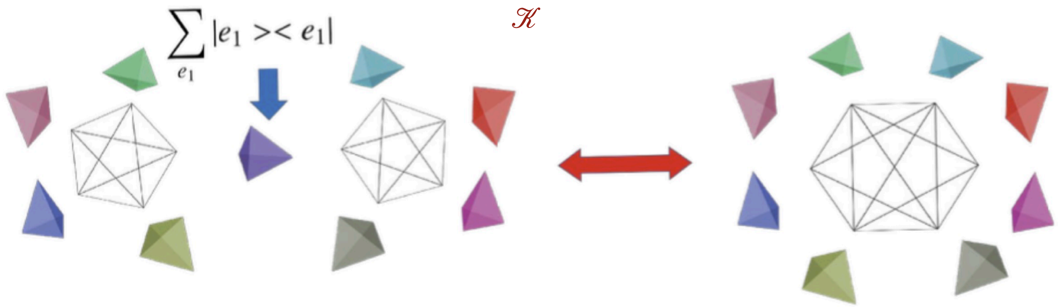

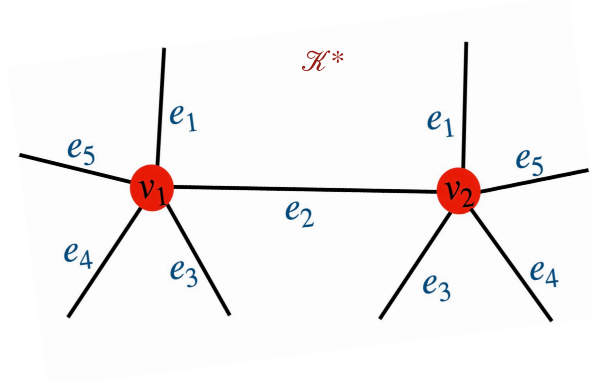

[J. Simao and S. Steinhaus, 2021], [H. Liu and M. Han, 2019], [W. Kaminski, M. Kisielowski, H. Sahlmann, 2018], [M. Han and M. Zhang, 2011], [H. Liu loops24' summer school lecture]

Spinfoam on a simplicial complex

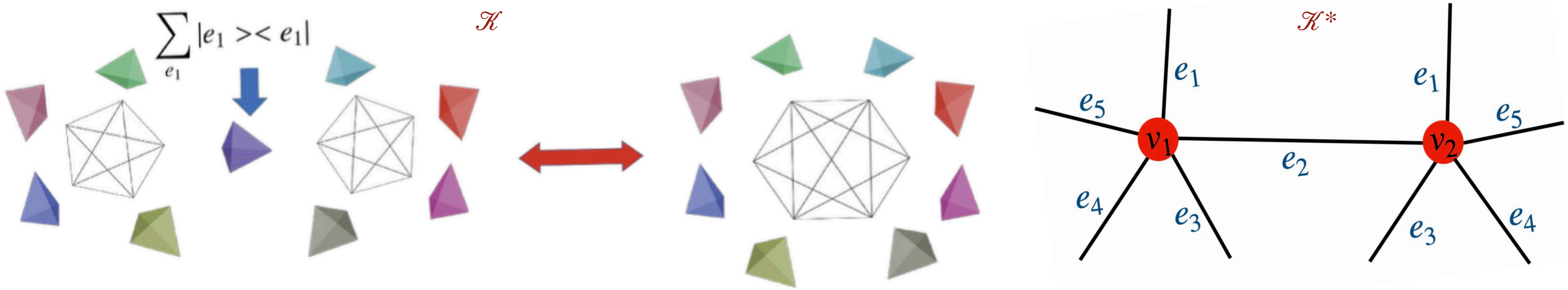

Start with 4D coordinates of each 4-simplex

$v_1: \quad P_1 = (0,0,0,0), \quad P_2 = (0,0,0,1), \quad P_3 = (0,0,1,1), \quad P_4 = (0,1,1,1), \quad P_5 = (\frac{1}{2},1,1,1)\,.$

$v_2: \quad \cdots, \quad \cdots, \quad P_{3'} = (0,1,0,1), \quad \cdots \quad \cdots\,.$

e_2 is a timelike tetrahedron

[J. Simao and S. Steinhaus, 2021], [H. Liu and M. Han, 2019], [W. Kaminski, M. Kisielowski, H. Sahlmann, 2018], [M. Han and M. Zhang, 2011], [H. Liu loops24' summer school lecture]

Spinfoam on a simplicial complex

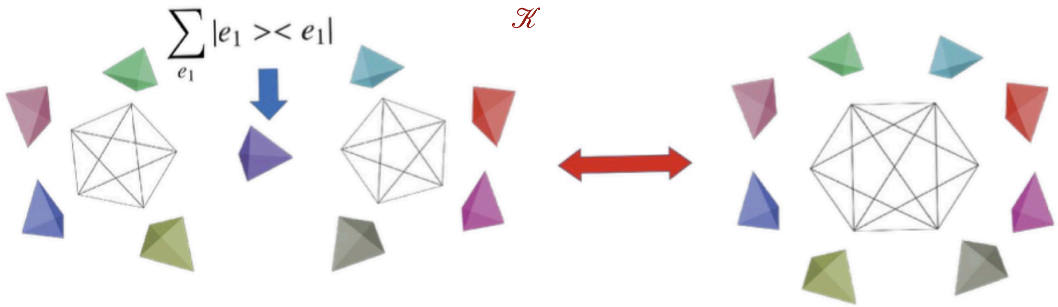

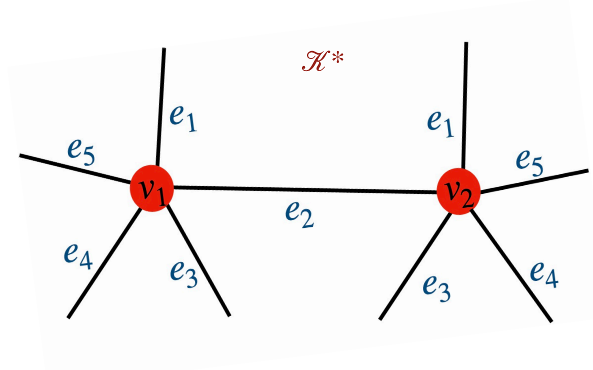

Start with 4D coordinates of each 4-simplex

v_1 : $P_1 = (0,0,0,0)$, $P_2 = (0,0,0,1)$, $P_3 = (0,0,1,1)$, $P_4 = (0,1,1,1)$, $P_5 = (\frac{1}{2},1,1,1)$.

v_2 : $\cdots$, $\cdots$, $P_{3'} = (0,1,0,1)$, $\cdots$ $\cdots$.

e_2 is a timelike tetrahedron

Repeat the 4-simplex algorithm to construct boundary data and critical point for v_1 and v_2 separately.

$(j_f, \tilde{\xi}_{ef}, l^{\pm}_{ef})$ and $(g^0_{v_1 e}, z^0_{v_1 f}, g^0_{v_2 e}, z^0_{v_2 f})$

[J. Simao and S. Steinhaus, 2021], [H. Liu and M. Han, 2019], [W. Kaminski, M. Kisielowski, H. Sahlmann, 2018], [M. Han and M. Zhang, 2011], [H. Liu loops24' summer school lecture]

Spinfoam on a simplicial complex

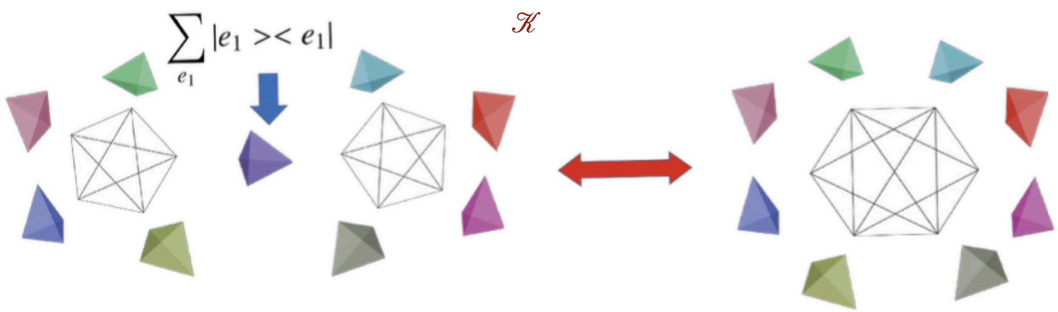

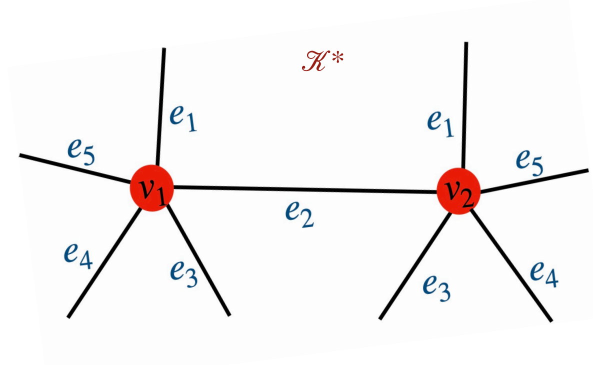

Start with 4D coordinates of each 4-simplex

$v_1: \quad P_1 = (0,0,0,0), \quad P_2 = (0,0,0,1), \quad P_3 = (0,0,1,1), \quad P_4 = (0,1,1,1), \quad P_5 = (\frac{1}{2},1,1,1)\,.$

$v_2: \quad \cdots, \quad \cdots, \quad P_{3'} = (0,1,0,1), \quad \cdots \quad \cdots\,.$

e_2 is a timelike tetrahedron

Repeat the 4-simplex algorithm to construct boundary data and critical point for v_1 and v_2 separately.

$(j_f, \tilde{\xi}_{ef}, l^{\pm}_{ef})$ and $(g^0_{v_1 e}, z^0_{v_1 f}, g^0_{v_2 e}, z^0_{v_2 f})$

Match face normals of e_2

[J. Simao and S. Steinhaus, 2021], [H. Liu and M. Han, 2019], [W. Kaminski, M. Kisielowski, H. Sahlmann, 2018], [M. Han and M. Zhang, 2011], [H. Liu loops24' summer school lecture]

Spinfoam on a simplicial complex

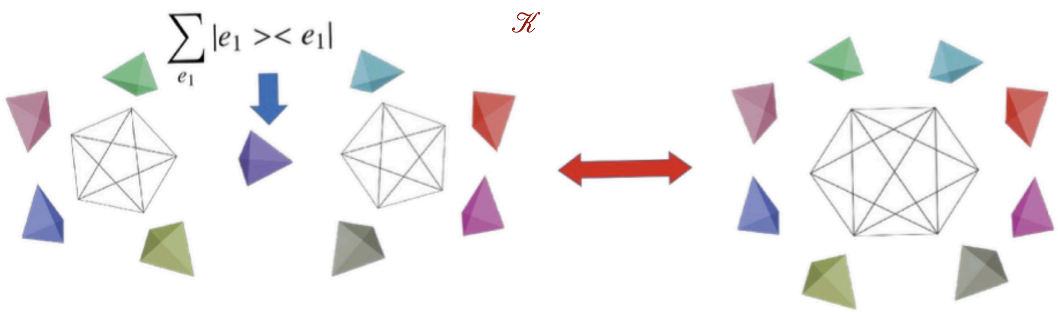

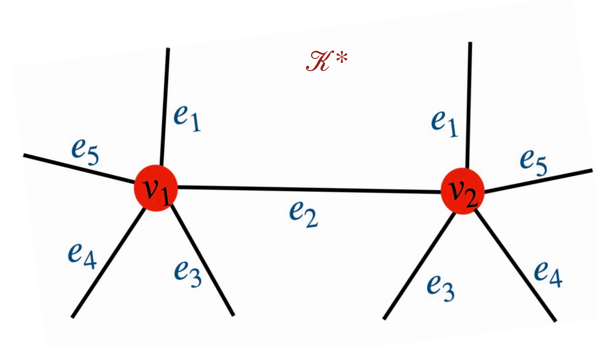

Start with 4D coordinates of each 4-simplex

$v_1: \quad P_1 = (0,0,0,0), \quad P_2 = (0,0,0,1), \quad P_3 = (0,0,1,1), \quad P_4 = (0,1,1,1), \quad P_5 = (\frac{1}{2},1,1,1)\,.$

$v_2: \quad \cdots, \quad \cdots, \quad P_{3'} = (0,1,0,1), \quad \cdots \quad \cdots\,.$

e_2 is a timelike tetrahedron

Repeat the 4-simplex algorithm to construct boundary data and critical point for v_1 and v_2 separately.

$(j_f, \tilde{\xi}_{ef}, l^{\pm}_{ef})$ and $(g^0_{v_1 e}, z^0_{v_1 f}, g^0_{v_2 e}, z^0_{v_2 f})$

Match face normals of e_2

Gauge fixings

Boundary data and critical point on the simplicial complex

[J. Simao and S. Steinhaus, 2021], [H. Liu and M. Han, 2019], [W. Kaminski, M. Kisielowski, H. Sahlmann, 2018], [M. Han and M. Zhang, 2011], [H. Liu loops24' summer school lecture]

Spinfoam on a simplicial complex

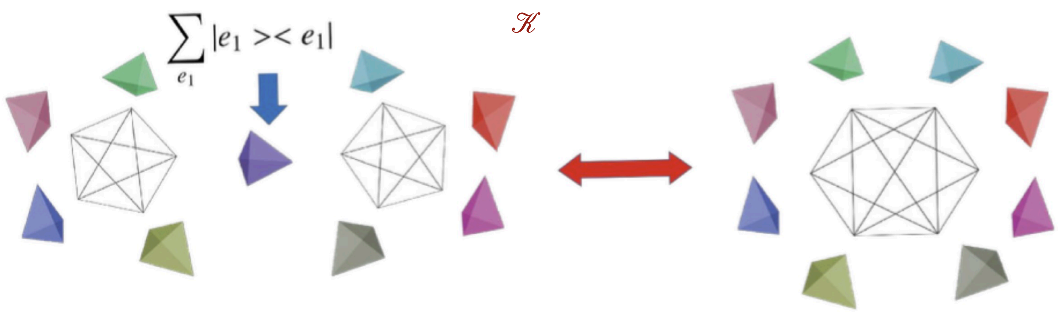

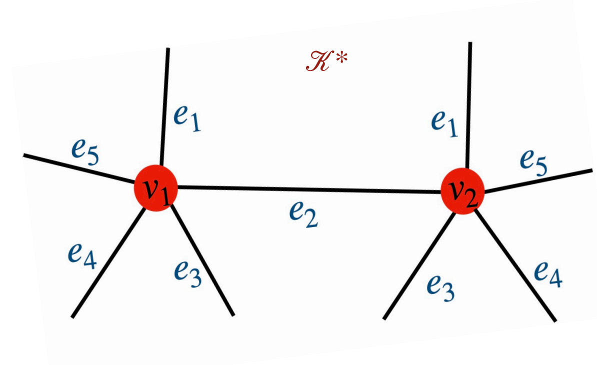

Start with 4D coordinates of each 4-simplex

$v_1: \quad P_1 = (0,0,0,0), \quad P_2 = (0,0,0,1), \quad P_3 = (0,0,1,1), \quad P_4 = (0,1,1,1), \quad P_5 = (\frac{1}{2},1,1,1)\,.$

$v_2: \quad \cdots, \quad \cdots, \quad P_{3'} = (0,1,0,1), \quad \cdots \quad \cdots\,.$

e_2 is a timelike tetrahedron

↓

Repeat the 4-simplex algorithm to construct boundary data and critical point for v_1 and v_2 separately.

↓ $(j_f, \tilde{\xi}_{ef}, l^{\pm}_{ef})$ and $(g^0_{v_1 e}, z^0_{v_1 f}, g^0_{v_2 e}, z^0_{v_2 f})$

Match face normals of e_2

↓

Gauge fixings

↓

Boundary data and critical point on the simplicial complex → Real parametrization g_{ve}, z_{vf} and $\xi^{\pm}_{eh}, l^{+}_{eh}$

[J. Simao and S. Steinhaus, 2021], [H. Liu and M. Han, 2019], [W. Kaminski, M. Kisielowski, H. Sahlmann, 2018], [M. Han and M. Zhang, 2011], [H. Liu loops24' summer school lecture]

Spinfoam on a simplicial complex

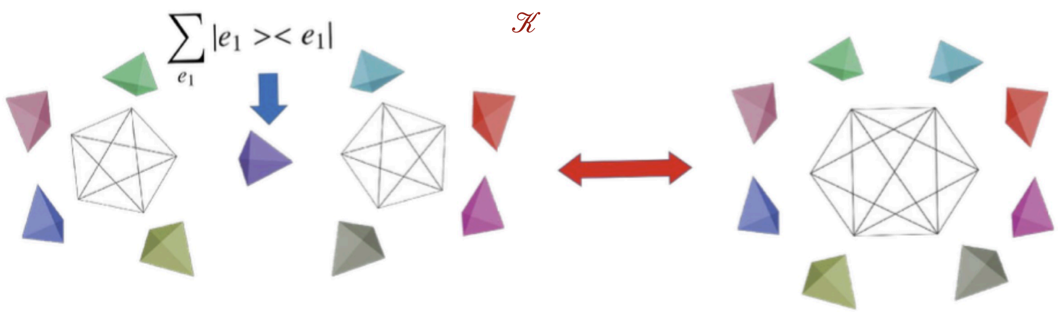

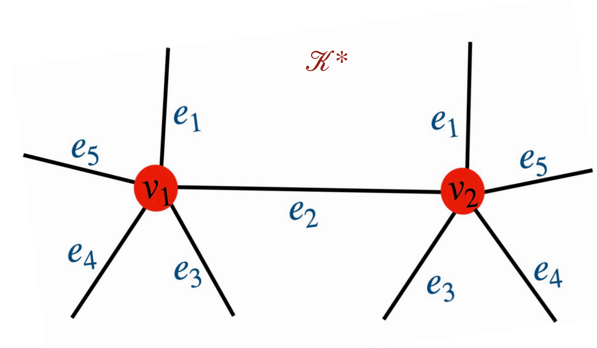

Start with 4D coordinates of each 4-simplex

$v_1: \quad P_1 = (0,0,0,0), \quad P_2 = (0,0,0,1), \quad P_3 = (0,0,1,1), \quad P_4 = (0,1,1,1), \quad P_5 = (\frac{1}{2},1,1,1)\,.$

$v_2: \quad \cdots, \quad \cdots, \quad P_{3'} = (0,1,0,1), \quad \cdots \quad \cdots\,.$

e_2 is a timelike tetrahedron

Repeat the 4-simplex algorithm to construct boundary data and critical point for v_1 and v_2 separately.

$(j_f, \xi_{ef}, l_{ef}^{\pm})$ and $(g_{v_1e}^0, z_{v_1f}^0, g_{v_2e}^0, z_{v_2f}^0)$

Match face normals of e_2

Gauge fixings

Boundary data and critical point on the simplicial complex

Real parametrization g_{ve}, z_{vf} and $\xi_{eh}^{\pm}, l_{eh}^{+}$

Spinfoam action on $\mathscr{K}$: $S[X; j_b, \xi_{eb}] = S(x_{ve}, y_{ve}, x_{vf}, y_{vf}, \theta_{eh}, \beta_{eh}, \zeta_{eh})$,

$S(x_{ve}, y_{ve}, x_{vf}, y_{vf})$ is a function of 91 real variables

[J. Simao and S. Steinhaus, 2021], [H. Liu and M. Han, 2019], [W. Kaminski, M. Kisielowski, H. Sahlmann, 2018], [M. Han and M. Zhang, 2011], [H. Liu loops24' summer school lecture]

Spinfoam on a simplicial complex

https://github.com/dqu2017/Real-and-Complex-Critical-Points

```
actionv1v3 = Refine[ActionComplex[gvariablesall, zvariablesall], Assumptions → _Symbol ∈ Reals] // Flatten // Total;
```

$$(0. + 2.82152\,i) + \frac{0. + 9.52013\,i}{\gamma}$$

```
daction = D[actionv1v3, {variablesAll}];
```

```
{0, 0, 0, 0, 0, 0, 0, 0, 0, 0, 0, 0, 0, 0, 0, 0, 0, 0, 0, 0, 0, 0,
 0, 0, 0, 0, 0, 0, 0, 0, 0, 0, 0, 0, 0, 0, 0, 0, 0, 0, 0, 0, 0, 0,
 0, 0, 0, 0, 0, 0, 0, 0, 0, 0, 0, 0, 0, 0, 0, 0, 0, 0, 0, 0, 0, 0,
 0, 0, 0, 0, 0, 0, 0, 0, 0, 0, 0, 0, 0, 0, 0, 0, 0, 0, 0, 0, 0, 0}
```

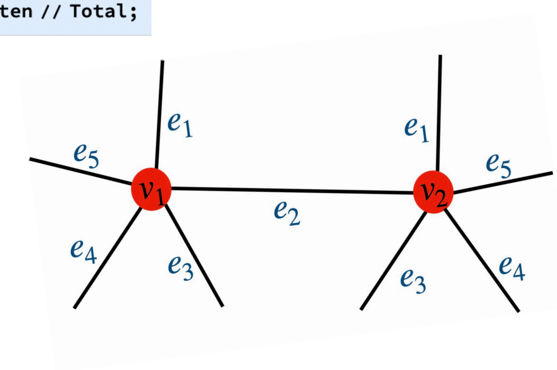

Spinfoam on a simplicial complex

https://github.com/dqu2017/Real-and-Complex-Critical-Points

```
actionv1v3 = Refine[ActionComplex[gvariablesall, zvariablesall], Assumptions → _Symbol ∈ Reals] // Flatten // Total;
```

$(0. + 2.82152\,i) + \frac{0. + 9.52013\,i}{\gamma}$

```
daction = D[actionv1v3, {variablesAll}];
```

```
{0, 0, 0, 0, 0, 0, 0, 0, 0, 0, 0, 0, 0, 0, 0, 0, 0, 0, 0, 0, 0, 0,
 0, 0, 0, 0, 0, 0, 0, 0, 0, 0, 0, 0, 0, 0, 0, 0, 0, 0, 0, 0, 0, 0,
 0, 0, 0, 0, 0, 0, 0, 0, 0, 0, 0, 0, 0, 0, 0, 0, 0, 0, 0, 0, 0, 0,
 0, 0, 0, 0, 0, 0, 0, 0, 0, 0, 0, 0, 0, 0, 0, 0, 0, 0, 0, 0, 0, 0}
```

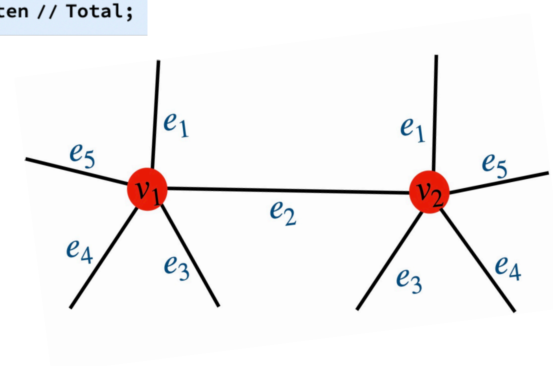

The algorithm of constructing boundary data and critical point can be generalized to *any simplicial complex*

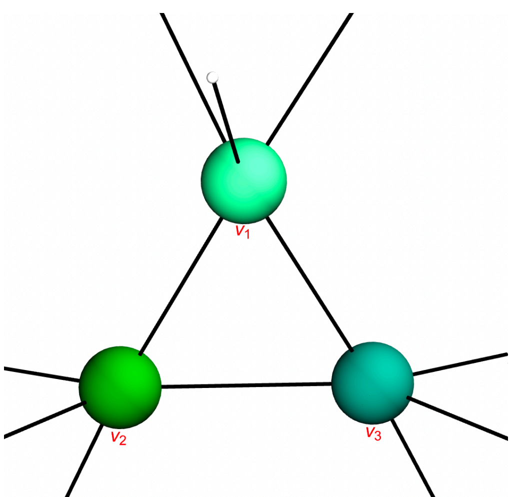

Δ_3 triangulation

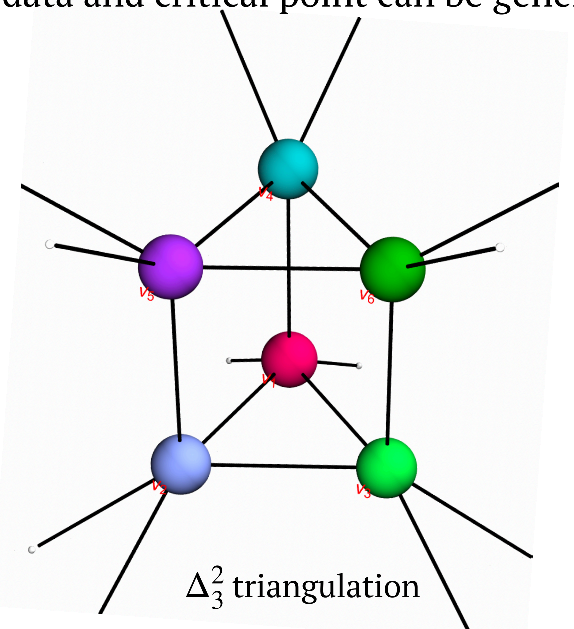

Δ_3^2 triangulation

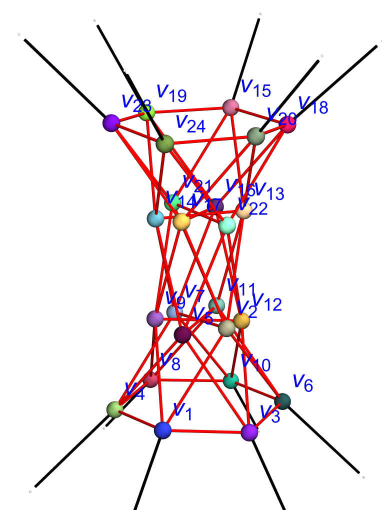

Hypercube triangulation

Outline

- Motivation
- Spinfoam overviews
- Real and complex critical point
  - Numerical algorithm of constructing boundary data and real critical point
  - Computing complex critical points
- Cosmological dynamics from spinfoam with scalar matter

Complex critical Points and Applications

arXiv: 2404.10563 (2023.01)

arXiv: 2404.10563 (2021.10)

M. Han, Z.Huang, H. Liu, DQ

Complex critical point

The full spinfoam amplitude on the simplicial $\mathscr{K}$ needs to sum over internal j:

$$A(\mathscr{K}) = \sum_{j_h} d_{j_h} \int d\mu(g, \mathbf{z})\, e^S, \quad S = \sum_h j_h F_h(g, \mathbf{z}) + \sum_b j_b F_b(g, \mathbf{z}, \xi)$$

Confusion of "***Flatness Problem***": the spin foam amplitude seems to be dominated only by ***flat*** *Regge geometries* in the large-j regime:

$$\delta_{j_h} S = 0 \Longrightarrow \text{deficit angles (discrete curvature) } \delta = 0 \text{ mod } 4\pi\mathbb{Z}/\gamma$$

[Hörmander, 1983] [Melin, Sjöstrand, 1975]

Complex critical point

The full spinfoam amplitude on the simplicial $\mathscr{K}$ needs to sum over internal j:

$$A(\mathscr{K}) = \sum_{j_h} d_{j_h} \int d\mu(g, \mathbf{z})\, e^S, \quad S = \sum_h j_h F_h(g, \mathbf{z}) + \sum_b j_b F_b(g, \mathbf{z}, \xi)$$

Confusion of "***Flatness Problem***": the spin foam amplitude seems to be dominated only by ***flat*** *Regge geometries* in the large-j regime:

$$\delta_{j_h} S = 0 \Longrightarrow \text{deficit angles (discrete curvature) } \delta = 0 \bmod 4\pi\mathbb{Z}/\gamma$$

[Hörmander, 1983] [Melin, Sjöstrand, 1975]

Complex critical point

The full spinfoam amplitude on the simplicial $\mathscr{K}$ needs to sum over internal j:

$$A(\mathscr{K}) = \sum_{j_h} d_{j_h} \int d\mu(g, \mathbf{z})\, e^{S}, \quad S = \sum_h j_h F_h(g, \mathbf{z}) + \sum_b j_b F_b(g, \mathbf{z}, \xi)$$

Confusion of "***Flatness Problem***": the spin foam amplitude seems to be dominated only by ***flat*** *Regge geometries* in the large-j regime:

$$\delta_{j_h} S = 0 \Longrightarrow \text{deficit angles (discrete curvature) } \delta = 0 \bmod 4\pi\mathbb{Z}/\gamma$$

We consider the large-λ integral:

$$\int_{\mathscr{K}} \mathrm{d}^N x\, \mu(x)\, e^{\lambda S(r,x)},$$

- $S(r, x)$ and $\mu(x)$ are analytic functions for $r \in U \subset \mathbb{R}^k, x \in K \subset \mathbb{R}^N$.
- $U \times K$ is a compact neighborhood of (r^0, x^0), x^0 is a real critical point.

[Hörmander, 1983] [Melin, Sjöstrand, 1975]

Complex critical point

The full spinfoam amplitude on the simplicial $\mathscr{K}$ needs to sum over internal j:

$$A(\mathscr{K}) = \sum_{j_h} d_{j_h} \int d\mu(g,\mathbf{z})\, e^{S}, \quad S = \sum_h j_h F_h(g,\mathbf{z}) + \sum_b j_b F_b(g,\mathbf{z},\xi)$$

Confusion of "~~***Flatness Problem***~~": the spin foam amplitude seems to be dominated only by ***flat*** *Regge geometries* in the large-j regime:

$$\delta_{j_h} S = 0 \Longrightarrow \text{deficit angles (discrete curvature) } \delta = 0 \bmod 4\pi\mathbb{Z}/\gamma$$

We consider the large-λ integral:

$$\int_{\mathscr{K}} \mathrm{d}^N x\, \mu(x)\, e^{\lambda S(r,x)},$$

- $S(r,x)$ and $\mu(x)$ are analytic functions for $r \in U \subset \mathbb{R}^k, x \in K \subset \mathbb{R}^N$.
- $U \times K$ is a compact neighborhood of (r^0, x^0), x^0 is a real critical point.

Analytic Extension: $x \to z \in \mathbb{C}^N, \quad S(r,x) \to \mathcal{S}(r,z)$

Complex critical points: $z = Z(r)$ are the solutions of the complex critical equation

$$\partial_z \mathcal{S} = 0$$

[Hörmander, 1983] [Melin, Sjöstrand, 1975]

Complex critical point

The full spinfoam amplitude on the simplicial $\mathscr{K}$ needs to sum over internal j:

$$A(\mathscr{K}) = \sum_{j_h} d_{j_h} \int d\mu(g, \mathbf{z})\, e^S, \quad S = \sum_h j_h F_h(g, \mathbf{z}) + \sum_b j_b F_b(g, \mathbf{z}, \xi)$$

Confusion of "~~***Flatness Problem***~~": the spin foam amplitude seems to be dominated only by ***flat*** *Regge geometries* in the large-j regime:

$$\delta_{j_h} S = 0 \Longrightarrow \text{deficit angles (discrete curvature) } \delta = 0 \bmod 4\pi\mathbb{Z}/\gamma$$

We consider the large-λ integral:

$$\int_{\mathscr{K}} \mathrm{d}^N x\, \mu(x)\, e^{\lambda S(r,x)},$$

- $S(r, x)$ and $\mu(x)$ are analytic functions for $r \in U \subset \mathbb{R}^k, x \in K \subset \mathbb{R}^N$.
- $U \times K$ is a compact neighborhood of (r^0, x^0), x^0 is a real critical point.

Analytic Extension: $x \to z \in \mathbb{C}^N, \quad S(r, x) \to \mathcal{S}(r, z)$

Complex critical points: $z = Z(r)$ are the solutions of the complex critical equation

$$\partial_z \mathcal{S} = 0$$

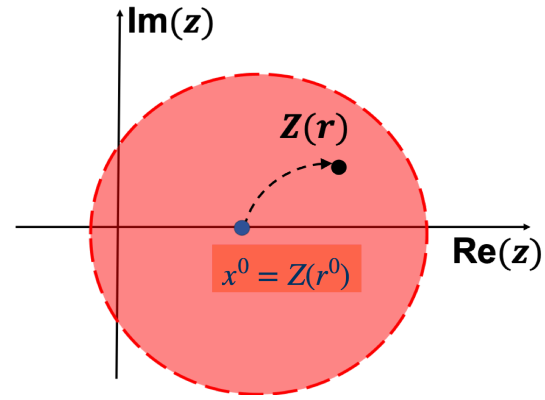

[Hörmander, 1983] [Melin, Sjöstrand, 1975]

Complex critical point

Large-λ asymptotic expansion for the integral:

$$\int_K \mathrm{d}^N x\, \mu(x) e^{\lambda S(r,x)} = \left(\frac{1}{\lambda}\right)^{\frac{N}{2}} \frac{e^{\lambda \mathcal{S}(r,Z(r))}\mu(Z(r))}{\sqrt{\det\left(-\delta^2_{z,z}\mathcal{S}(r,Z(r))/2\pi\right)}}\left[1+O(1/\lambda)\right]$$

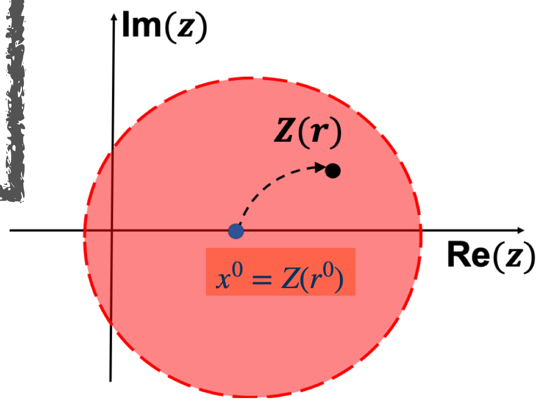

[Hörmander, 1983] [Melin, Sjöstrand, 1975]

Complex critical point

Large-λ asymptotic expansion for the integral:

$$\int_K \mathrm{d}^N x\, \mu(x) e^{\lambda S(r,x)} = \left(\frac{1}{\lambda}\right)^{\frac{N}{2}} \frac{e^{\lambda \mathcal{S}(r,Z(r))}\mu(Z(r))}{\sqrt{\det\left(-\delta^2_{z,z}\mathcal{S}(r,Z(r))/2\pi\right)}}\left[1+O(1/\lambda)\right]$$

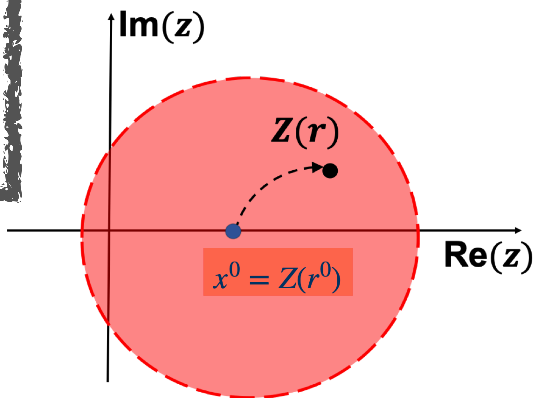

- There exists constant $C > 0$ such that

[Hörmander, 1983] [Melin, Sjöstrand, 1975]

Complex critical point

Large-λ asymptotic expansion for the integral:

$$\int_K \mathrm{d}^N x\, \mu(x) e^{\lambda S(r,x)} = \left(\frac{1}{\lambda}\right)^{\frac{N}{2}} \frac{e^{\lambda \mathcal{S}(r,Z(r))}\mu(Z(r))}{\sqrt{\det\left(-\delta^2_{z,z}\mathcal{S}(r,Z(r))/2\pi\right)}}\left[1+O(1/\lambda)\right]$$

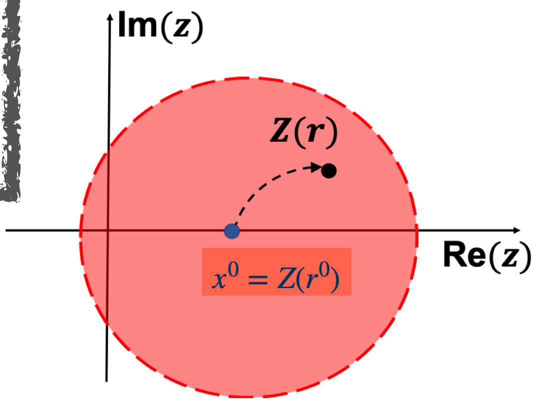

- There exists constant $C > 0$ such that

$$\mathrm{Re}(\mathcal{S}) \leq -C\,|\,\mathrm{Im}(Z)\,|^2 .$$

[Hörmander, 1983] [Melin, Sjöstrand, 1975]

Complex critical point

Large-λ asymptotic expansion for the integral:

$$\int_K \mathrm{d}^N x\, \mu(x) e^{\lambda S(r,x)} = \left(\frac{1}{\lambda}\right)^{\frac{N}{2}} \frac{e^{\lambda \mathcal{S}(r,Z(r))}\mu(Z(r))}{\sqrt{\det\left(-\delta^2_{z,z}\mathcal{S}(r,Z(r))/2\pi\right)}}\left[1+O(1/\lambda)\right]$$

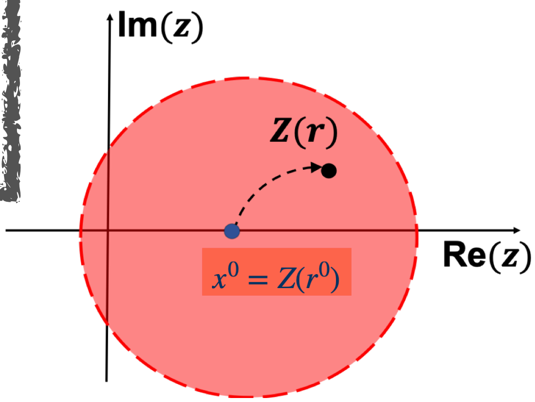

- There exists constant $C > 0$ such that

$$\mathrm{Re}(\mathcal{S}) \leq -C\,|\,\mathrm{Im}(Z)\,|^2 .$$

- Interpolating two regimes:

[Hörmander, 1983] [Melin, Sjöstrand, 1975]

Complex critical point

Large-λ asymptotic expansion for the integral:

$$\int_K \mathrm{d}^N x\, \mu(x) e^{\lambda S(r,x)} = \left(\frac{1}{\lambda}\right)^{\frac{N}{2}} \frac{e^{\lambda \mathcal{S}(r,Z(r))}\mu(Z(r))}{\sqrt{\det\left(-\delta^2_{z,z}\mathcal{S}(r,Z(r))/2\pi\right)}} \left[1 + O(1/\lambda)\right]$$

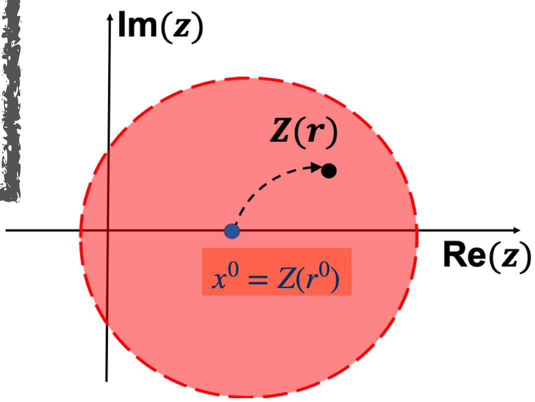

- There exists constant $C > 0$ such that

$$\mathrm{Re}(\mathcal{S}) \leq -C\,|\,\mathrm{Im}(Z)\,|^2 .$$

- Interpolating two regimes:

$$\begin{cases} r = r^0, & \mathrm{Re}(\mathcal{S}(r^0, Z(r^0)) = 0, \quad \text{oscillatory phase}\,. \\ r \neq r^0, & \mathrm{Re}(\mathcal{S}(r, Z(r)) < 0, \quad \text{exponentially decaying amplitude } e^{\lambda \mathrm{Re}(\mathcal{S})}\,. \end{cases}$$

[Hörmander, 1983] [Melin, Sjöstrand, 1975]

Complex critical point

Large-λ asymptotic expansion for the integral:

$$\int_K \mathrm{d}^N x\, \mu(x) e^{\lambda S(r,x)} = \left(\frac{1}{\lambda}\right)^{\frac{N}{2}} \frac{e^{\lambda \mathcal{S}(r,Z(r))}\mu(Z(r))}{\sqrt{\det\left(-\delta^2_{z,z}\mathcal{S}(r,Z(r))/2\pi\right)}}\left[1+O(1/\lambda)\right]$$

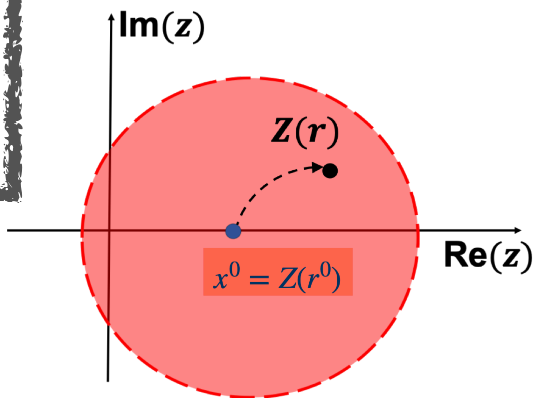

- There exists constant $C > 0$ such that

$$\mathrm{Re}(\mathcal{S}) \leq -C\,|\,\mathrm{Im}(Z)\,|^2 .$$

- Interpolating two regimes:

$$\begin{cases} r = r^0, & \mathrm{Re}(\mathcal{S}(r^0, Z(r^0)) = 0, \quad \text{oscillatory phase}. \\ r \neq r^0, & \mathrm{Re}(\mathcal{S}(r, Z(r)) < 0, \quad \text{exponentially decaying amplitude } e^{\lambda \mathrm{Re}(\mathcal{S})}. \end{cases}$$

It gives a smooth description of the asymptotics in the parameter space of r

For given λ, there always exists small Im(Z) such that Re$(\mathcal{S})$ is not small

[Hörmander, 1983] [Melin, Sjöstrand, 1975]

Complex critical point

Large-λ asymptotic expansion for the integral:

$$\int_K d^N x\, \mu(x) e^{\lambda S(r,x)} = \left(\frac{1}{\lambda}\right)^{\frac{N}{2}} \frac{e^{\lambda \mathcal{S}(r,Z(r))}\mu(Z(r))}{\sqrt{\det\left(-\delta^2_{z,z}\mathcal{S}(r,Z(r))/2\pi\right)}}\left[1+O(1/\lambda)\right]$$

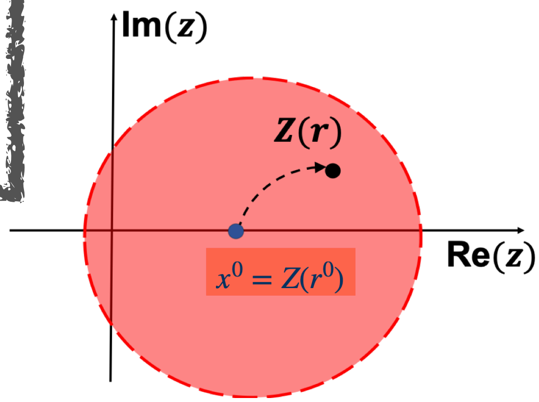

- There exists constant $C > 0$ such that

$$\mathrm{Re}(\mathcal{S}) \leq -C\,|\,\mathrm{Im}(Z)\,|^2 .$$

- Interpolating two regimes:

$$\begin{cases} r = r^0, & \mathrm{Re}(\mathcal{S}(r^0, Z(r^0))) = 0, \quad \text{oscillatory phase} . \\ r \neq r^0, & \mathrm{Re}(\mathcal{S}(r, Z(r))) < 0, \quad \text{exponentially decaying amplitude } e^{\lambda \mathrm{Re}(\mathcal{S})} . \end{cases}$$

It gives a smooth description of the asymptotics in the parameter space of r

For given λ, there always exists small Im(Z) such that Re$(\mathcal{S})$ is not small

https://github.com/dqu2017/Real-and-Complex-Critical-Points

```
GammaValue = 1 / 100;
ComplexSoln = getComplexSoln[GammaValue, Flatsoln];
```

[Hörmander, 1983] [Melin, Sjöstrand, 1975]

Complex critical point

Large-λ asymptotic expansion for the integral:

$$\int_K \mathrm{d}^N x\, \mu(x) e^{\lambda S(r,x)} = \left(\frac{1}{\lambda}\right)^{\frac{N}{2}} \frac{e^{\lambda \mathcal{S}(r,Z(r))}\mu(Z(r))}{\sqrt{\det\left(-\delta^2_{z,z}\mathcal{S}(r,Z(r))/2\pi\right)}}\left[1+O(1/\lambda)\right]$$

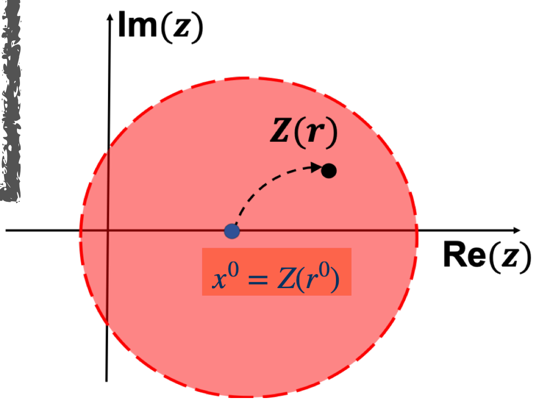

- There exists constant $C > 0$ such that

$$\mathrm{Re}(\mathcal{S}) \leq -C\,|\mathrm{Im}(Z)|^2 .$$

- Interpolating two regimes:

$$\begin{cases} r = r^0, & \mathrm{Re}(\mathcal{S}(r^0, Z(r^0)) = 0, \quad \text{oscillatory phase} . \\ r \neq r^0, & \mathrm{Re}(\mathcal{S}(r, Z(r)) < 0, \quad \text{exponentially decaying amplitude } e^{\lambda \mathrm{Re}(\mathcal{S})} . \end{cases}$$

It gives a smooth description of the asymptotics in the parameter space of r

For given λ, there always exists small Im(Z) such that Re$(\mathcal{S})$ is not small

https://github.com/dqu2017/Real-and-Complex-Critical-Points

```
GammaValue = 1 / 100;
ComplexSoln = getComplexSoln[GammaValue, Flatsoln];
```

[Hörmander, 1983] [Melin, Sjöstrand, 1975]

Complex critical point

Large-λ asymptotic expansion for the integral:

$$\int_K \mathrm{d}^N x\, \mu(x) e^{\lambda S(r,x)} = \left(\frac{1}{\lambda}\right)^{\frac{N}{2}} \frac{e^{\lambda \mathcal{S}(r,Z(r))}\mu(Z(r))}{\sqrt{\det\left(-\delta^2_{z,z}\mathcal{S}(r,Z(r))/2\pi\right)}}\left[1+O(1/\lambda)\right]$$

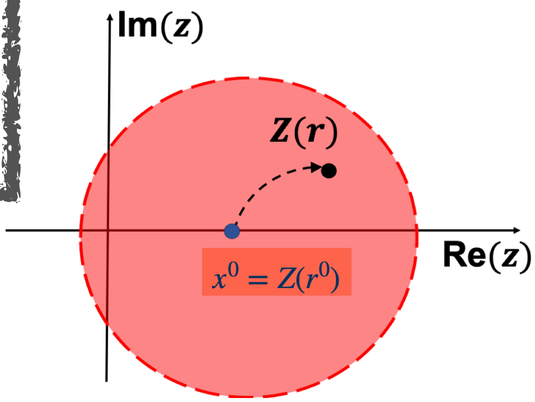

- There exists constant $C > 0$ such that

$$\mathrm{Re}(\mathcal{S}) \leq -C\,|\,\mathrm{Im}(Z)\,|^2 .$$

- Interpolating two regimes:

$$\begin{cases} r = r^0, & \mathrm{Re}(\mathcal{S}(r^0, Z(r^0)) = 0, \quad \text{oscillatory phase} . \\ r \neq r^0, & \mathrm{Re}(\mathcal{S}(r, Z(r)) < 0, \quad \text{exponentially decaying amplitude } e^{\lambda \mathrm{Re}(\mathcal{S})} . \end{cases}$$

It gives a smooth description of the asymptotics in the parameter space of r

For given λ, there always exists small Im(Z) such that Re$(\mathcal{S})$ is not small

https://github.com/dqu2017/Real-and-Complex-Critical-Points

```
GammaValue = 1 / 100;
ComplexSoln = getComplexSoln[GammaValue, Flatsoln];
```

```
actionDelta3 /. γ → GammaValue /. ComplexSoln // ExpandAll
```

```
-1.41654 × 10^-8 + 1276.02 i
```

[Hörmander, 1983] [Melin, Sjöstrand, 1975]

Applications: 4-simplex and Δ_3 triangulation

- For boundary data $r = r^0 = \{j_f, \xi_{eb}\}$ of Lorentzian Regge geometry (tetrahedra are glued with shape matching): 2 solutions and 2 oscillatory phases in the asymptotic: $A_v \simeq \lambda^{-12}\left(N_+ e^{i\lambda S_{Regge}} + N_- e^{-i\lambda S_{Regge}}\right)$.

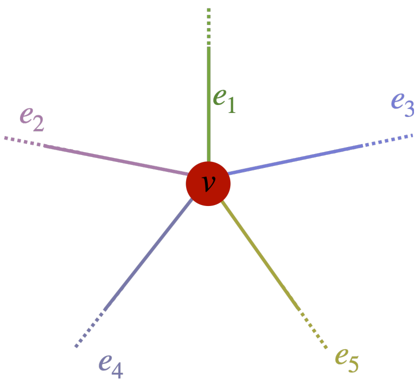

- For $r \neq r^0$, it leads to no solutions, and A_v will be exponentially suppressed.

Applications: 4-simplex and Δ_3 triangulation

- For boundary data $r = r^0 = \{j_f, \xi_{eb}\}$ of Lorentzian Regge geometry (tetrahedra are glued with shape matching): 2 solutions and 2 oscillatory phases in the asymptotic: $A_v \simeq \lambda^{-12}\left(N_+ e^{i\lambda S_{Regge}} + N\_e^{-i\lambda S_{Regge}}\right)$.

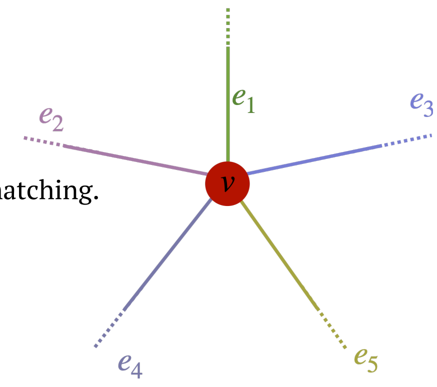

- For $r \neq r^0$, it leads to no solutions, and A_v will be exponentially suppressed.

δz_4 is the deviation from shape matching: $\delta z_4 \neq 0$, tetrahedra are glued with only area-matching but without shape-matching.

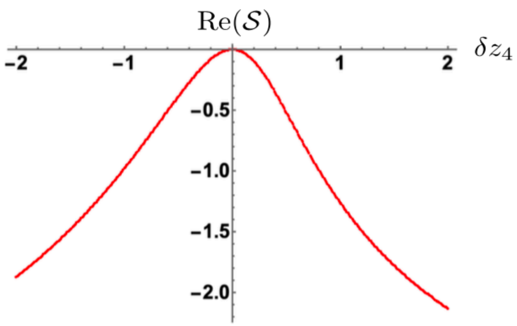

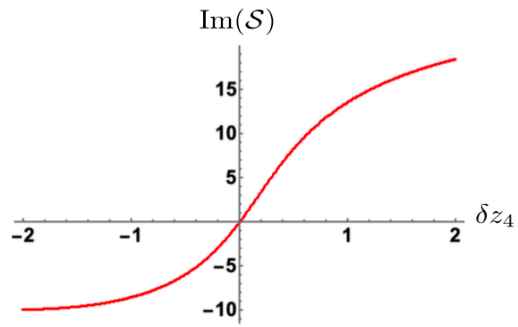

For any given λ, there exists small deformation, such that the amplitude is not suppressed.

Applications: 4-simplex and Δ_3 triangulation

- For boundary data $r = r^0 = \{j_f, \xi_{eb}\}$ of Lorentzian Regge geometry (tetrahedra are glued with shape matching): 2 solutions and 2 oscillatory phases in the asymptotic: $A_v \simeq \lambda^{-12}\left(N_+ e^{i\lambda S_{Regge}} + N\_e^{-i\lambda S_{Regge}}\right)$.

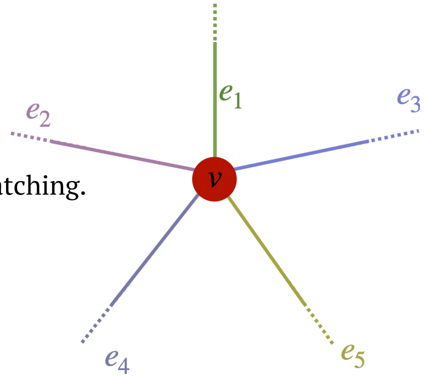

- For $r \neq r^0$, it leads to no solutions, and A_v will be exponentially suppressed.

δz_4 is the deviation from shape matching: $\delta z_4 \neq 0$, tetrahedra are glued with only area-matching but without shape-matching.

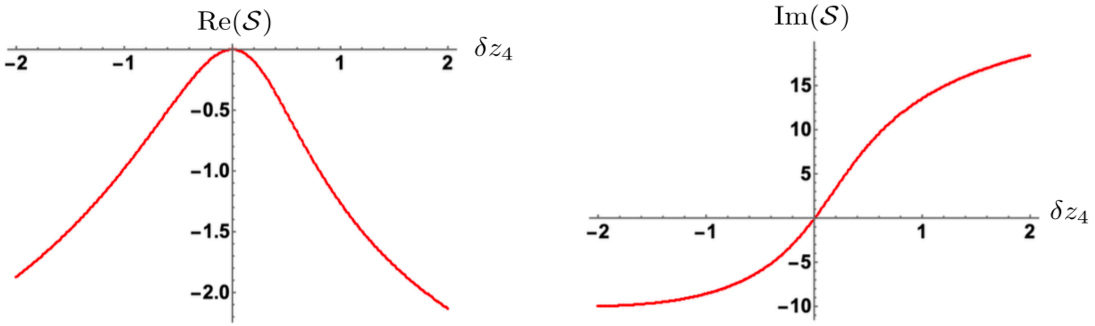

For any given λ, there exists small deformation, such that the amplitude is not suppressed.

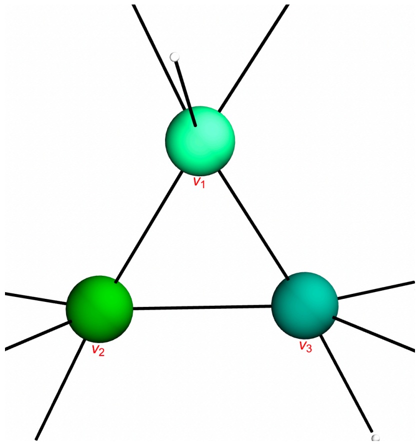

Applications: 4-simplex and Δ_3 triangulation

- For boundary data $r = r^0 = \{j_f, \xi_{eb}\}$ of Lorentzian Regge geometry (tetrahedra are glued with shape matching): 2 solutions and 2 oscillatory phases in the asymptotic: $A_v \simeq \lambda^{-12}\left(N_+ e^{i\lambda S_{Regge}} + N_- e^{-i\lambda S_{Regge}}\right).$

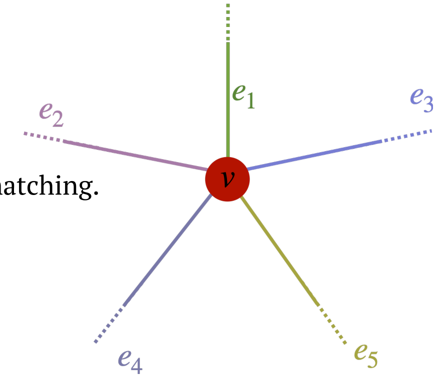

- For $r \neq r^0$, it leads to no solutions, and A_v will be exponentially suppressed.

δz_4 is the deviation from shape matching: $\delta z_4 \neq 0$, tetrahedra are glued with only area-matching but without shape-matching.

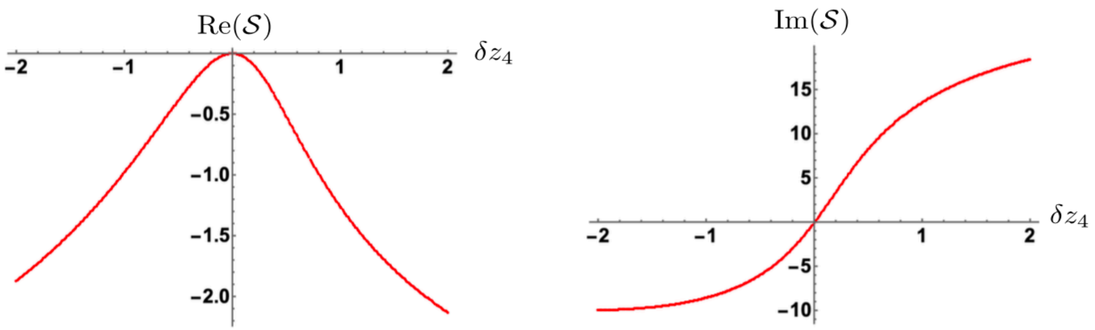

For any given λ, there exists small deformation, such that the amplitude is not suppressed.

Flatness problem:

- For the boundary data corresponds to a flat Regge geometry, there is a real critical point and the amplitude gives an oscillatory phase.
- For the boundary data corresponds to a curved Regge geometry, there is no real critical points and the amplitude is exponentially suppressed.

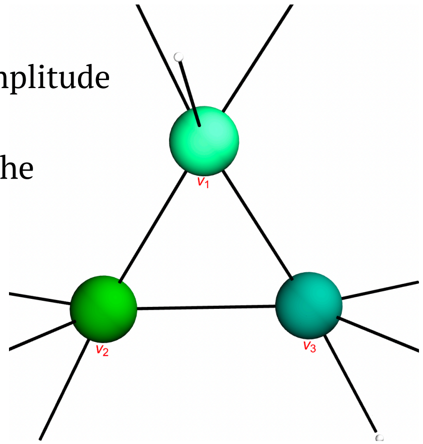

Applications: 4-simplex and Δ_3 triangulation

- For boundary data $r = r^0 = \{j_f, \xi_{eb}\}$ of Lorentzian Regge geometry (tetrahedra are glued with shape matching): 2 solutions and 2 oscillatory phases in the asymptotic: $A_v \simeq \lambda^{-12}\left(N_+ e^{i\lambda S_{Regge}} + N_- e^{-i\lambda S_{Regge}}\right).$

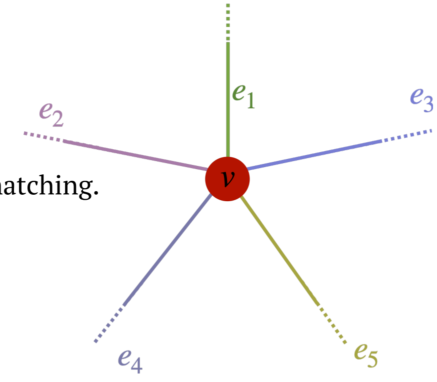

- For $r \neq r^0$, it leads to no solutions, and A_v will be exponentially suppressed.

δz_4 is the deviation from shape matching: $\delta z_4 \neq 0$, tetrahedra are glued with only area-matching but without shape-matching.

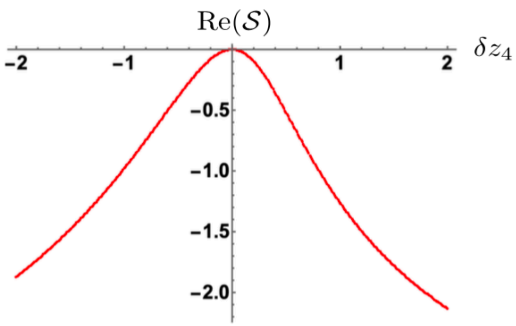

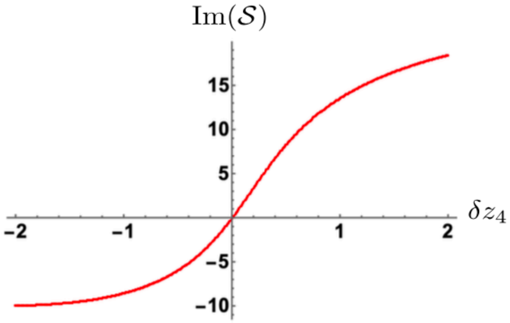

For any given λ, there exists small deformation, such that the amplitude is not suppressed.

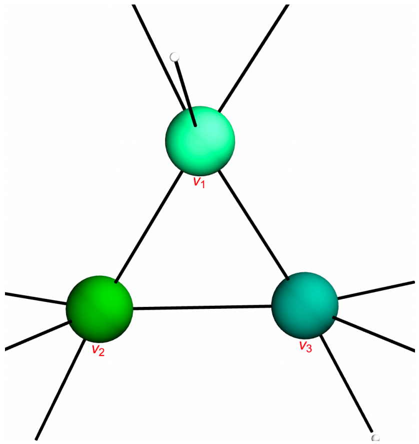

Applications: 4-simplex and Δ_3 triangulation

- For boundary data $r = r^0 = \{j_f, \xi_{eb}\}$ of Lorentzian Regge geometry (tetrahedra are glued with shape matching): 2 solutions and 2 oscillatory phases in the asymptotic: $A_v \simeq \lambda^{-12}\left(N_+ e^{i\lambda S_{Regge}} + N\_e^{-i\lambda S_{Regge}}\right)$.

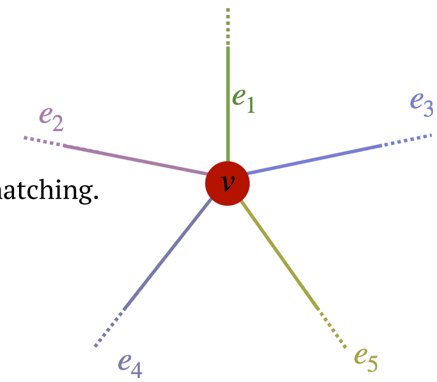

- For $r \neq r^0$, it leads to no solutions, and A_v will be exponentially suppressed.

δz_4 is the deviation from shape matching: $\delta z_4 \neq 0$, tetrahedra are glued with only area-matching but without shape-matching.

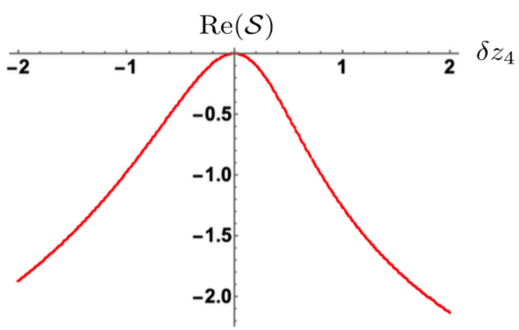

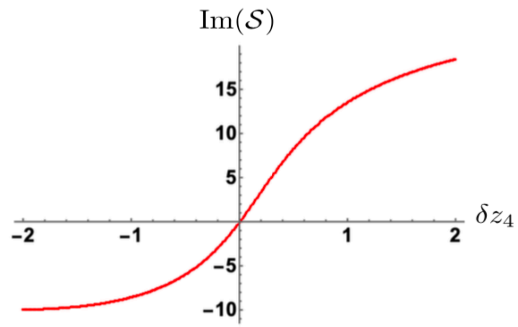

For any given λ, there exists small deformation, such that the amplitude is not suppressed.

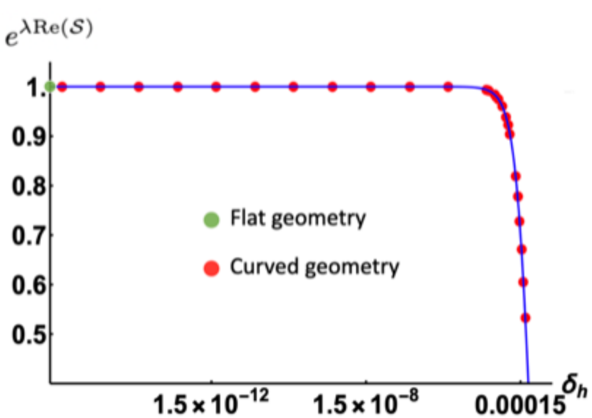

- Real critical point $\Longleftrightarrow$ Flat geometry
- Complex critical point $\Longleftrightarrow$ Curved geometry

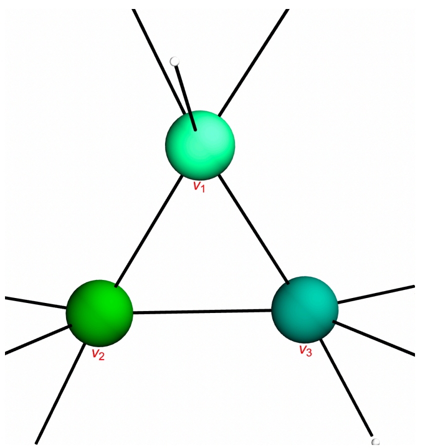

Applications: Δ_3^2 triangulation

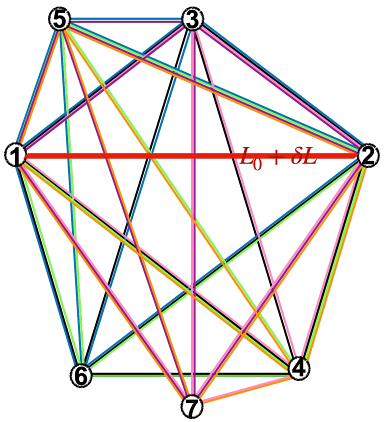

- Δ_3 triangulation has no internal edge: trivial Regge dynamics
- 1 internal edges $l_{12} = L_0 + \delta L$ on double-Δ_3 triangulation: non-trivial Regge dynamics.
- The spinfoam amplitude and the splitting j-variables:

$$A(\mathscr{K}) = \int \mathrm{d}j_{h_o} \mathcal{Z}_{\mathscr{K}}\left(j_{h_o}\right), \quad \mathcal{Z}_{\mathscr{K}}\left(j_{h_o}\right) = \int \prod_{\bar{h}} \mathrm{d}j_{\bar{h}} \prod_{h} \left(2\lambda\, d_{\lambda j_h}\right) \int [\mathrm{d}g\, \mathrm{d}\mathbf{z}] e^{\lambda S}.$$

$$\mathcal{Z}_{\mathscr{K}}\left(j_{h_o}\right) \sim e^{\lambda \mathcal{S}\left(j_{h_o}\right)}$$ Effective action

- changing variable $j_{h_o} \to l_{12} : A(\mathscr{K}) \sim \int \mathrm{d}l_{12}\, e^{\lambda \mathcal{S}(l_{12})}$, similar to path integral of Regge

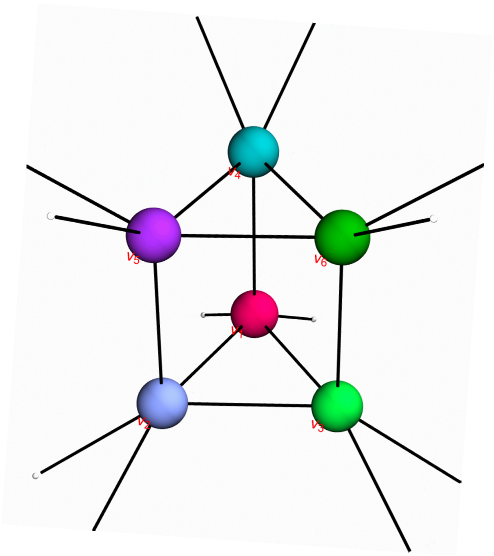

Applications: Δ_3^2 triangulation

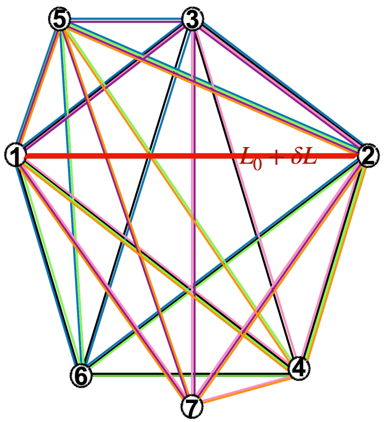

- Δ_3 triangulation has no internal edge: trivial Regge dynamics
- 1 internal edges $l_{12} = L_0 + \delta L$ on double-Δ_3 triangulation: non-trivial Regge dynamics.
- The spinfoam amplitude and the splitting j-variables:

$$A(\mathscr{K}) = \int \mathrm{d}j_{h_o} \mathcal{Z}_{\mathscr{K}}\left(j_{h_o}\right), \quad \mathcal{Z}_{\mathscr{K}}\left(j_{h_o}\right) = \int \prod_{\bar{h}} \mathrm{d}j_{\bar{h}} \prod_{h} \left(2\lambda\, d_{\lambda j_h}\right) \int [\mathrm{d}g\, \mathrm{d}\mathbf{z}] e^{\lambda S}.$$

$$\mathcal{Z}_{\mathscr{K}}\left(j_{h_o}\right) \sim e^{\lambda \mathcal{S}\left(j_{h_o}\right)}$$ Effective action

- changing variable $j_{h_o} \to l_{12} : A(\mathscr{K}) \sim \int \mathrm{d}l_{12}\, e^{\lambda \mathcal{S}(l_{12})}$, similar to path integral of Regge

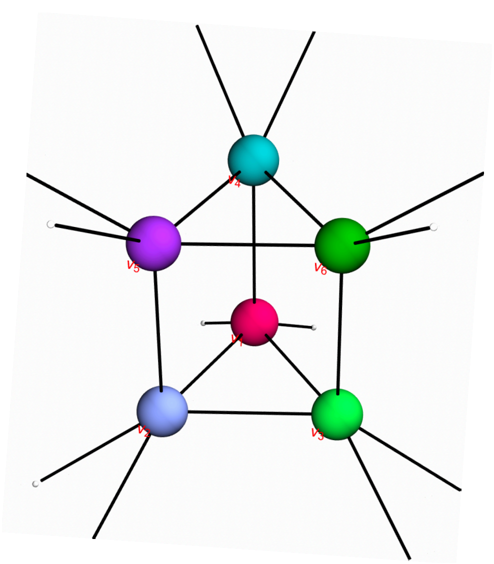

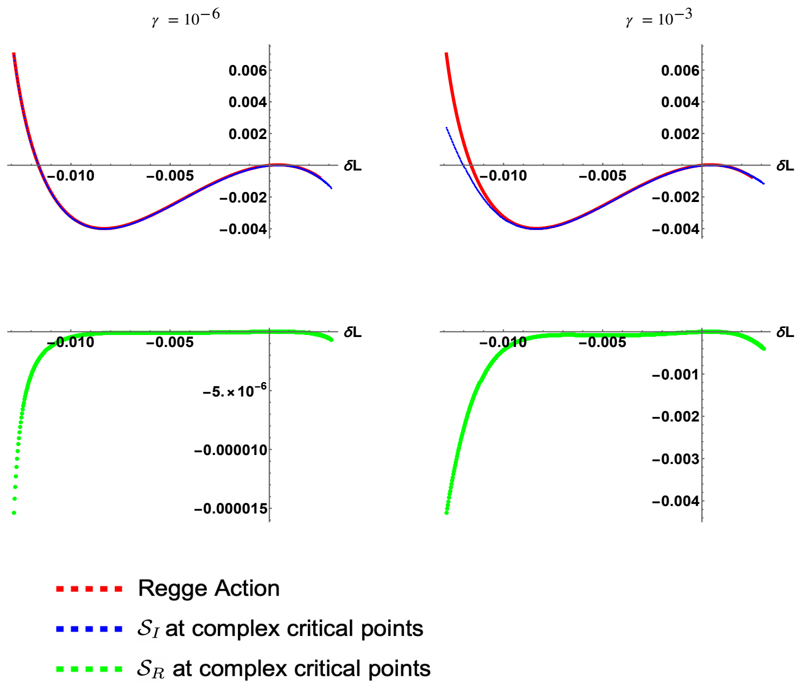

Regge dynamics is reproduced for small γ, and gets corrections for finite γ

Outline

- Motivation
- Spinfoam overviews
- Real and complex critical point
  - Numerical algorithm of constructing boundary data and real critical point
  - Computing complex critical points
- Cosmological dynamics from spinfoam with scalar matter

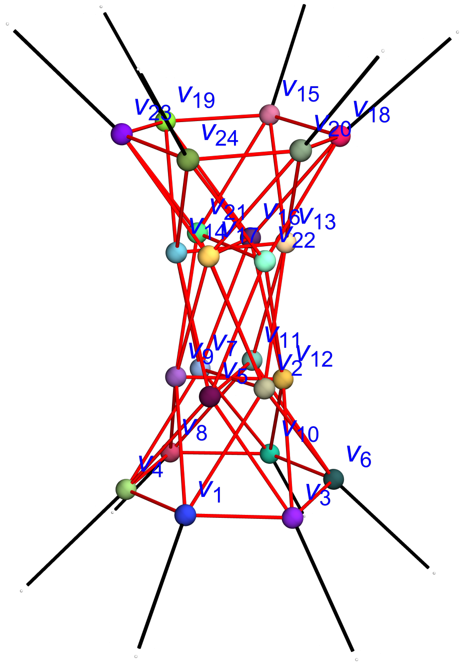

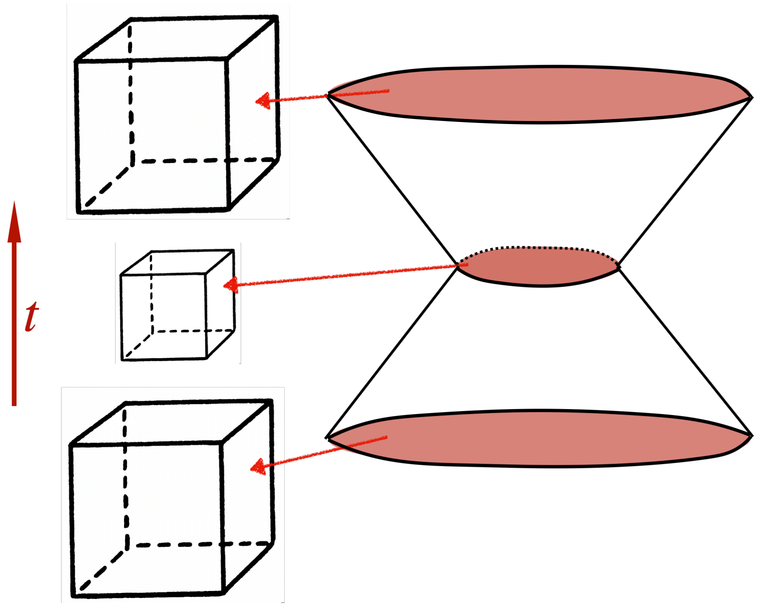

Cosmological Dynamics from Covariant Loop Quantum Gravity with Scalar Matter

arXiv: 2402.07984 (2024.02)

M. Han, H. Liu, F. Vidotto, DQ and C. Zhang

Hypercube complex

A hypercube consists of 24 4-simplices: $(v_1, v_2, \cdots, v_{24})$.

- Flat hypercube: $a_f = a_i$.
- Curved hypercube: $a_f = a_i - 2\delta a, \quad \delta a \neq 0$

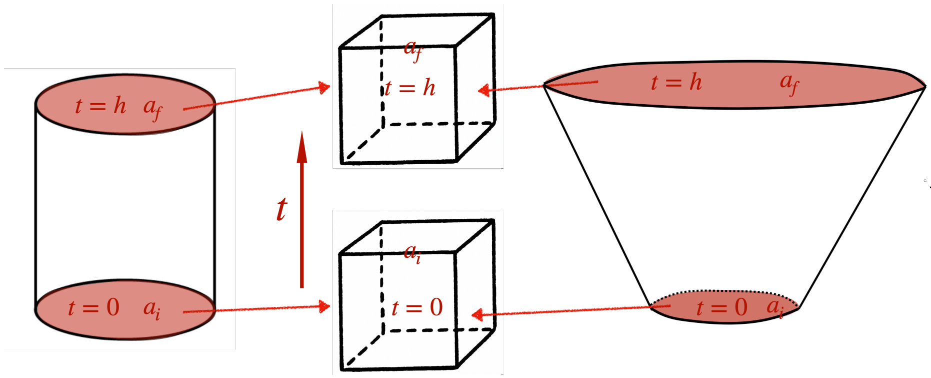

Periodic boundary condition

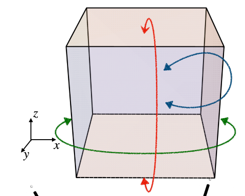

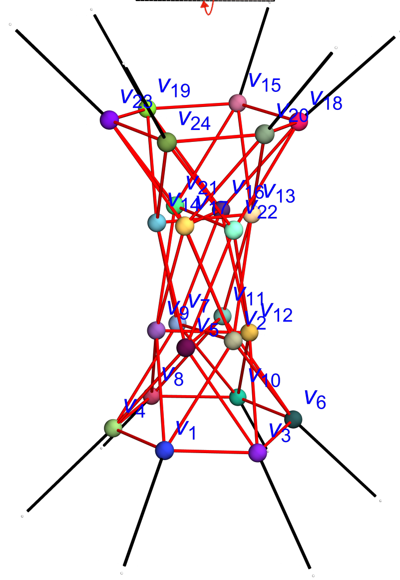

Hypercube complex

A hypercube consists of 24 4-simplices: $(v_1, v_2, \cdots, v_{24})$.

- Flat hypercube: $a_f = a_i$.
- Curved hypercube: $a_f = a_i - 2\delta a, \quad \delta a \neq 0$

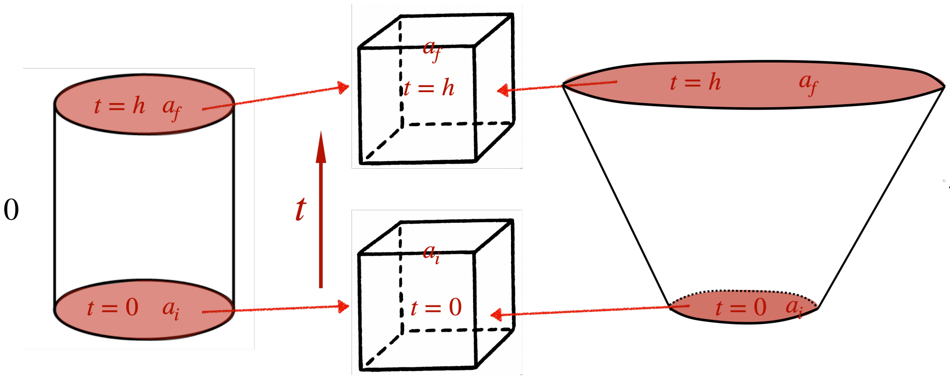

Periodic boundary condition

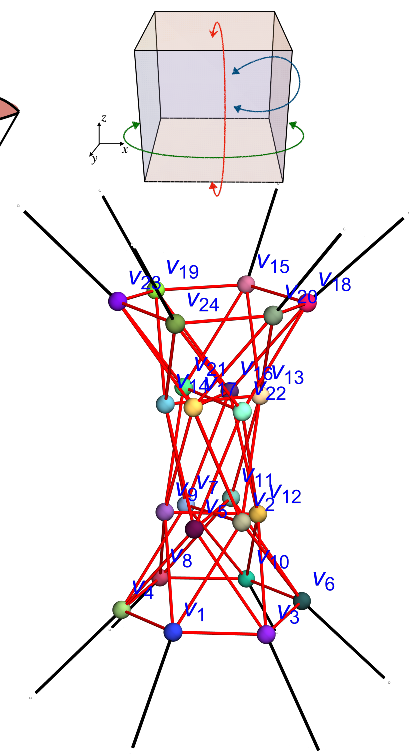

- The spinfoam action with a coherent spin-network boundary state is

Extrinsic curvature

$$S_{\mathrm{SF}} = S[j_h, X; j_b, \xi_{eb}] + \left[i \sum_{b_f} \gamma \vartheta^0_{b_f} \left(j_{b_f} - j^0_{b_f} \right) - i \sum_{b_i} \gamma \vartheta^0_{b_i} \left(j_{b_i} - j^0_{b_i} \right) - \sum_b \frac{1}{2 j^0_b} \left(j_b - j^0_b \right)^2 \right].$$

- The scalar field action with the coherent state as the boundary state

$$S_{\mathrm{Scalar}}(\boldsymbol{g}, \varphi_v; \phi_{v_{b_{i(f)}}}, \pi_{v_{b_{i(f)}}}) = \frac{i}{2} \sum_{b_{vv'}} \rho_{vv'} \left(\varphi_v - \varphi_{v'} \right)^2 + \frac{1}{4\hbar} \sum_{v_{b_i}} \left(z^2_{v_{b_i}} - 2 \left(\varphi_{v_{b_i}} - z_{v_{b_i}} \right)^2 - z_{v_{b_i}} \bar{z}_{v_{b_i}} \right) + \frac{1}{4\hbar} \sum_{v_{b_f}} \left(\bar{z}^2_{v_{b_f}} - 2 \left(\varphi_{v_{b_f}} - \bar{z}_{v_{b_f}} \right)^2 - z_{v_{b_f}} \bar{z}_{v_{b_f}} \right)$$

where the initial and final scalar data are $z_{v_{b_i}} = \phi_{v_{b_i}} + i \pi_{v_{b_i}}, \quad z_{v_{b_f}} = \phi_{v_{b_f}} + i \pi_{v_{b_f}}$.

Hypercube complex

A hypercube consists of 24 4-simplices: $(v_1, v_2, \cdots, v_{24})$.

- Flat hypercube: $a_f = a_i$.
- Curved hypercube: $a_f = a_i - 2\delta a, \quad \delta a \neq 0$

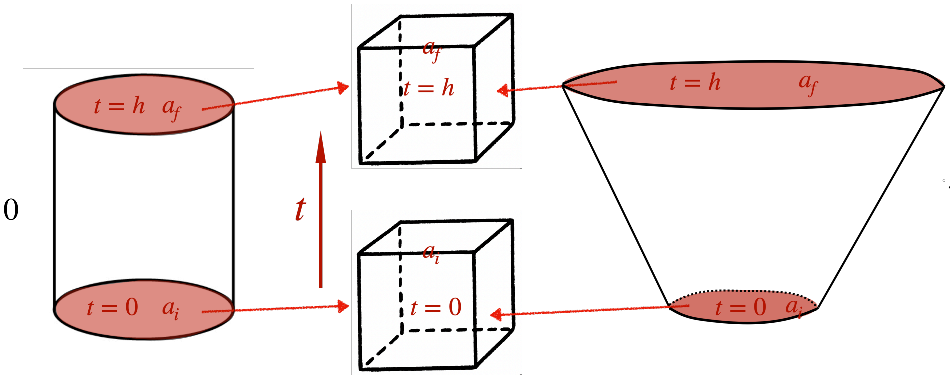

Periodic boundary condition

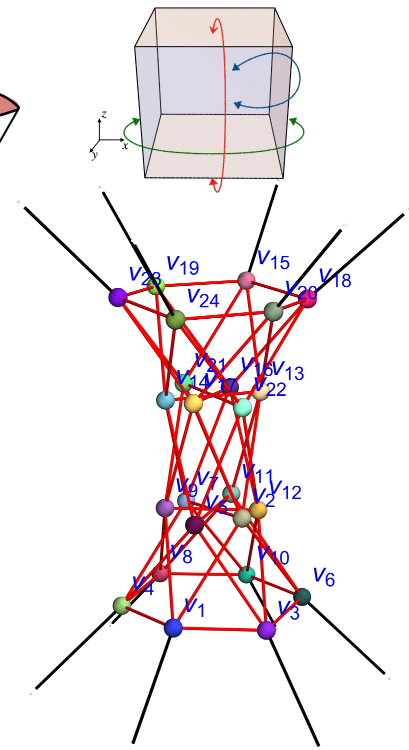

Hypercube complex

A hypercube consists of 24 4-simplices: $(v_1, v_2, \cdots, v_{24})$.

- Flat hypercube: $a_f = a_i$.
- Curved hypercube: $a_f = a_i - 2\delta a, \quad \delta a \neq 0$

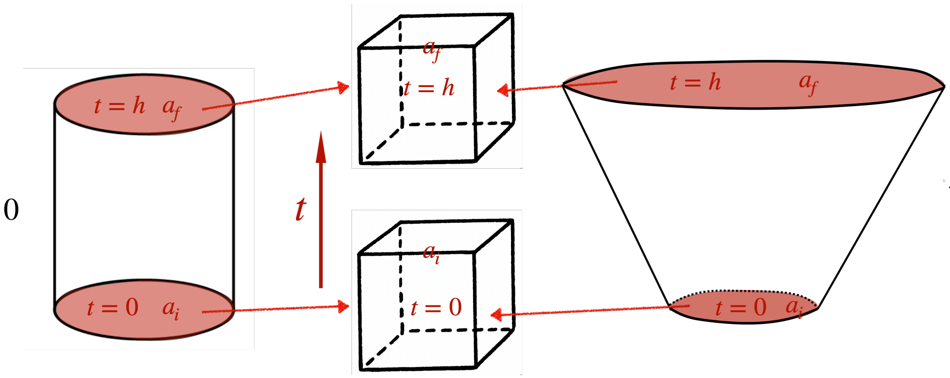

Periodic boundary condition

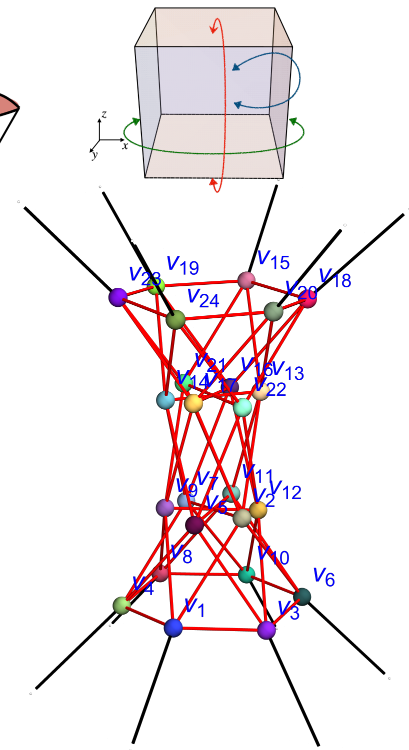

The spinfoam amplitude coupled with scalar matter:

$$\int \prod_{I=1}^{N_{\text{out}}} \mathrm{d}j_I^{\text{out}} \mathcal{Z}_{\mathcal{K}}\left(j_I^{\text{out}}, \xi_{eb}, K_{i(f)}, \phi_{i(f)}, \pi_{i(f)}\right), \qquad \mathcal{Z}_{\mathcal{K}} = \int \mathrm{d}^N \mathbf{x}\, \mu(\mathbf{x})\, e^{S_{\text{tot}}(r,\mathbf{x})}, \qquad S_{\text{tot}}(r, \mathbf{x}) = S_{\text{SF}} + S_{\text{Scalar}}\,.$$

- External data $r = (a_{i(f)}, K_{i(f)}, \phi_{i(f)}, \pi_{i(f)})$.
- The integration variables $\mathbf{x} = \{g_{ve}, z_{vf}, \xi_{eh}^{\pm}, l_{eh}^{+}, j_{\bar{h}}, \varphi_v\} \Longrightarrow$ 1192 real variables

Numerical Result of Hypercube Complex

- When r^0 is determined by $a_i = a_f = 1$, fixed h value, and $K_b = \phi_{v_b} = \pi_{v_b} = 0 \Longrightarrow$ Real critical point.
- When $r = r^0 + \delta r \Longrightarrow$ Complex critical point.

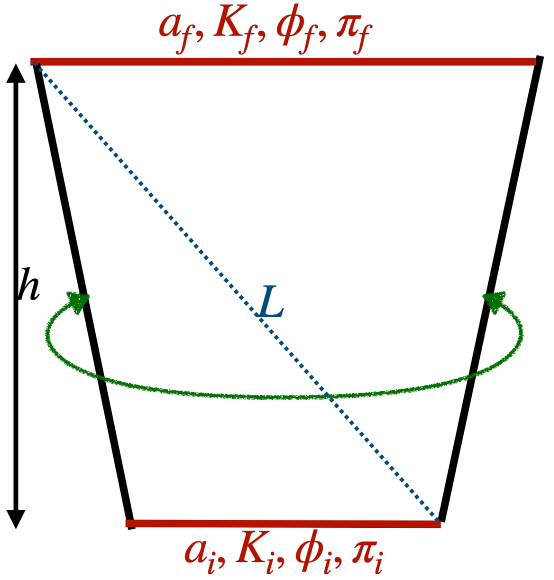

Numerical Result of Hypercube Complex

- When r^0 is determined by $a_i = a_f = 1$, fixed h value, and $K_b = \phi_{v_b} = \pi_{v_b} = 0 \Longrightarrow$ Real critical point.
- When $r = r^0 + \delta r \Longrightarrow$ Complex critical point.

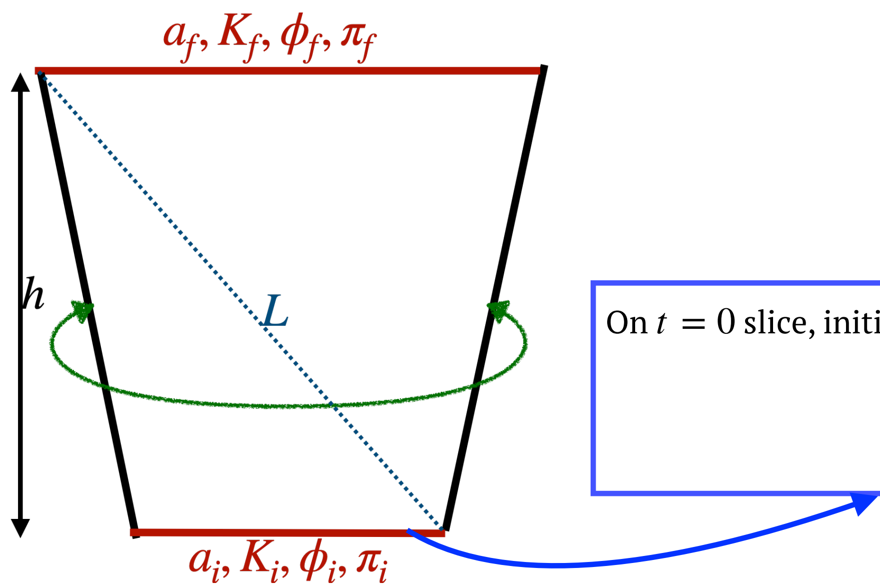

On $t = 0$ slice, initial data $(a_i, K_i, \phi_i, \pi_i)$ satisfy the Friedmann equation:

$$\left(\frac{\dot{a}_i}{a_i}\right)^2 = \frac{8\pi G\rho_i}{3} \Longrightarrow K_i^2 = \frac{3\pi_i^2}{2a_i^6}$$

Numerical Result of Hypercube Complex

- When r^0 is determined by $a_i = a_f = 1$, fixed h value, and $K_b = \phi_{v_b} = \pi_{v_b} = 0 \Longrightarrow$ Real critical point.
- When $r = r^0 + \delta r \Longrightarrow$ Complex critical point.

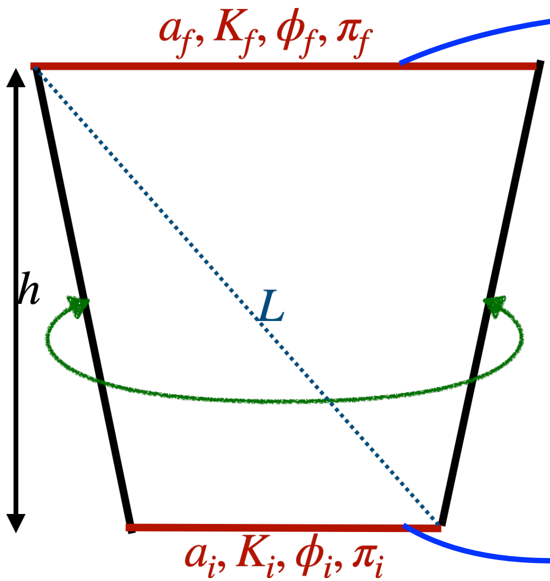

On $t = h$ slice, the final data $(a_f, K_f, \phi_f, \pi_f)$ are given with the condition:

$$a_f > a_i, \quad \phi_f > \phi_i, \quad K_f > 0, \quad \pi_f > 0$$

On $t = 0$ slice, initial data $(a_i, K_i, \phi_i, \pi_i)$ satisfy the Friedmann equation:

$$\left(\frac{\dot{a}_i}{a_i}\right)^2 = \frac{8\pi G \rho_i}{3} \Longrightarrow K_i^2 = \frac{3\pi_i^2}{2a_i^6}$$

Each sample (K_f, ϕ_f, π_f), we can find the numerical solutions to $\partial_{\mathbf{z}} \mathcal{S}_{\text{tot}}(r, \mathbf{z}) = 0 \Longrightarrow Z(r)$ is the complex critical point

Numerical Result of Hypercube Complex

The maximum of spinfoam amplitude corresponds to the Hamiltonian constraint (modified Friedmann equation)

[E. Bianchi, C. Rovelli, F. Vidotto, 2010]

Numerical Result of Hypercube Complex

The maximum of spinfoam amplitude corresponds to the Hamiltonian constraint (modified Friedmann equation)

[E. Bianchi, C. Rovelli, F. Vidotto, 2010]

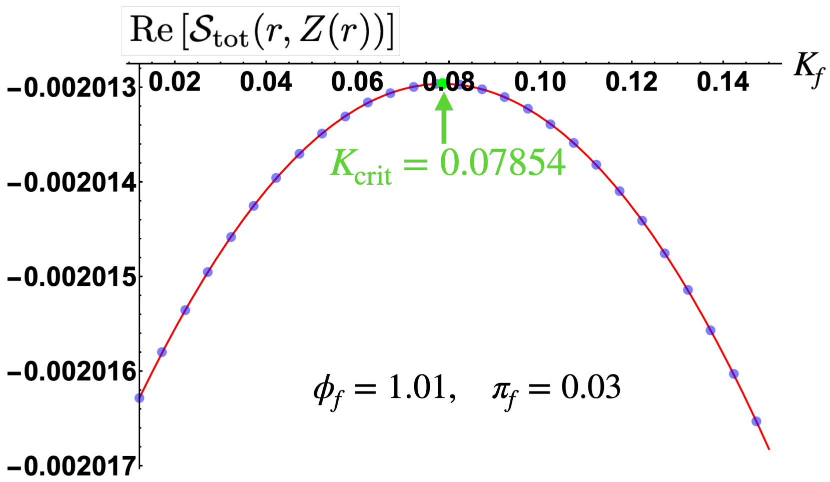

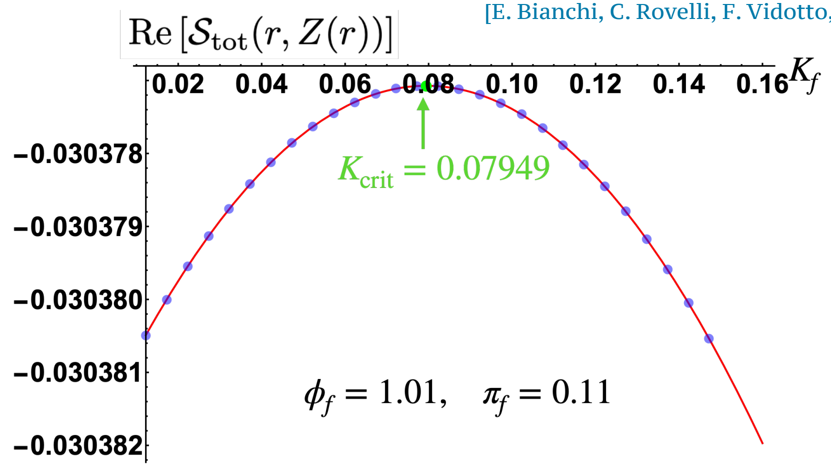

Numerical Result of Hypercube Complex

The maximum of spinfoam amplitude corresponds to the Hamiltonian constraint (modified Friedmann equation)

[E. Bianchi, C. Rovelli, F. Vidotto, 2010]

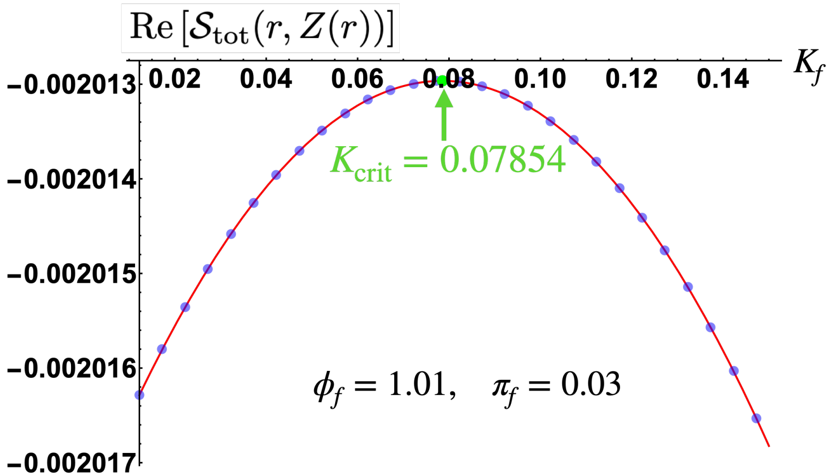

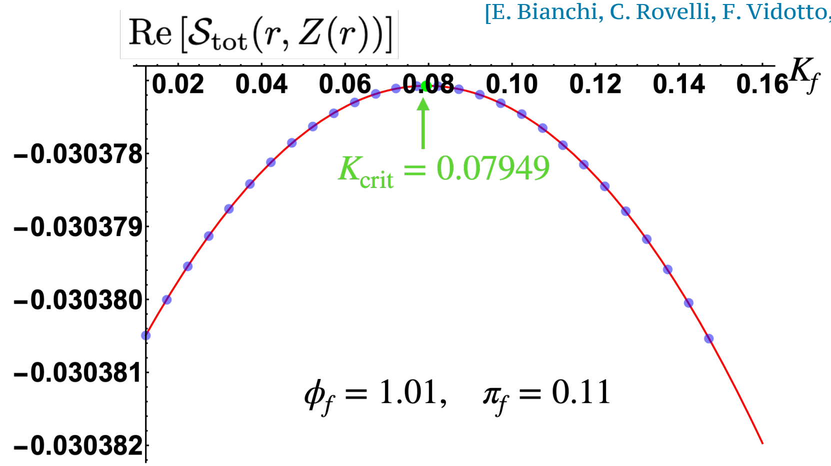

Fixing ϕ_f and varying π_f

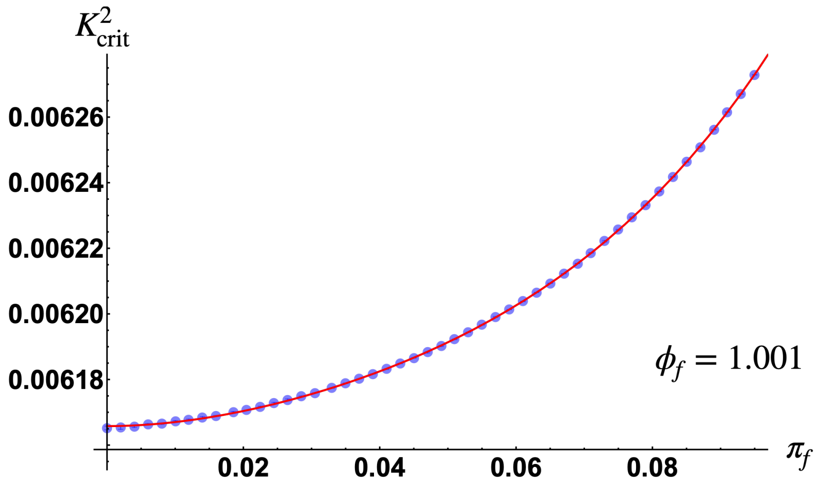

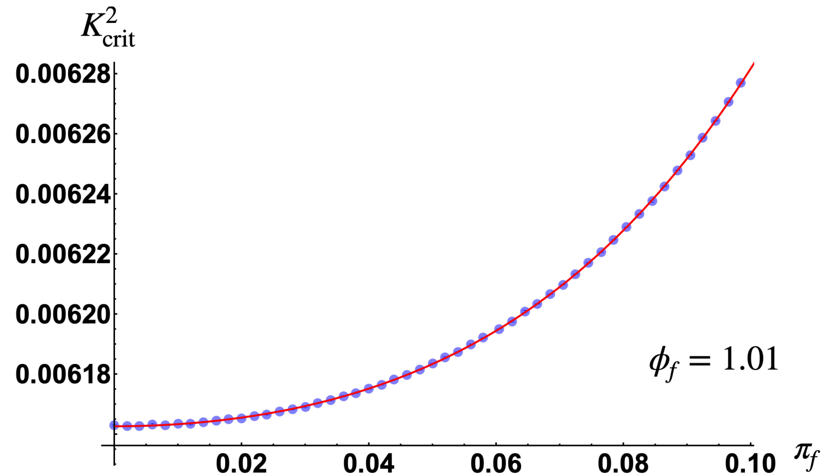

Numerical Result of Hypercube Complex

The constraint equation of K_f and π_f is given by

$$K_{\text{crit}}^2 = \alpha_0 + \alpha_2\pi_f^2 + \alpha_3\pi_f^3 + \alpha_4\pi_f^4 + O(\pi_f^5)$$

For $\phi_f = 1.001$:

$\alpha_0 = 0.00617_{\pm 1.08\times 10^{-8}}, \quad \alpha_2 = 0.0133_{\pm 6.32\times 10^{-5}},$

$\alpha_3 = -0.113_{\pm 1.52\times 10^{-3}}, \quad \alpha_4 = 1.034_{\pm 9.39\times 10^{-3}}.$

For $\phi_f = 1.01$:

$\alpha_0 = 0.00616_{\pm 1.56\times 10^{-8}}, \quad \alpha_2 = 0.00690_{\pm 4.38\times 10^{-5}},$

$\alpha_3 = 0.00518_{\pm 1.05\times 10^{-3}}, \quad \alpha_4 = 0.447_{\pm 6.50\times 10^{-3}}.$

Numerical Result of Hypercube Complex

The constraint equation of K_f and π_f is given by

$$K_{\text{crit}}^2 = \alpha_0 + \alpha_2\pi_f^2 + \alpha_3\pi_f^3 + \alpha_4\pi_f^4 + O(\pi_f^5)$$

For $\phi_f = 1.001$:

$$\alpha_0 = 0.00617_{\pm 1.08\times 10^{-8}}, \quad \alpha_2 = 0.0133_{\pm 6.32\times 10^{-5}},$$
$$\alpha_3 = -0.113_{\pm 1.52\times 10^{-3}}, \quad \alpha_4 = 1.034_{\pm 9.39\times 10^{-3}}.$$

For $\phi_f = 1.01$:

$$\alpha_0 = 0.00616_{\pm 1.56\times 10^{-8}}, \quad \alpha_2 = 0.00690_{\pm 4.38\times 10^{-5}},$$
$$\alpha_3 = 0.00518_{\pm 1.05\times 10^{-3}}, \quad \alpha_4 = 0.447_{\pm 6.50\times 10^{-3}}.$$

Compare to classical Friedmann equation $K_i^2 = 8\pi G \frac{3\pi_i^2}{2a_i^6}$:

Numerical Result of Hypercube Complex

The constraint equation of K_f and π_f is given by

$$K^2_{\text{crit}} = \alpha_0 + \alpha_2\pi_f^2 + \alpha_3\pi_f^3 + \alpha_4\pi_f^4 + O(\pi_f^5)$$

For $\phi_f = 1.001$:

$\alpha_0 = 0.00617_{\pm 1.08\times 10^{-8}}, \quad \alpha_2 = 0.0133_{\pm 6.32\times 10^{-5}},$

$\alpha_3 = -0.113_{\pm 1.52\times 10^{-3}}, \quad \alpha_4 = 1.034_{\pm 9.39\times 10^{-3}}.$

For $\phi_f = 1.01$:

$\alpha_0 = 0.00616_{\pm 1.56\times 10^{-8}}, \quad \alpha_2 = 0.00690_{\pm 4.38\times 10^{-5}},$

$\alpha_3 = 0.00518_{\pm 1.05\times 10^{-3}}, \quad \alpha_4 = 0.447_{\pm 6.50\times 10^{-3}}.$

Compare to classical Friedmann equation $K_i^2 = 8\pi G \dfrac{3\pi_i^2}{2a_i^6}$:

- An effective scalar density ρ_{eff}: π_f^2 terms and higher derivative terms with π_f^3 and π_f^4.

Numerical Result of Hypercube Complex

The constraint equation of K_f and π_f is given by

$$K_{\text{crit}}^2 = \alpha_0 + \alpha_2\pi_f^2 + \alpha_3\pi_f^3 + \alpha_4\pi_f^4 + O(\pi_f^5)$$

For $\phi_f = 1.001$:

$\alpha_0 = 0.00617_{\pm 1.08\times 10^{-8}}, \quad \alpha_2 = 0.0133_{\pm 6.32\times 10^{-5}},$

$\alpha_3 = -0.113_{\pm 1.52\times 10^{-3}}, \quad \alpha_4 = 1.034_{\pm 9.39\times 10^{-3}}.$

For $\phi_f = 1.01$:

$\alpha_0 = 0.00616_{\pm 1.56\times 10^{-8}}, \quad \alpha_2 = 0.00690_{\pm 4.38\times 10^{-5}},$

$\alpha_3 = 0.00518_{\pm 1.05\times 10^{-3}}, \quad \alpha_4 = 0.447_{\pm 6.50\times 10^{-3}}.$

Compare to classical Friedmann equation $K_i^2 = 8\pi G \dfrac{3\pi_i^2}{2a_i^6}$:

- An effective scalar density ρ_{eff}: π_f^2 terms and higher derivative terms with π_f^3 and π_f^4.
- $\alpha_0(\phi_f)$ is understood as an effective scalar potential.

Numerical Result of Hypercube Complex

The constraint equation of K_f and π_f is given by

$$K^2_{\text{crit}} = \alpha_0 + \alpha_2 \pi_f^2 + \alpha_3 \pi_f^3 + \alpha_4 \pi_f^4 + O(\pi_f^5)$$

For $\phi_f = 1.001$:

$\alpha_0 = 0.00617_{\pm 1.08\times 10^{-8}}, \quad \alpha_2 = 0.0133_{\pm 6.32\times 10^{-5}},$

$\alpha_3 = -0.113_{\pm 1.52\times 10^{-3}}, \quad \alpha_4 = 1.034_{\pm 9.39\times 10^{-3}}.$

For $\phi_f = 1.01$:

$\alpha_0 = 0.00616_{\pm 1.56\times 10^{-8}}, \quad \alpha_2 = 0.00690_{\pm 4.38\times 10^{-5}},$

$\alpha_3 = 0.00518_{\pm 1.05\times 10^{-3}}, \quad \alpha_4 = 0.447_{\pm 6.50\times 10^{-3}}.$

Compare to classical Friedmann equation $K_i^2 = 8\pi G \dfrac{3\pi_i^2}{2a_i^6}$:

- An effective scalar density ρ_{eff}: π_f^2 terms and higher derivative terms with π_f^3 and π_f^4.
- $\alpha_0(\phi_f)$ is understood as an effective scalar potential.
- $\alpha_0 > 0$ plays a role similar to an effective positive cosmological constant.

Numerical Result of Hypercube Complex

The constraint equation of K_f and π_f is given by

$$K_{\text{crit}}^2 = \alpha_0 + \alpha_2 \pi_f^2 + \alpha_3 \pi_f^3 + \alpha_4 \pi_f^4 + O(\pi_f^5)$$

For $\phi_f = 1.001$:

$\alpha_0 = 0.00617_{\pm 1.08 \times 10^{-8}}, \quad \alpha_2 = 0.0133_{\pm 6.32 \times 10^{-5}},$

$\alpha_3 = -0.113_{\pm 1.52 \times 10^{-3}}, \quad \alpha_4 = 1.034_{\pm 9.39 \times 10^{-3}}.$

For $\phi_f = 1.01$:

$\alpha_0 = 0.00616_{\pm 1.56 \times 10^{-8}}, \quad \alpha_2 = 0.00690_{\pm 4.38 \times 10^{-5}},$

$\alpha_3 = 0.00518_{\pm 1.05 \times 10^{-3}}, \quad \alpha_4 = 0.447_{\pm 6.50 \times 10^{-3}}.$

Compare to classical Friedmann equation $K_i^2 = 8\pi G \dfrac{3\pi_i^2}{2a_i^6}$:

- An effective scalar density ρ_{eff}: π_f^2 terms and higher derivative terms with π_f^3 and π_f^4.
- $\alpha_0(\phi_f)$ is understood as an effective scalar potential.
- $\alpha_0 > 0$ plays a role similar to an effective positive cosmological constant.
- $\alpha_0 \neq 0$ indicates that on the final slice $K_{\text{crit}} > K_i$, implying the accelerating expansion of the universe.

Double Hypercube Complex

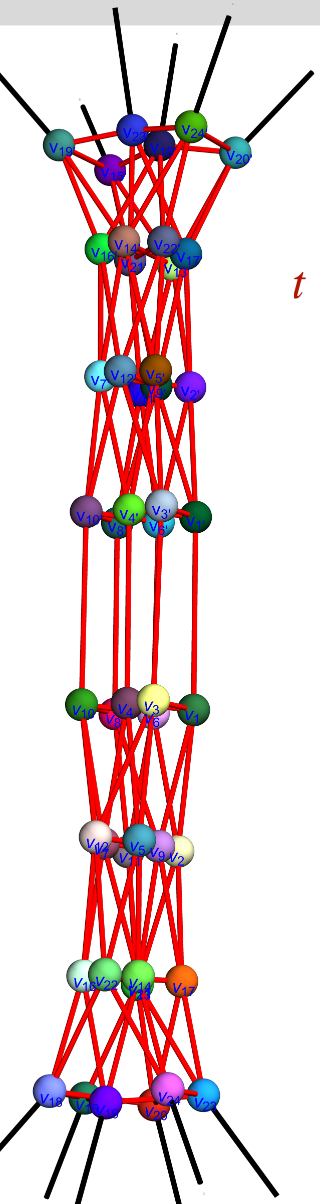

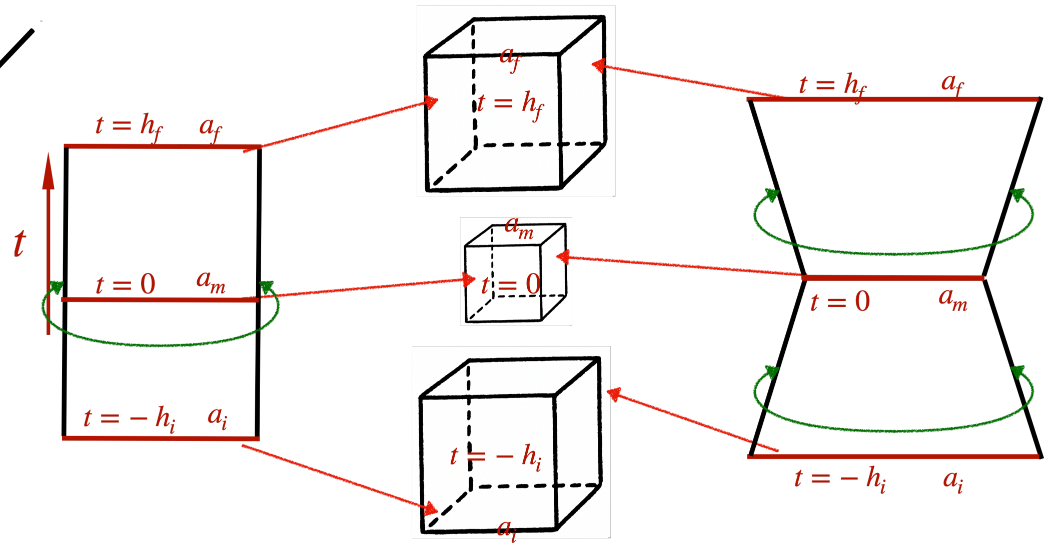

- Flat geometry: $a_f = a_i = a_m$.
- Curved geometries: $a_f = a_i = a$,

$$a_m = a - 2\delta a, \quad 0 < \delta a < \frac{a}{2}.$$

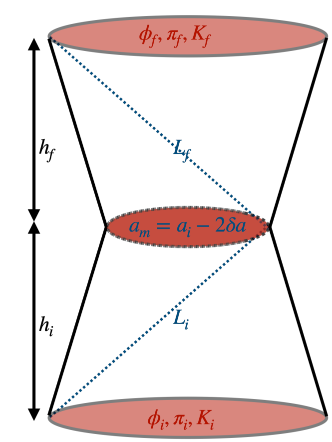

Double Hypercube Complex

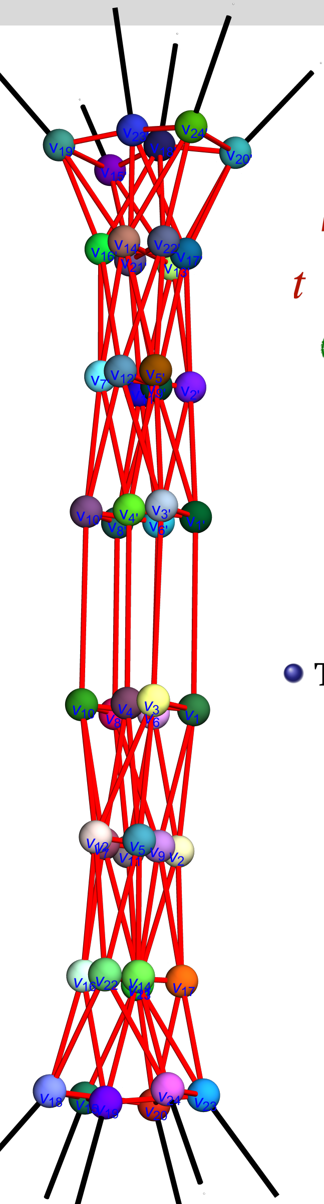

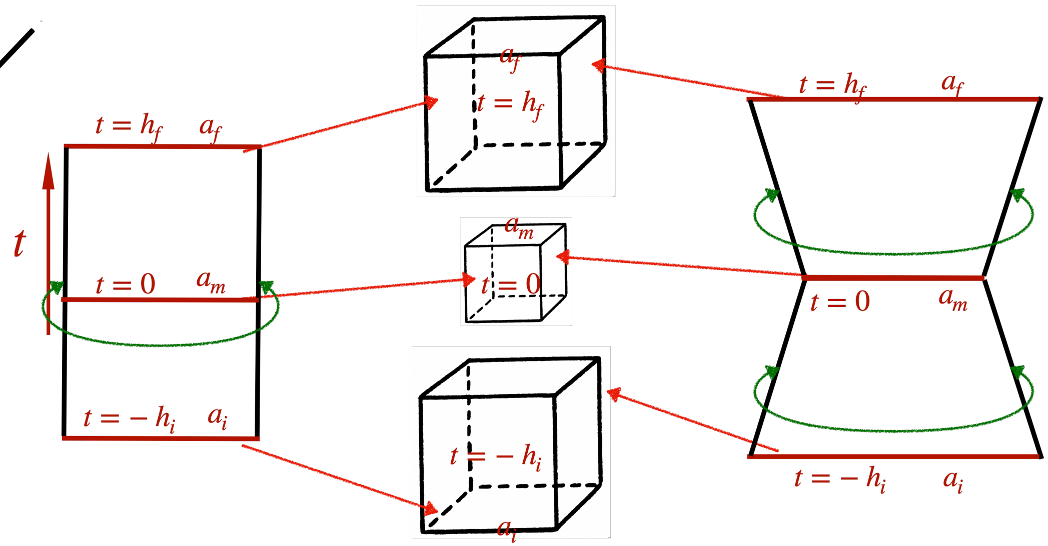

- Flat geometry: $a_f = a_i = a_m$.
- Curved geometries: $a_f = a_i = a$,

$$a_m = a - 2\delta a, \quad 0 < \delta a < \frac{a}{2}.$$

- This model consists of two hypercubes: 48 4-simplices.

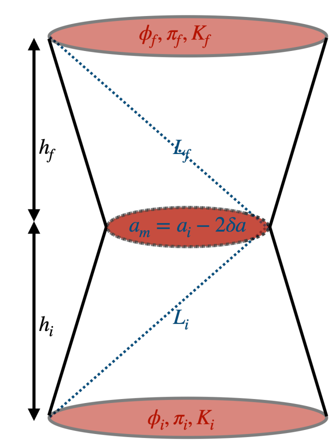

Double Hypercube Complex

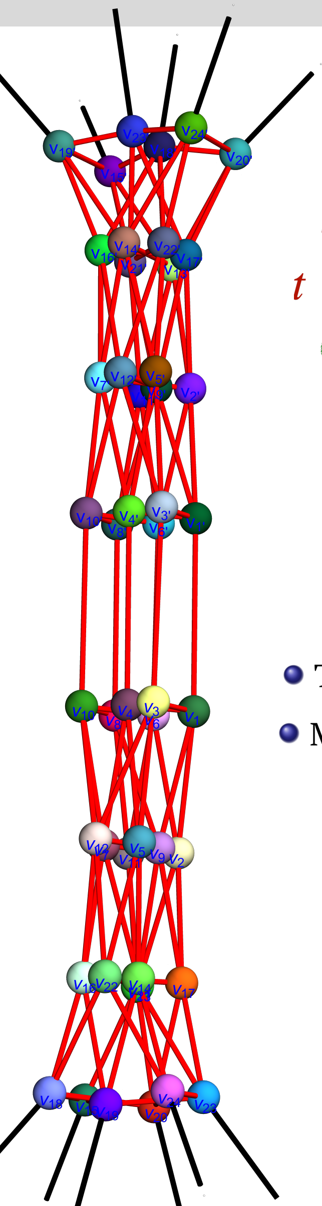

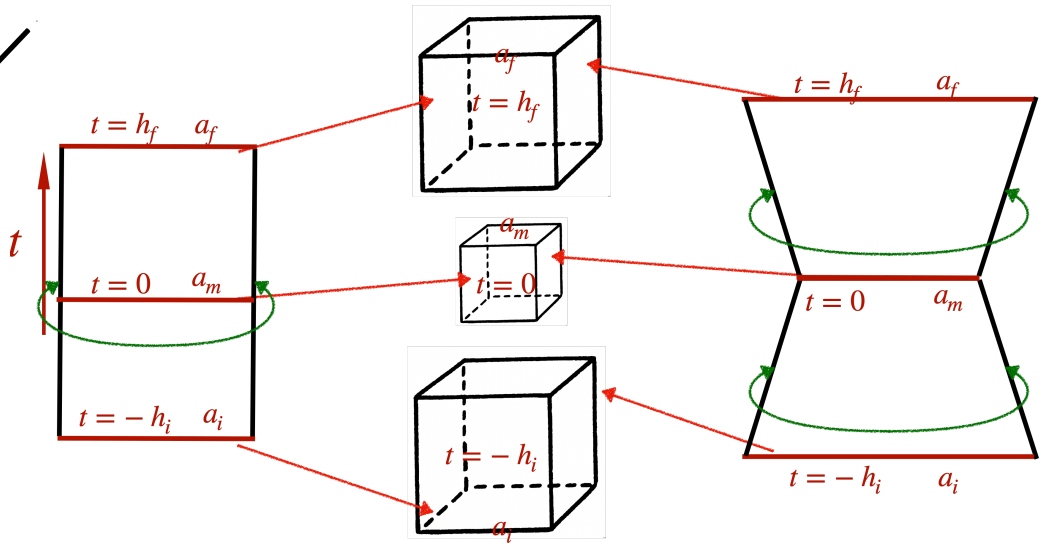

- Flat geometry: $a_f = a_i = a_m$.
- Curved geometries: $a_f = a_i = a$,

$$a_m = a - 2\delta a, \quad 0 < \delta a < \frac{a}{2}.$$

- This model consists of two hypercubes: 48 4-simplices.
- Make an analog of the (time-reversal) symmetric cosmic bounce.

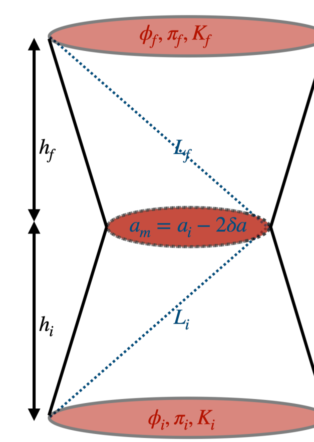

Double Hypercube Complex

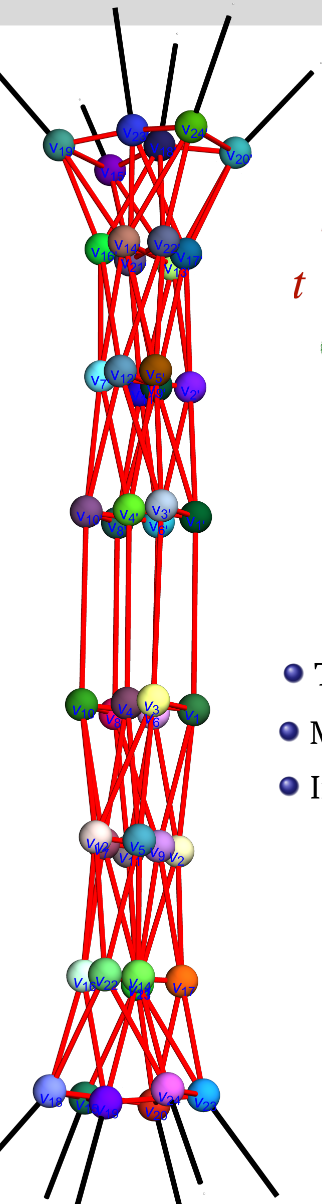

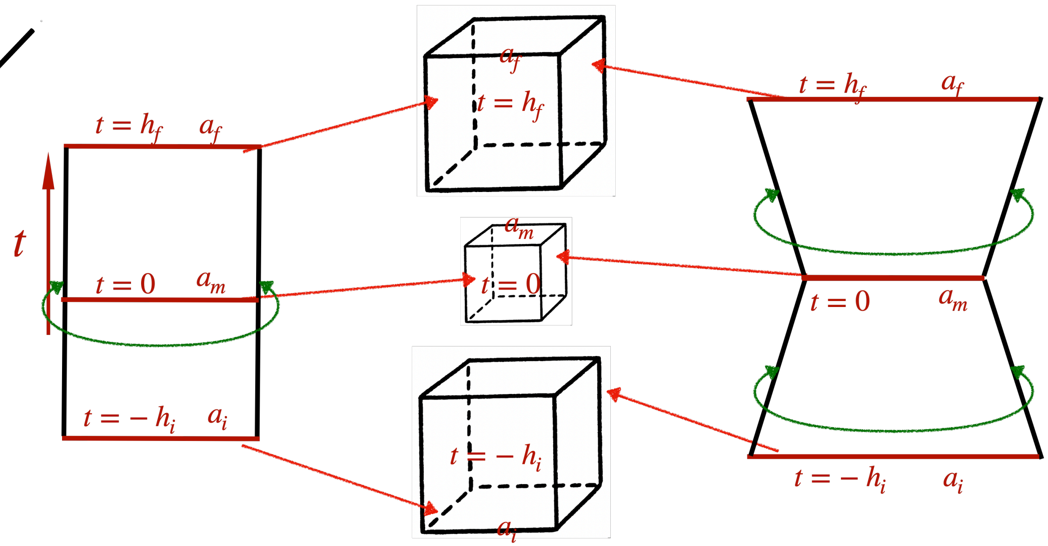

- Flat geometry: $a_f = a_i = a_m$.
- Curved geometries: $a_f = a_i = a$,

$$a_m = a - 2\delta a, \quad 0 < \delta a < \frac{a}{2}.$$

- This model consists of two hypercubes: 48 4-simplices.
- Make an analog of the (time-reversal) symmetric cosmic bounce.
- Impose the following conditions for the initial and final data:

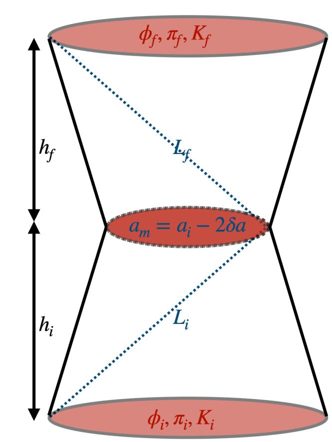

Double Hypercube Complex

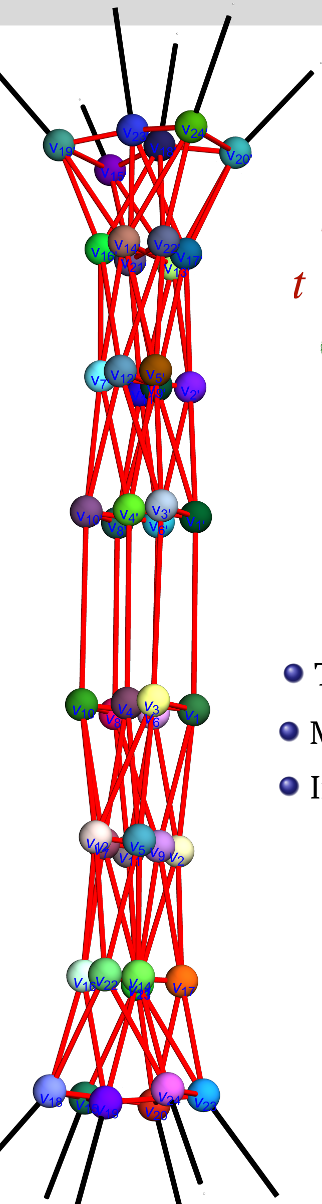

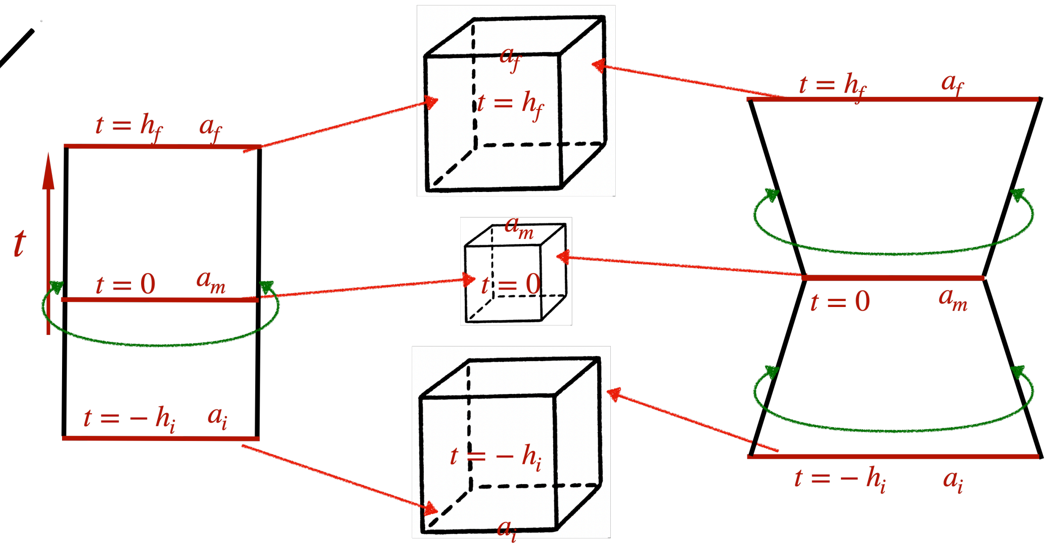

- Flat geometry: $a_f = a_i = a_m$.
- Curved geometries: $a_f = a_i = a$,

$$a_m = a - 2\delta a, \quad 0 < \delta a < \frac{a}{2}.$$

- This model consists of two hypercubes: 48 4-simplices.
- Make an analog of the (time-reversal) symmetric cosmic bounce.
- Impose the following conditions for the initial and final data:

$$a_i = a_f = a, \quad K_f = -K_i > 0, \quad \phi_f = -\phi_i > 0, \quad \pi_f = \pi_i > 0.$$

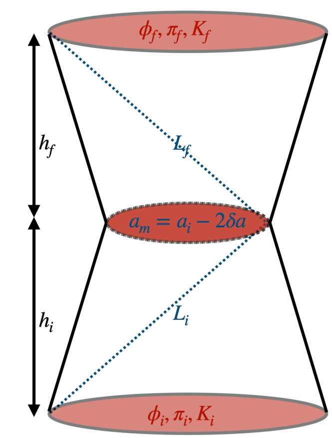

Double Hypercube Complex

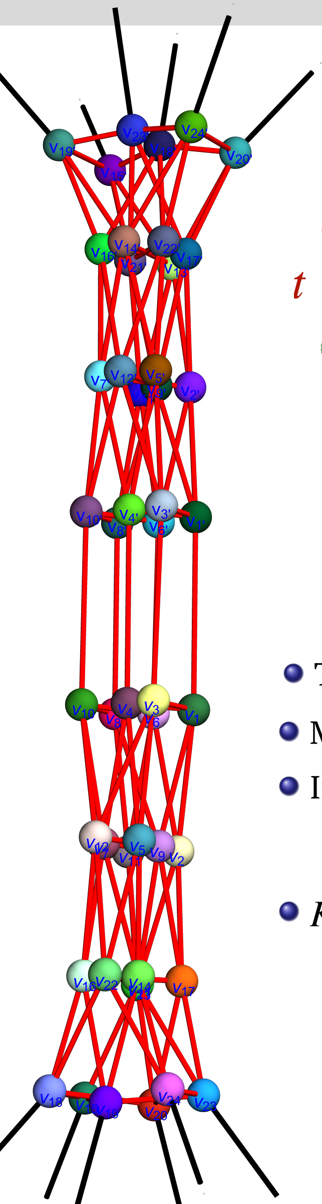

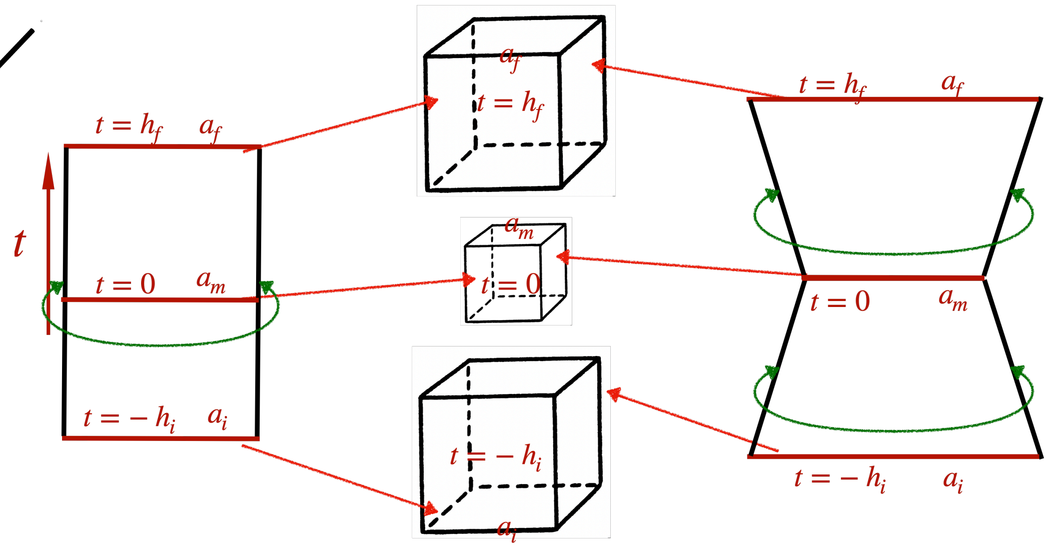

- Flat geometry: $a_f = a_i = a_m$.
- Curved geometries: $a_f = a_i = a$,

$$a_m = a - 2\delta a, \quad 0 < \delta a < \frac{a}{2}.$$

- This model consists of two hypercubes: 48 4-simplices.
- Make an analog of the (time-reversal) symmetric cosmic bounce.
- Impose the following conditions for the initial and final data:

$$a_i = a_f = a, \quad K_f = -K_i > 0, \quad \phi_f = -\phi_i > 0, \quad \pi_f = \pi_i > 0.$$

- $K_i < 0$ and $K_f > 0 \rightarrow$ contracting and expanding universes at the initial and final slices.

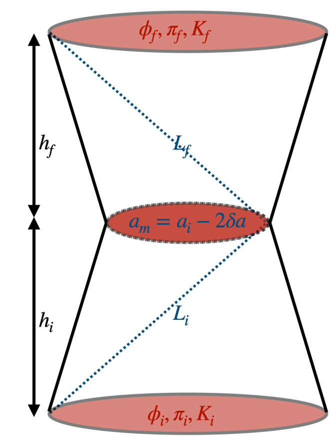

Double Hypercube Complex

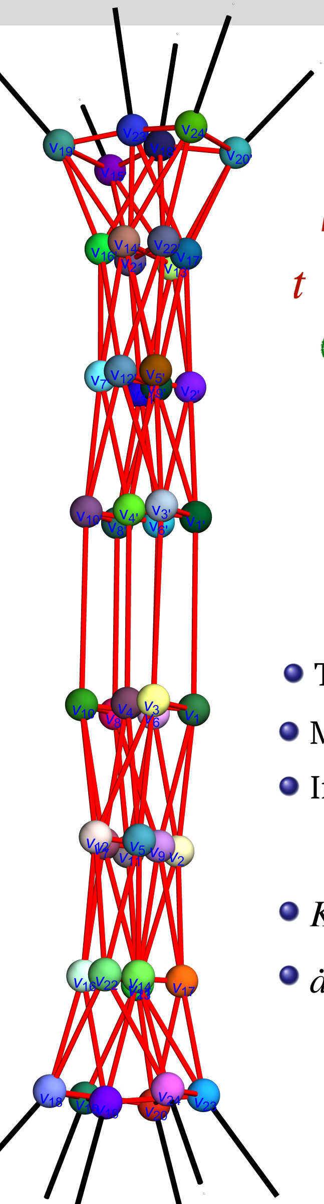

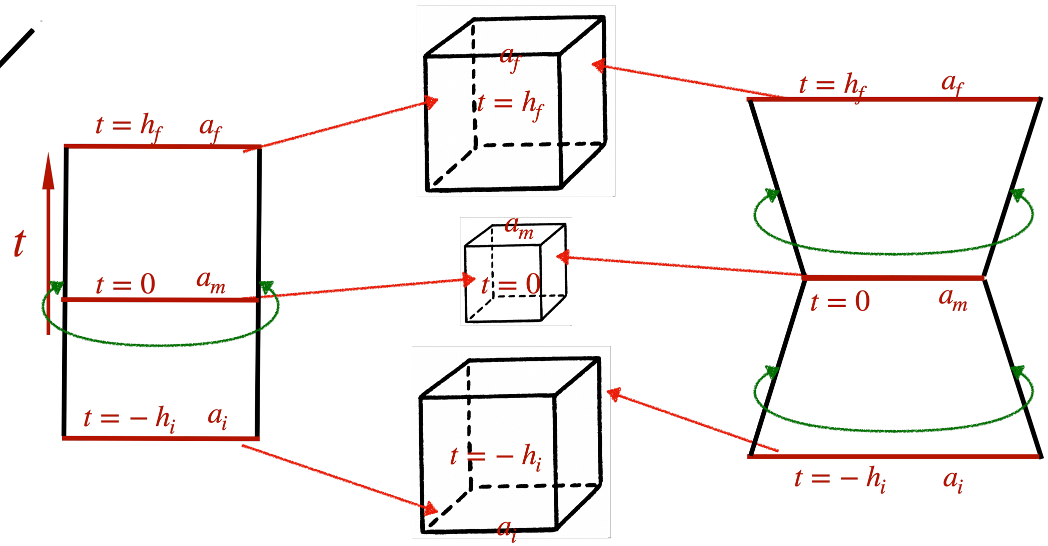

- Flat geometry: $a_f = a_i = a_m$.
- Curved geometries: $a_f = a_i = a$,

$$a_m = a - 2\delta a, \quad 0 < \delta a < \frac{a}{2}.$$

- This model consists of two hypercubes: 48 4-simplices.
- Make an analog of the (time-reversal) symmetric cosmic bounce.
- Impose the following conditions for the initial and final data:

$$a_i = a_f = a, \quad K_f = -K_i > 0, \quad \phi_f = -\phi_i > 0, \quad \pi_f = \pi_i > 0.$$

- $K_i < 0$ and $K_f > 0 \rightarrow$ contracting and expanding universes at the initial and final slices.
- $\dot{a}$ evolves from negative to positive $\rightarrow$ a cosmic bounce occurring in the evolution.

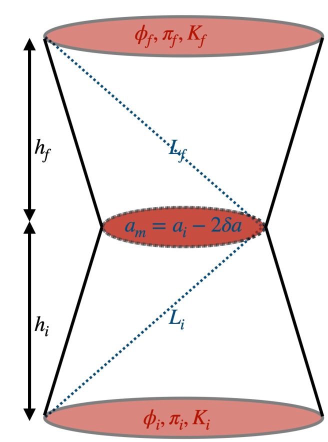

Numerical Result of Double-Hypercube Complex

Numerical Result of Double-Hypercube Complex

Each sample (K_i, ϕ_i, π_i), we can find the numerical solutions to $\partial_{\mathbf{z}} \mathcal{S}_{\text{tot}}(r, \mathbf{z}) = 0 \Longrightarrow Z(r)$ is the complex critical point

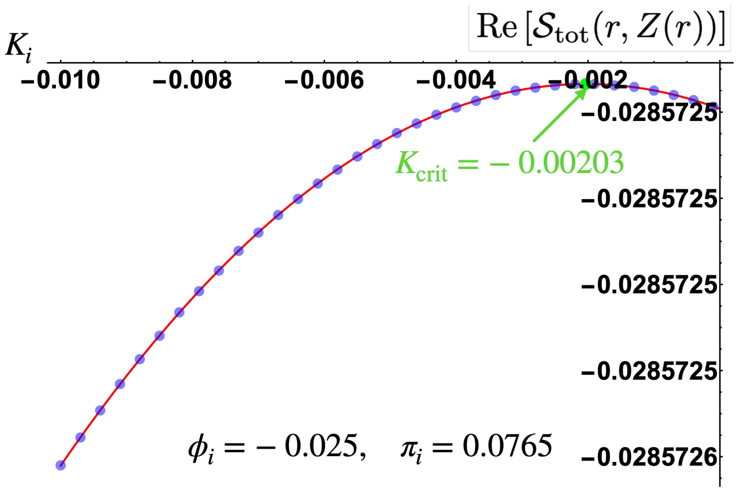

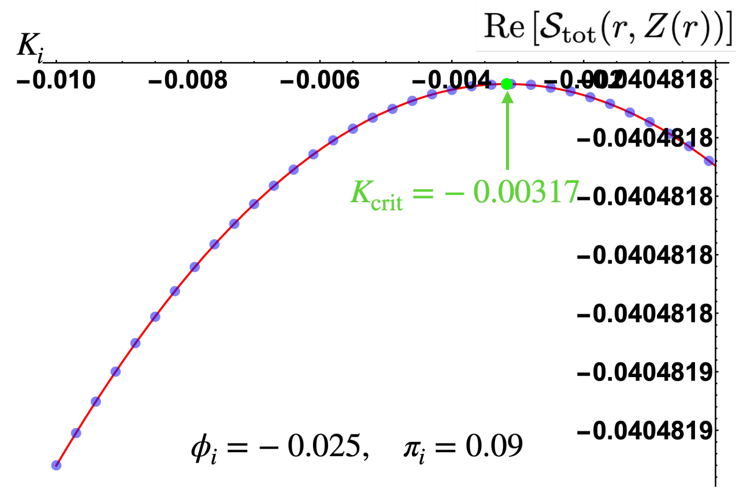

$K_i = -K_f = K_{\text{crit}}$ should have the interpretation as the quantum analog of a cosmic bounce.

Numerical Result of Double-Hypercube Complex

Each sample (K_i, ϕ_i, π_i), we can find the numerical solutions to $\partial_{\mathbf{z}}\mathcal{S}_{\text{tot}}(r, \mathbf{z}) = 0 \Longrightarrow Z(r)$ is the complex critical point

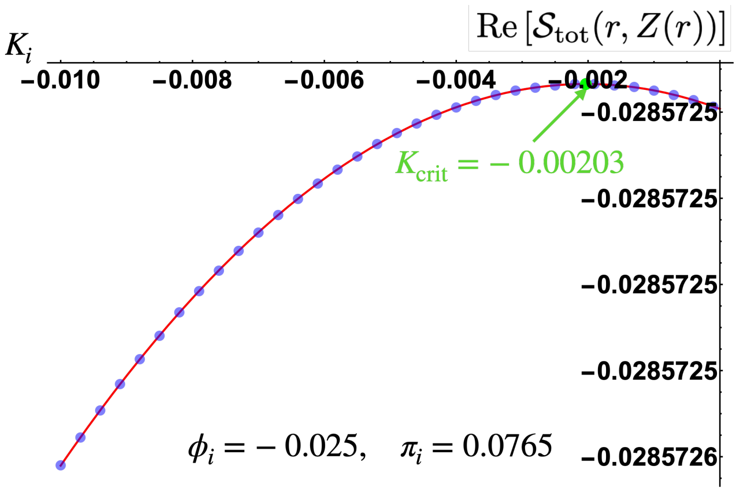

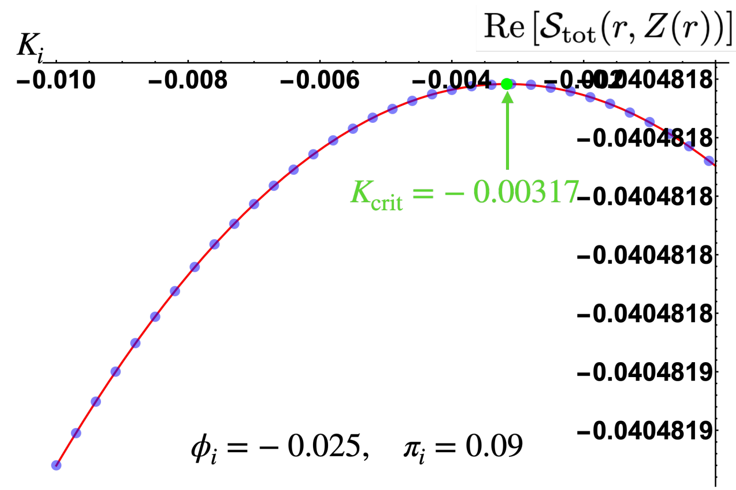

$K_i = -K_f = K_{\text{crit}}$ should have the interpretation as the quantum analog of a cosmic bounce.

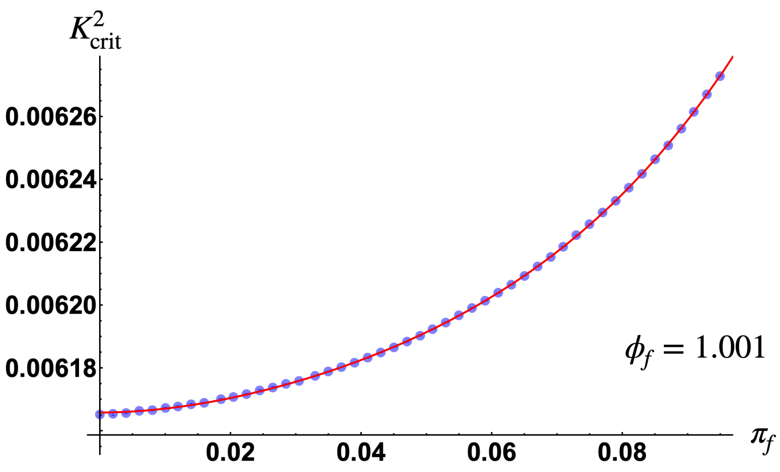

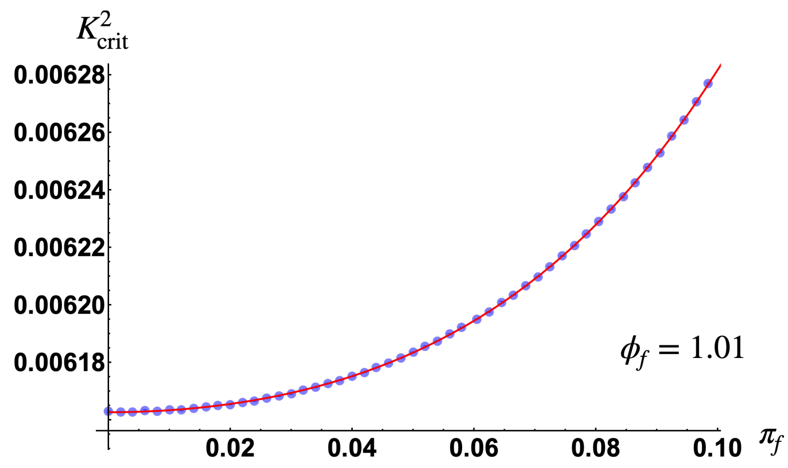

Numerical Result of Double-Hypercube Complex

The constraint equation between K^2_{crit} and π_i:

$$K^2_{\text{crit}} = \alpha_2(\phi_i)\pi_i^2 + \alpha_3(\phi_i)\pi_i^3 + \alpha_4(\phi_i)\pi_i^4 + \mathcal{O}(\pi_i^5)\,.$$

For $\phi_i = -0.025$:

$$\alpha_2 = 0.000146_{\pm 8.40\times 10^{-6}},$$
$$\alpha_3 = -0.0197_{\pm 2.14\times 10^{-4}}, \quad \alpha_4 = 0.354_{\pm 0.00133}\,.$$

For $\phi_i = -0.04$:

$$\alpha_2 = 0.00170_{\pm 1.56\times 10^{-5}},$$
$$\alpha_3 = -0.0571_{\pm 3.44\times 10^{-4}}, \quad \alpha_4 = 0.465_{\pm 0.00190}\,.$$

Numerical Result of Double-Hypercube Complex

The constraint equation between K^2_{crit} and π_i:

$$K^2_{\text{crit}} = \alpha_2(\phi_i)\pi_i^2 + \alpha_3(\phi_i)\pi_i^3 + \alpha_4(\phi_i)\pi_i^4 + \mathcal{O}(\pi_i^5)\,.$$

For $\phi_i = -0.025$:

$$\alpha_2 = 0.000146_{\pm 8.40\times 10^{-6}},$$
$$\alpha_3 = -0.0197_{\pm 2.14\times 10^{-4}}, \quad \alpha_4 = 0.354_{\pm 0.00133}\,.$$

For $\phi_i = -0.04$:

$$\alpha_2 = 0.00170_{\pm 1.56\times 10^{-5}},$$
$$\alpha_3 = -0.0571_{\pm 3.44\times 10^{-4}}, \quad \alpha_4 = 0.465_{\pm 0.00190}\,.$$

- A modified Friedmann equation when a symmetric bounce happens.

Numerical Result of Double-Hypercube Complex

The constraint equation between $K_{\rm crit}^2$ and π_i:

$$K_{\rm crit}^2 = \alpha_2(\phi_i)\pi_i^2 + \alpha_3(\phi_i)\pi_i^3 + \alpha_4(\phi_i)\pi_i^4 + \mathcal{O}(\pi_i^5)\,.$$

For $\phi_i = -0.025$:

$$\alpha_2 = 0.000146_{\pm 8.40\times 10^{-6}},$$
$$\alpha_3 = -0.0197_{\pm 2.14\times 10^{-4}}, \quad \alpha_4 = 0.354_{\pm 0.00133}\,.$$

For $\phi_i = -0.04$:

$$\alpha_2 = 0.00170_{\pm 1.56\times 10^{-5}},$$
$$\alpha_3 = -0.0571_{\pm 3.44\times 10^{-4}}, \quad \alpha_4 = 0.465_{\pm 0.00190}\,.$$

- A modified Friedmann equation when a symmetric bounce happens.
- The effective scalar density $\rho_{\rm eff}$, which contains higher derivative terms with π_i^3 and π_i^4.

Numerical Result of Double-Hypercube Complex

The constraint equation between K^2_{crit} and π_i:

$$K^2_{\text{crit}} = \alpha_2(\phi_i)\pi_i^2 + \alpha_3(\phi_i)\pi_i^3 + \alpha_4(\phi_i)\pi_i^4 + \mathcal{O}(\pi_i^5)\,.$$

For $\phi_i = -0.025$:

$$\alpha_2 = 0.000146_{\pm 8.40\times 10^{-6}},$$
$$\alpha_3 = -0.0197_{\pm 2.14\times 10^{-4}}, \quad \alpha_4 = 0.354_{\pm 0.00133}\,.$$

For $\phi_i = -0.04$:

$$\alpha_2 = 0.00170_{\pm 1.56\times 10^{-5}},$$
$$\alpha_3 = -0.0571_{\pm 3.44\times 10^{-4}}, \quad \alpha_4 = 0.465_{\pm 0.00190}\,.$$

- A modified Friedmann equation when a symmetric bounce happens.
- The effective scalar density ρ_{eff}, which contains higher derivative terms with π_i^3 and π_i^4.
- The scalar potential vanishes due to no constant term.

Conclusion

- The numerical method of real and complex critical points is a powerful tool to study spinfoam amplitude.
- Our work provides a general procedure to numerically construct the critical points of the spinfoam amplitude on the simplicial complex.
- For the cases that real critical point is absent, we use the method of complex critical points.
- We can use the method of complex critical points to study more physical scenario - quantum cosmology.
- The coupling of scalar matter to spinfoam yields nontrivial physical implications for the effective cosmological dynamics.
- Similar studies have been carried out to the black-to-white-hole transition. [Cong Zhang's talk]

Outlook

Numerical Algorithm

- The algorithm of computing the Next-to-leading order in stationary phase approximation
  [Haida Li's talk]
- Compare to the result of sl2cfoam based on $15j$ + boosters.
- Lefschetz thimble from the complex critical point to compute spinfoam propagator on curved spacetime

Outlook

Numerical Algorithm

- The algorithm of computing the Next-to-leading order in stationary phase approximation [Haida Li's talk]
- Compare to the result of sl2cfoam based on $15j$ + boosters.
- Lefschetz thimble from the complex critical point to compute spinfoam propagator on curved spacetime

Physical Application

- More hypercubes along t-direction, leading to a more accurate representation of cosmology.
- Develop techniques for fitting the constraint among $(a_{i(f)}, K_{i(f)}, \phi_{i(f)}, \pi_{i(f)})$ within a higher-dimensional parameter space.
- Compare to LQC. [A. Ashtekar, M. Campiglia, A. Henderson, 2010]

Thank you for your attention!